TRANSITIONS IN THE LUBRICATION

OF CONCENTRATED CONTACTS

PROEFSCHRIFT

ter verkrijging van
de graad van doctor aan de Universiteit Twente,
op gezag van de rector magnificus,
prof. dr. ir. J.H.A. de Smit,
volgens besluit van het College van Dekanen
in het openbaar te verdedigen
op vrijdag 28 oktober te 16.00 uur.

door

Dirk Jan SCHIPPER

geboren op 30 mei 1955 te Kampen

Dit proefschrift is goedgekeurd door de promotor:

Prof. ir. R. Bosma

aan mijn ouders

aan Agnieszka en David.

CONTENTS

ABSTRACT

SAMENVATTING

ABSTRACT.

This thesis deals with the different lubrication modes present in lubricated concentrated contacts. Attention is paid to the lubrication of concentrated contacts in the mixed lubrication regime, especially the transitions from elasto-hydrodynamic lubrication (EHL) to mixed lubrication (ML) and mixed lubrication to boundary lubrication (BL).

In the introduction, chapter 1, problems are discussed with respect to friction and wear in the mixed lubrication regime. In chapter 2 an outline is given of the present knowledge with regard to mixed lubrication and the above mentioned transitions gained from experimental and theoretical developments.

Chapter 3 describes friction in concentrated contacts under conditions of EHL and BL. This as a function of the operational conditions (operational variables and element properties), under which such contacts operate. A lubrication number is derived from the parameters characteristic for friction in lubricated concentrated contacts. This lubrication number consists of the operational variables (implicit) and of the relevant element properties which determine the operational conditions under which a lubricated contact is functioning. This number is also applicable for lubricated systems operating at low pressures.

In order to study friction and the transitions as a function of this lubrication number friction measurements were carried out, as described in chapter 5. The tribometers used and the most applied testprocedure are described in chapter 4. The measured friction curves, which show the different lubrication modes EHL, ML and Bl, are obtained at different operational conditions. Transitions from one lubrication mode to the other are obtained from these friction curves (Stribeck-like) as a function of the derived lubrication number. An important phenomenon in friction of lubricated concentrated contacts is the solid-like behaviour of the lubricant at conditions of relatively high pressures and low temperatures. Also the existence of micro-EHL is shown.

The most important conclusions are analysed in chapter 6. A transition diagram is presented to determine the lubrication mode of a lubricated concentrated contact. In the discussion a comparison is made between the presented results and results known from literature.

Finally, some recommendations for further research are presented.

TRANSITIES BIJ DE SMERING VAN GECONCENTREERDE CONTACTEN.

SAMENVATTING.

Dit proefschrift handelt over de verschillende smeringsvormen aanwezig in gesmeerde geconcentreerde contacten. De aandacht gaat uit naar gemengde smering en met name de transities van elastohydrodynamische smering (EHL) naar gemengde smering (ML) en gemengde smering (ML) naar grenssmering (BL).

Als inleiding wordt in Hoofdstuk 1 het probleem gebied geschetst. De huidige kennis met betrekking tot gemengde smering en de transities is in hoofdstuk 2 uiteengezet aan de hand van experimentele en theoretische ontwikkelingen.

In Hoofdstuk 3 wordt de hedendaagse kennis besproken m.b.t. de wrijving in geconcentreerde contacten onder EHL en BL condities. Dit als funktie van de operationele condities waaronder dergelijke contacten werken. Met de variabelen die karakteristiek zijn voor de wrijving in gesmeerde geconcentreerde contacten is een smeringskental afgeleid. Dit smeringskental bevat de operationele variabelen (impliciet) en relevante elementeigenschappen welke de operationele condities bepalen waaronder dergelijke contacten functioneren. Het kental is ook toepasbaar voor gesmeerde contactsituaties waarbij lage contactdrukken heersen.

Teneinde de wrijving en de transities als funktie van dit smeringskental te onderzoeken zijn wrijvingsexperimenten uitgevoerd onder nagenoeg isotherme contactsituaties, beschreven in Hoofdstuk 5. De tribometers waarop deze metingen zijn uitgevoerd alsmede de meest gehanteerde testprocedure zijn beschreven in Hoofdstuk 4. De gemeten wrijvingscurves, waarin de smeringsvormen EHL, ML en BL te onderscheiden zijn, zijn gemeten onder verschillende operationele condities. De transities van de ene smeringsvorm naar de andere zijn bepaald, a.d.h.v. deze gemeten (Stribeck-achtige) wrijvingskrommen, als funktie van het smeringskental. Een belangrijk fenomeen dat optreed bij wrijving in gesmeerde geconcentreerde contacten is het vaste-stof gedrag van het smeermiddel onder relatief hoge drukken en lage temperaturen. Tevens blijkt dat micro-EHL op kan treden in de contacten die gevormd worden door de met elkaar interacterende ruwheden.

In Hoofdstuk 6 worden de belangrijkste conclusies geanalyseerd. Een transitie diagram is gepresenteerd waarmee de smeringvorm in een gesmeerd geconcentreerd contact kan worden bepaald. In de discussie wordt een vergelijking gemaakt met bestaande kennis uit de literatuur. Tot slot worden aanbevelingen voor verder onderzoek gegeven.

CHAPTER 1   INTRODUCTION

1.1   LUBRICATED CONTACTS

In many applications concentrated contacts can be found by which
forces, motion, etc. are transmitted from one body to another.
Examples are gears, traction drives, cam & tappet mechanisms and
roller bearings. These concentrated contacts are lubricated by a
lubricant to avoid wear and if required, to establish a low friction
between the two approaching and relatively moving surfaces. The ideal
type of lubrication occurs if these surfaces are fully separated by a
lubricant film. In that situation the properties of the lubricant
control the friction and wear is negligible. However, in many
practical situations the pressure, generated in the lubricant, is not
able to ensure a complete separation of the surfaces. The separation
is not large enough to avoid contact between the asperities of the
opposing surfaces. This occurs, for instance, at operating conditions
of low velocities and/or high normal forces and/or high temperatures.
The influence of the operating conditions on pressure generation is
demonstrated by integrating twice the Reynolds equation (2.1) for the
one-dimensional, incompressible and stationary situation, which reads:

$$\frac{dp}{dx} = 6\ \eta\ V_+\ \frac{h - h_0}{h^3}$$

$$p = \int_{-\infty}^{+\infty} 6\ \eta\ V_+\ \frac{h - h_0}{h^3}\ dx$$

(1.1)

where: p   = generated pressure.

       x   = Cartesian coordinate in the direction of motion
              of the surfaces.

       η = dynamic viscosity.

V_+ = sum velocity of the surfaces.

h = h(x), lubricant film thickness.

h_0 = integration constant: $h = h_0$ for dp/dx = 0.

Equation (1.1) shows that for the just mentioned (severe) operating conditions the generated pressure is becoming too small compared to the required pressure (applied load), when h is limited to decrease further by surface roughness. In these situations, the load applied to the system is not only transmitted from one surface to the other by pressure in the lubricant film but also by solid contact of the interacting asperities. Under even more severe operating conditions, the load will be transmitted entirely by asperity interactions. Fortunately, in practice surfaces are covered with protecting boundary layers, which then mainly control friction and wear. If these boundary layers are not present or not able to avoid direct contact between one surface and the other then dry friction occurs at these asperity interfaces. Wear will be high in these situations.

The following three modes of lubrication can be expected in a lubricated concentrated contact (LCC)[*].

Firstly, complete separation of the surfaces by a lubricant, as shown in fig. 1.1[a]. The applied load is transmitted by the pressure in the lubricant and all shear caused by the relatively moving surfaces takes place in the lubricant. In general, this is referred to as hydrodynamic lubrication (HL). Since in many contact situations the pressure in the film is relatively low, hence, with the presence of a high elasticity modulus, the elastic deformation of the surfaces will be negligible. The film shape will then be determined by the geometry of the surfaces. In the case of concentrated contacts where the pressures are high, or when using materials with a low elasticity modulus, the elastic deformation of the surfaces becomes significant with respect to film shape and pressure distribution. Hydrodynamic

[*]note: In the next chapters the abbreviations, introduced in this chapter will be used as much as possible.

lubrication (HL) with elastically deformable surfaces, such as in lubricated concentrated contacts, is referred to as elasto hydrodynamic lubrication (EHL).

Secondly, the applied load is fully transmitted by the interacting asperities, fig. 1.1[b]. In that case shear is determined by the following contact situations i.e., A: Boundary layers (mainly) protect the two surfaces; shear takes place in the boundary layers or at the interface of these boundary layers. This lubrication mode is known as boundary lubrication (BL), B: Direct contact between the interacting asperities predominates and dry friction (DF) occurs. Shear takes place at the interface or in the weaker asperities, leading to material transfer from one surface to the other, C: A combination of boundary lubrication (BL) and dry friction (DF) occurs between the interacting asperities.
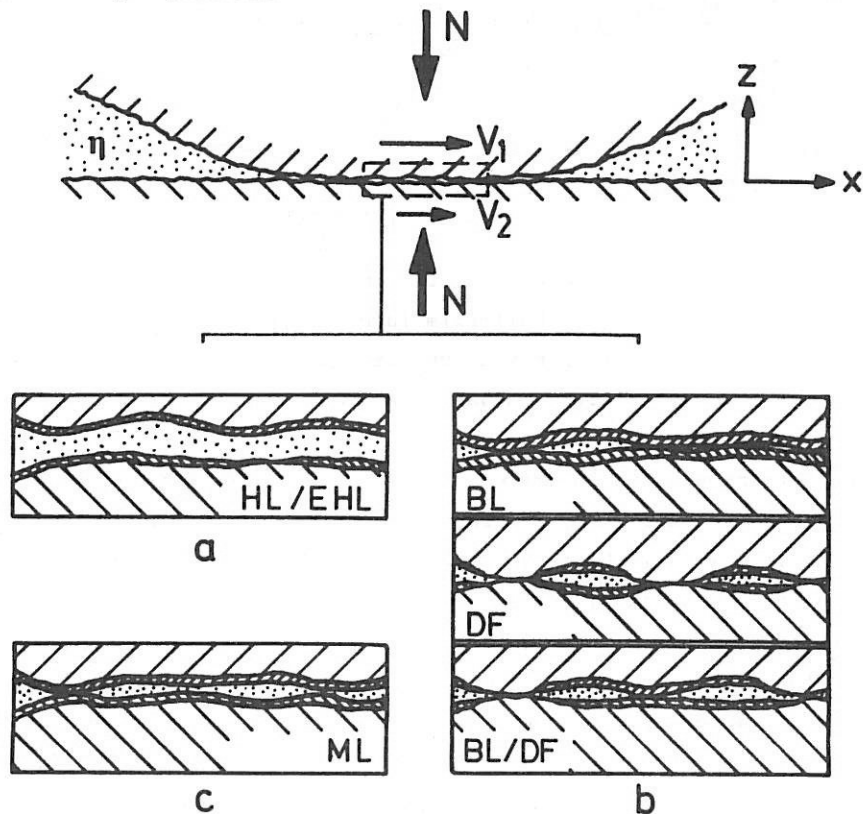
Fig. 1.1: Lubrication modes.

Thirdly, the intermediate stage between boundary lubrication/dry friction and (elasto) hydrodynamic lubrication, were the applied load is both carried by the interacting asperities and the pressure in the lubricant film, fig. 1.1^C. This lubrication mode is referred to as mixed lubrication (ML).

Each lubrication mode has its own characteristic frictional behaviour, which can be represented in the generalized Stribeck curve, as shown in fig. 1.2.
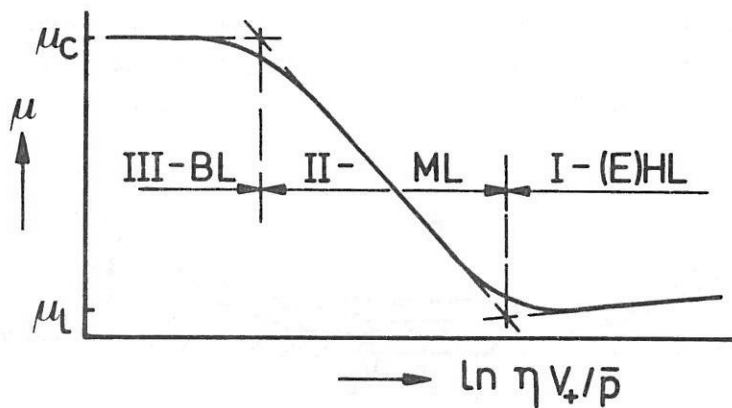
Fig. 1.2: Generalized Stribeck curve.

    I : Full-film lubrication (E)HL

    II : Mixed lubrication ML

    III: Boundary lubrication BL

The ordinate represents the value of the coefficient of friction $\mu = F/N$. The abscissa depicts the logarithm of $\eta \cdot V_+/\bar{p}$, in which η is the lubricant viscosity in Pa.s, V_+ the sum velocity in m/s and $\bar{p}$ the mean pressure in the contact in Pa.

The work in this thesis will be specially focused on the mixed lubrication regime and on the transitions from this regime to the neighbouring modes of contact.

Wear, the unwanted removal of material from the rubbing surfaces, usually shows a corresponding behaviour; i.e. at high values of $\eta \cdot V_+/\bar{p}$ wear becomes negligible but under more severe operating conditions (low values of $\eta \cdot V_+/\bar{p}$) wear can become very high.

Friction and wear are important tribological properties with respect to the functional behaviour of lubricated concentrated contacts. These two variables determine whether a lubricated concentrated contact fails or not. In principle, failure will take place when the contact no longer fulfills the function for which it was designed. The most common failure situation is that of high friction (energy losses) and/or high wear (damage of the surfaces).

For LCC's a failure transition diagram has been established by the International Research Group on Wear of Engineering Materials (IRG). This IRG-transition diagram, de Gee et al.(1984)[*], defines the lubrication conditions of LCC's as a function of the normal force N and sliding velocity V_. It shows three regions which are separated by two transition curves, as shown in figure 1.3. Region I, II and III are identified by the coefficient of friction in time and wear characteristics as present in the different regions.
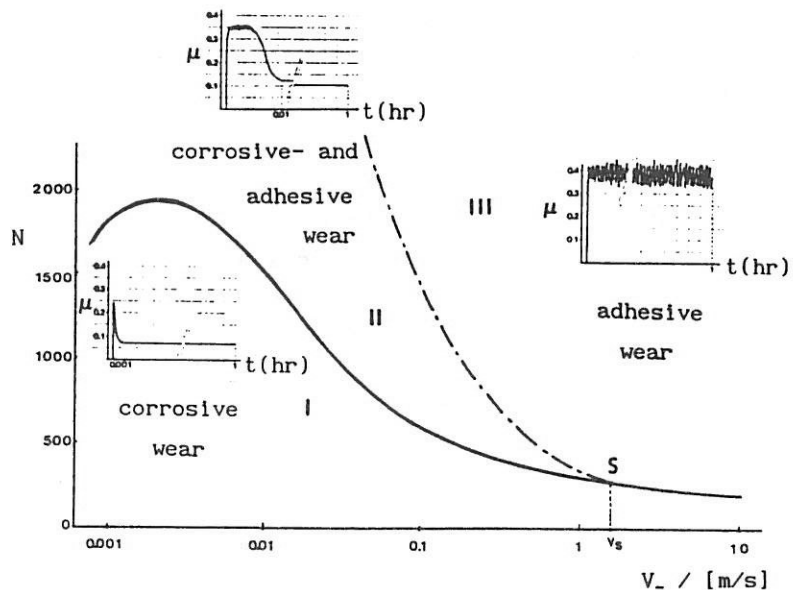
Fig. 1.3 : IRG-transition diagram for LCC's.
Reproduced from the Gee et al.(1984).

[*] Literature is listed in appendix G.

In region I, an LCC operates in the lubrication modes as presented in figure 1.2. Once the LCC operates in region III, failure by adhesive wear takes place. Region II is an intermediate region where oxidation of the surfaces prevent total destruction by adhesive wear and BL prevails.

However, a lubricated concentrated contact can also fail if wear is virtually absent and the induced friction is too low, for instance in a traction drive. This failure description is called the functional failure of a tribosystem, Czichos (1974[c], 1978). Thus, a lubricated concentrated contact not only fails when "severe" wear take place, on which some failure criteria have been build, Blok (1937), Matveevsky (1965), Ku (1978[a,b]), etc., but it can fail in every lubrication mode.

Difficulties arise when one wants to estimate friction and wear or make a prediction about failure for these lubrication modes, in which contact takes place between the opposing surfaces.

For (elasto) hydrodynamic lubrication, prediction of friction on the basis of a theoretical model is sufficiently established. Prediction of friction for the boundary lubricated contact situation relies on data from experiments. In fact, prediction of friction for mixed- and boundary lubrication is still in its infancy.

Friction in the mixed lubrication regime is a combination of friction arising at the asperity interfaces and friction caused by shearing the lubricant film in the rest of the contact region.

For friction and normal force can be written[**]:

$$F = F_c + F_l$$

$$N = N_c + N_l$$

(1.2)

[**] Nomenclature is given in appendix A.

If the next relationship is assumed to be valid at the interfaces, for all asperity contacts:

$$\bar{\mu}_c = F_c/N_c \qquad (1.3)$$

and for the lubricant:

$$\bar{\mu}_l = F_l/N_l \qquad (1.4)$$

then, the following simplified equations can be given for the coefficient of friction in the mixed lubrication regime.

$$\bar{\mu} = \bar{\mu}_c + (\bar{\mu}_l - \bar{\mu}_c) \cdot N_l/N$$

$$\qquad (1.5)$$

$$\text{or} \qquad \bar{\mu} = \bar{\mu}_l + (\bar{\mu}_c - \bar{\mu}_l) \cdot N_c/N$$

This equation is often proposed and used in literature, Altrogge (1950), Blok (1963), etc. The main disadvantage of this equation is that, at the moment, no relation is available, which estimates the part of the load carried by the pressure in the lubricant, N_l, or that by asperity contacts, N_c, as a function of the operating variables, i.e. normal force N, velocity V and temperature θ and element properties like roughness. Frequently, even the lubrication mode of a particular concentrated contact as a function of the operating conditions is unknown. Known is only that at the boundaries of the mixed lubrication regime N_c or N_l is equal to N. The value of μ_l depends on the operational variables valid for the lubricant, while μ_c is mainly determined by the shear strength of the formed surface layers, which is generally also unknown.

The next problem is wear, which can be divided into four basic mechanisms, i.e., surface fatigue, abrasive-, corrosive- and adhesive wear, Burwell (1957). The more a concentrated contact approaches or enters the mixed lubrication regime, the more one can expect any of these wear mechanisms to occur. Apart from some empirical relations, the knowledge in predicting wear is still virtually absent.

1.8

Summarizing: "When a lubricated concentrated contact is operating in the mixed- or boundary lubrication regime, friction and wear are largely unpredictable".

1.2   AIM OF THE PRESENT INVESTIGATION

In the previous section it was indicated in which lubrication mode a lubricated concentrated contact can operate and what are the consequences for friction and wear.

It is necessary to know the behaviour of friction and wear in these lubrication modes. Only then it is possible to improve the reliability of predictions with regard to the failure of lubricated concentrated contacts. Friction and wear are very complicated phenomena and the desire to solve this problem at once would be too ambitious, the number of variables involved are enormous. For an engineer, it would already be an advantage if, (s)he could predict in advance in which lubrication mode a particular lubricated concentrated contact will operate and which measures can be taken in that situation to reduce the risk of functional failure to a minimum.

The aim of this investigation is twofold;
Firstly, to carry out a study of the frictional behaviour of a lubricated concentrated contact in the different lubrication modes, in particular the mixed lubrication regime.
Secondly, to locate the transitions between the different modes of lubrication for lubricated concentrated contacts and represent them by numbers.
With the obtained numbers it is then possible to discriminate the modes of lubrication and, with the variables which are involved in these numbers, which measures have to be taken to avoid a specific unwanted lubrication mode. The results of this work are applicable to region I of the IRG-transition diagram.

To study these transitions, i.e. from elastohydrodynamic lubrication to mixed lubrication and from mixed lubrication to boundary lubrication, the generalized Stribeck curve will be used as a guide.

CHAPTER 2   MIXED LUBRICATION : A RETROSPECTIVE VIEW

2.1   INTRODUCTION

Previous work with regard to ML can in general be divided into two parts. Firstly, ML under conditions of relatively low pressures as in HL. Secondly, ML under conditions of high pressures, as present in EHL- contacts. The essential difference between these two conditions is the influence of the elastic deformation of the surfaces and the behaviour of the lubricant under conditions of high pressures. This thesis also treats ML at low pressures, because it will be assumed that the frictional features of the micro-contacts formed by asperity interaction, are virtually independent of the macroscopic contact conditions.

The following sections describe previously published experimental and theoretical work on ML, both under HL and EHL conditions.

2.2   MIXED LUBRICATION EXPERIMENTS AT LOW AND HIGH PRESSURES

2.2.1   Low pressures

In 1902 Stribeck published a series of articles concerning measurements of friction on journal bearings as a function of load, velocity and temperature. These measurements showed a transition from the HL- to the ML regime. Biel (1920) concluded from his own work and that of Stribeck that this transition, as characterized by the position of the minimum coefficient of friction, is controlled by the product of viscosity and sliding velocity. McKee (1927) used the relation $Z \cdot n / p_{proj.}$ to characterize the transition from HL to ML. ($Z \cdot n / p_{proj.}$ is the product of Z, viscosity in cP, with n, the number of revolutions per minute of the shaft divided by $p_{proj.}$, the load per unit projected area, lbs/inch^2). This parameter was proposed by Hersey (1915) to describe the frictional behaviour of journal bearings. McKee

showed that running-in of journal bearings has two effects on the transition HL-ML, i.e., the position of the minimum coefficient of friction shifts to lower values of $Z \cdot n / p_{proj}$. and the value of this minimum coefficient of friction decreases. Until now, in many books and published papers, this number $Z \cdot n / p_{proj}$. or $Z \cdot \omega / p_{proj}$. is still in use, where ω is the angular velocity in radians per second.

a.

DETAILED OBSERVATIONS AT THE LOWER VALUES OF ZN/P; $C/D = 1,450$
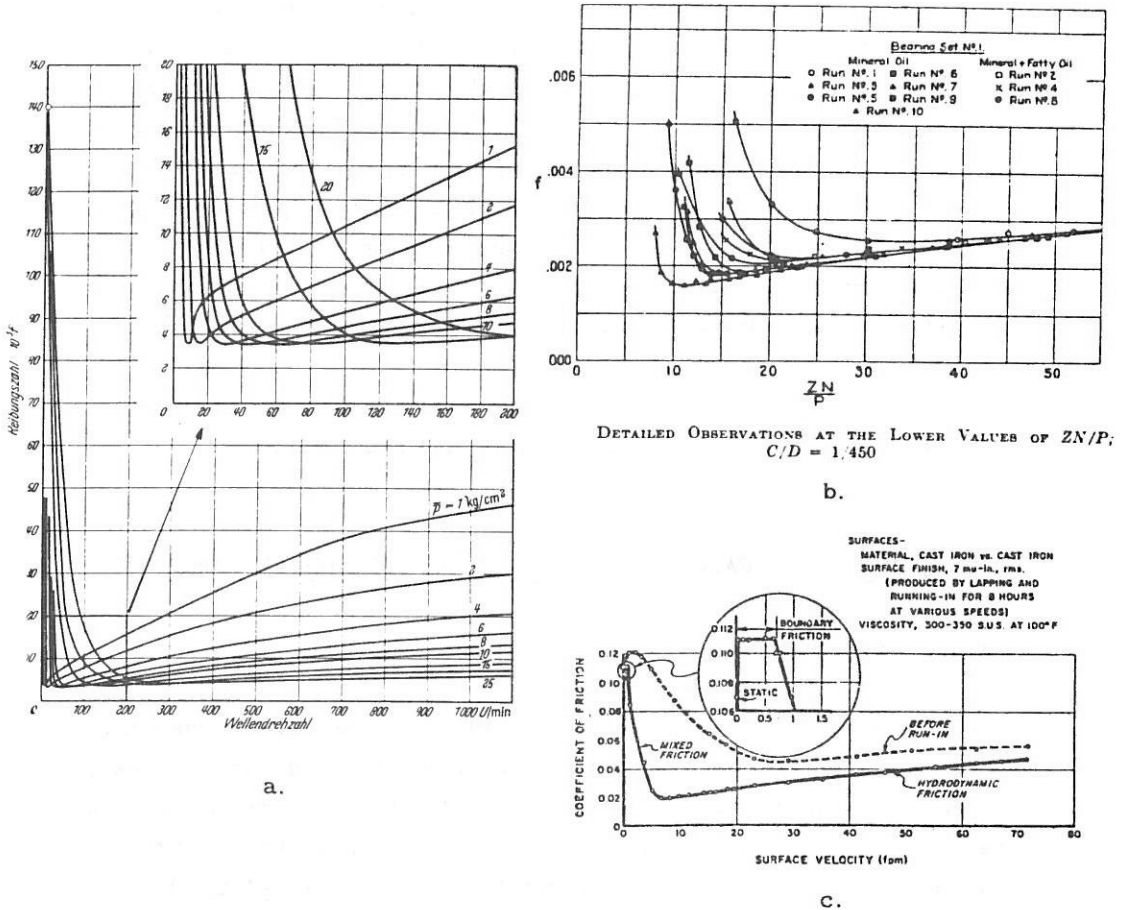
b.

c.

Fig. 2.1: Friction curves by:

a — Stribeck (1902)

b — McKee (1927)

c — Lenning (1960)

Altrogge (1950) measured the hydrodynamic pressure in the ML regime. These measurements showed that a pressure generation is present in the lubricant film until the BL regime is reached. He also found that the ratio $\omega/p_{proj.}$ is nearly constant for the position of the minimum coefficient of friction and that surface roughness has a significant influence on the value of the minimum coefficient of friction. With increasing surface roughness, μ_{min} obtains higher values and it shifts to higher transition velocities. This agrees with McKee's results. The results of Vogelpohl (1954, 1958) show a transition from HL to ML for $\eta \cdot V/p_{proj.}$-values of appr. $6 \cdot 10^{-9}$ to $9 \cdot 10^{-9}$ (m). Also, instead of the number $Z \cdot n/p_{proj.}$, the "Sommerfeld Number" was used which is equal to $Z \cdot n/(p_{proj.} \cdot \phi^2)$, where ϕ is the clearance-diameter ratio. However, no improvement was realized, i.e., to fit all the "Stribeck like" curves (measured at different conditions) into one master curve. Based on previous work of Vogelpohl (1958), Herrebrugh (1968) and Spiegel (1973), de Gee (1976, 1988) related the value of $\eta \cdot \omega/p_{proj.}$, at which the first asperity interactions occur, to the elastic deformation of the contacting surfaces, the bearing clearance ΔR and a "critical roughness measure" R_λ respectively. The above results were all carried out at journal bearings. For this reason, the speed n in rpm or ω in rad/s is used as a characteristic variable. From a hydrodynamic point of view, not n nor ω but the sum velocity V_+ is the important variable with relation to friction and the transition from HL to ML.

Stribeck-like curves have also been measured at flat sliding surfaces such as thrust bearings, seals, etc. The same features for the transition HL-ML as with journal bearings were found. In these experiments the sliding velocity is the common parameter. As a dimensionless number, $\eta \cdot V_-/W$ is used, in which W is the normal force per unit of length. Lenning (1960) investigated the transition ML to BL for flat sliding thrust bearings. He found that the transition velocity, characterizing the transition from ML to BL, is greatly reduced with increasing viscosity. The transition velocity also reduces with reducing surface roughness. The use of polar additives does not affect the transition from ML to BL. Only the value of the coefficient of friction in the BL-regime, μ_{BL}, reduces with it. μ_{BL} is only slightly affected by surface finish. In fact, these experiments confirm Altrogge's (1950) findings i.e. the presence of pressure

generation in the ML regime and, due to this, the enormous influence of viscosity and velocity on this transition. Hata et al. (1980) studied the transition from HL to ML for flat sliding thrust bearings with different loads, i.e., pressures of $1.4 \cdot 10^4$ to $2.7 \cdot 10^4$ Pa. These measurements show that the transition HL-ML is controlled by the product of viscosity and velocity.

Summarizing, Stribeck curves measured at low pressures show the following characteristic features. A low coefficient of friction in the HL regime, decreasing to a minimum of appr. $2 \cdot 10^{-3}$ with decreasing "Load"-parameter. Then it rises steeply to a constant value of roughly 0.15, the BL regime. The steep rise represents the area of mixed lubrication. Viscosity and velocity play an important role in the transitions HL-ML and ML-BL. Roughness results in a shift of the transitions to higher values of the "Load" parameters with increasing surface roughness. Typically for most of the published results concerning ML is that usually no roughness values are given. Because of the low coefficient of friction in the HL regime, in many calculations μ_l is neglected in estimating N_l or N_c with the measured μ.

Apart from these publications not many more relevant experimental contributions to ML under HL conditions can be found in literature. After the "fifties" some more theoretical work became available, see section 2.3.

2.2.2 High pressures

Smith (1958/1959) studied lubricant behaviour between a sphere and a cylinder under high pressures. These experiments also include measurements of the transition from EHL to ML for smooth and rough surfaces. When the roughness increases, the transition shifts to higher transition velocities. Furey (1962, 1963) studied the influence of viscosity and roughness on friction in sliding LCC's. From these experiments the conclusion can be drawn that the transition from ML to BL is controlled by viscosity and that, with increasing contact pressure at constant sliding velocity, this transition occurs at lower values of the surface roughness. Also, these experiments show that surface roughness has almost no effect on the coefficient of friction

in the BL regime. Tallian and coworkers (1965) pointed out that the ratio of film thickness and combined surface roughness is a correct parameter for describing the operating severity of LCC's. A good relationship between this parameter and the failure of these concentrated contacts by pitting was also found. This parameter, h/σ_t, is generally used nowadays. Niemann and Gartner (1966) measured the hydrodynamic film pressure in the mixed lubrication regime between two cylinders. From this the normal force transmitted by the lubricant was calculated, as Altrogge did in 1950. Poon and Haines (1966/1967) measured the transition from EHL- to the ML regime at a "sphere and cylinder combination". They separated the ML regime into two regions, i.e., the secondary- and primary transition region.
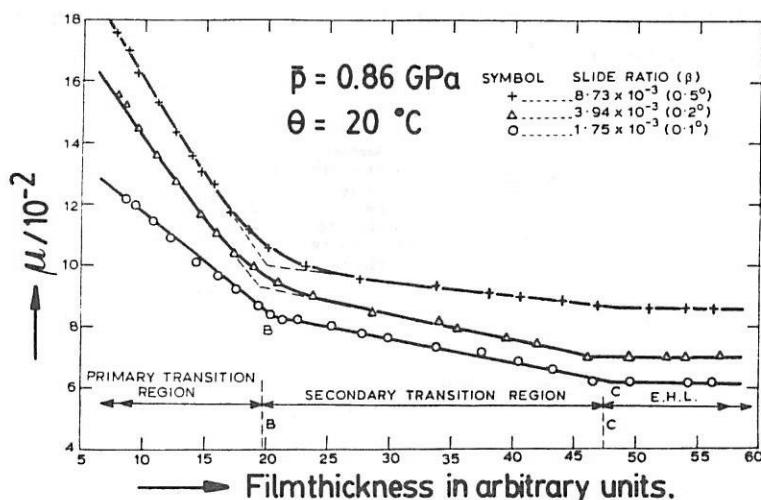
Fig. 2.2: The primary- and secondary transition region according to Poon and Haines (1966/1967). Note: Horizontal, film thickness in arbitrary units.

With measurements of the electrical conductivity they proved that asperity contact takes place in the primary- as well as in the secondary region. It turned out that friction is inversely proportional to the calculated lubricant film thickness. The transition from EHL to the secondary region occurred at values of λ = 2.0 - 2.4 and from the secondary- to the primary region at values of λ = 1.0 - 1.2. With $\lambda = h/\sigma_t$, where h is the calculated average film

thickness and σ_t is the combined RMS roughness of the two surfaces, σ_t = $(\sigma_1{}^2 + \sigma_2{}^2)^{1/2}$. Dowson and Whomes (1967/1968) used the peak to valley roughness divided by the theoretically calculated minimum film thickness as a parameter. This parameter was used to show its significance in forecasting the number of cycles before pitting failure to occur. These measurements show that the transition from EHL to ML shifts to higher values of this parameter, or to lower values of λ, with increasing pressure. Bair and Winer (1982) found that for values of λ, less then appr. 2 the LCC moves from the EHL- to the ML-regime. This transition is represented by plotting the reduced friction coefficient against the logarithm of lambda, see figure 2.3. The reduced friction coefficient is equal to the measured coefficient of friction divided by the ratio of limiting shear stress of the lubricant and pressure, τ_l/p.
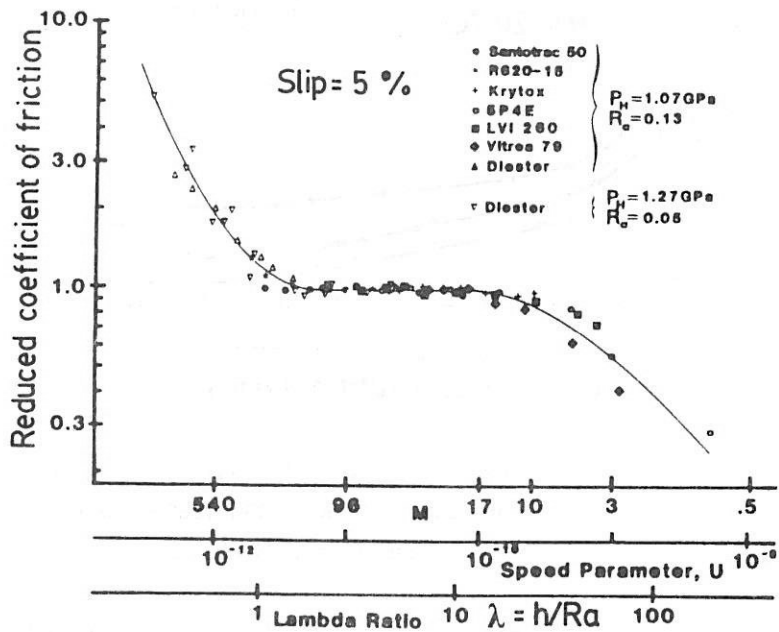

Fig. 2.3: Reproduced from Bair and Winer (1982). Reduced friction coefficient as a function of λ, M and U.

Recently, Evans and Johnson (1987) studied the effects of roughness on elastohydrodynamic friction. It was shown that for lambda values

between 0.5 and 6 the effect of asperity interaction on friction is still governed by the bulk rheological properties of the oil, at a pressure corresponding to the calculated mean contact pressure at the interacting asperities. For lambda values less then appr. 0.5 it is to be expected that boundary lubrication prevails at the asperity interactions.

Summarizing, in EHL the common parameter to express the severity of the operational conditions under which an LCC is functioning is the ratio h/σ_t. Physically, this parameter relates the film thickness to the combined roughness of the surfaces. When the calculated lubricant film thickness becomes comparable to the height of the surface asperities, contact between the surfaces is to be expected. For $h/\sigma_t>3$ full-film lubrication will occur and for values of $h/\sigma_t<3$ ML can be expected. At h/σ_t ratios of 0.5 or less, BL prevails.

The value of h/σ_t in the ML-regime is somewhat doubtful for two reasons. Firstly, the calculated film thickness is based on the smooth surface theory and will not be valid in the ML-regime. Secondly, the actual roughness at high pressures, i.e. at deformed surfaces, is not really known.

2.3   THEORETICAL WORK

The hydrodynamic action of the lubricant between two smooth solid surfaces is described by the Reynolds equation (1886):

$$\frac{\partial}{\partial x}\left[\frac{\rho h^3}{\eta}\frac{\partial p}{\partial x}\right] + \frac{\partial}{\partial y}\left[\frac{\rho h^3}{\eta}\frac{\partial p}{\partial y}\right] = 6\ V_+\frac{\partial}{\partial x}(\rho h) + 12\frac{\partial}{\partial t}(\rho h) \qquad (2.1)$$

where   p   = hydrodynamic pressure across the film thickness.

   x   = Cartesian coordinate in the direction of motion of
         the surfaces, considered as almost parallel.

   y   = Cartesian coordinate perpendicular to x.

   h   = thickness of the lubricant film.

   η = dynamic viscosity of the lubricant.

ρ = density.

V_+ = sum velocity of the moving surfaces.

t = time.

In the stationary situation the last term in (2.1) disappears.

In the last two decades many studies were made to understand the effect of roughness on hydrodynamics in HL- and EHL-contacts. The Reynolds equation is therefore combined with a deterministic- or a statistical description of the micro-geometry.

Initiated by Michell (1950) and Tzeng and Saibel (1967), who pointed out the importance of roughness with relation to lubrication in journal bearings, many investigators tried to formulate a modified Reynolds equation, including the effects of the micro-geometry. Besides roughness effects on pressure and film thickness, also the consequence of roughness on friction could then be obtained. A statistical description of rough surfaces in combination with the Reynolds equation is studied by Christensen (1971), Tonder and Christensen (1972), Christensen and Tonder (1973) and Tonder (1977[a,b]). They gave modified Reynolds equations for longitudinal-, transversal- and for two dimensionally oriented roughness. A high summit density is assumed.

Longitudinal roughness:

$$\frac{\partial}{\partial x} \left\{ E(H^3) \ \frac{\partial \overline{p}}{\partial x} \right\} + \frac{\partial}{\partial y} \left\{ \frac{1}{E(1/H^3)} \ \frac{\partial \overline{p}}{\partial y} \right\} = 6 \ \eta \ V_+ \ \frac{\partial}{\partial x} \ E(H) \qquad (2.2)$$

Transverse roughness:

$$\frac{\partial}{\partial x} \left\{ \frac{1}{E(1/H^3)} \ \frac{\partial \overline{p}}{\partial x} \right\} + \frac{\partial}{\partial y} \left\{ E(H^3) \ \frac{\partial \overline{p}}{\partial y} \right\} = 6 \ \eta \ V_+ \ \frac{\partial}{\partial x} \ \frac{E(1/H^2)}{E(1/H^3)} \qquad (2.3)$$

Two-dimensional roughness:

$$\frac{\partial}{\partial x} \left\{ E(H^3) \ \frac{\partial \overline{p}}{\partial x} \right\} + \frac{\partial}{\partial y} \left\{ E(H^3) \ \frac{\partial \overline{p}}{\partial y} \right\} = 6 \ \eta \ V_+ \frac{\partial}{\partial x} \ E(H) \qquad (2.4)$$

where: - E ( ) is the expectancy operator defined by:

$$E \ (H^n) = \int\limits_{-\infty}^{+\infty} H^n \ f \ (\ \delta \ ) \ d\delta \qquad (2.5)$$

- H is the film thickness defined by $H = h + \delta$. h denotes the nominal, smooth part of the film geometry while δ is the part due to the surface roughness as measured from the nominal level.
- $\overline{p}$ the expectation of the pressure.

These equations are valid for a stationary rough and a moving smooth surface. Elrod (1973) studied surfaces possessing striated roughness or grooving and made a distinction between "Reynolds roughness" and "Stokes roughness". If Δ is the mean wavelength of the roughness and h the film thickness then, for $\Delta/h \gg 1$, the Reynolds equation may be applied and for $\Delta/h \ll 1$ the Stokes equations should be used. Berthe and Godet (1973) derived a complicated modified time dependent Reynolds equation for rough moving surfaces. This equation should be used instead of the classical Reynolds equation when the surface profiles and the velocity envelope are not identical. However, the equation which they propose is not valid for two rough moving surfaces. Chow and Cheng (1976) studied the effect of surface roughness (rigid) on the average film thickness. They rewrote the time dependent term in the Reynolds equation, which is caused by the relative moving asperities, into a stationary one. Sun and Chen (1977) applied the Stokes equations to surfaces with transverse roughness and concluded that if Δ/h equals appr. 1, the difference between the calculated friction and the load capacity is large compared with the results obtained with the Reynolds equation. Elrod (1977) did the same study only with a sinusoidal roughness. His results are not so

dramatic as those reported by Sun and Chen (1977). Patir and Cheng (1978, 1979) introduced the flow-factor method. To the Reynolds equation are added pressure flow-factors (ϕ_x, ϕ_y) and a shear flow-factor (ϕ_s). They define the flow as follows:

$$\bar{q}_x = - \phi_x \frac{h^3}{12\eta} \frac{\partial \bar{p}}{\partial x} + \frac{V_+}{2} \bar{h}_t + \frac{V_-}{2} \sigma_t \phi_s \qquad (2.6)$$

$$\bar{q}_y = - \phi_y \frac{h^3}{12\eta} \frac{\partial \bar{p}}{\partial y} \qquad (2.7)$$

where $h_t = h + \delta_1 + \delta_2$, h is the nominal film thickness and δ_1, δ_2 are roughness amplitudes of the surfaces measured from their mean levels.

σ_t = is the standard deviation of the combined roughness δ.

Substitution of (2.6) and (2.7) in the mean flow balance $\partial \bar{q}_x / \partial x + \partial \bar{q}_y / \partial y = - \partial \bar{h}_t / \partial t$ gives the next modified Reynolds equation:

$$\frac{\partial}{\partial x} \left[\phi_x \frac{h^3}{12\eta} \frac{\partial \bar{p}}{\partial x} \right] + \frac{\partial}{\partial y} \left[\phi_y \frac{h^3}{12\eta} \frac{\partial \bar{p}}{\partial y} \right] = \frac{V_+}{2} \frac{\partial h_t}{\partial x} + \frac{V_-}{2} \sigma_t \frac{\partial \phi_s}{\partial x} + \frac{\partial \bar{h}_t}{\partial t} \qquad (2.8)$$

These flow-factors are obtained by numerical flow simulation with a randomly generated roughness for a finite rectangular bearing element. ϕ_x, ϕ_y and ϕ_s are dependent on the nominal film thickness/combined RMS ratio and a surface texture parameter γ, defined as the ratio of x and y correlation lengths of the combined roughness. The results with relation to hydrodynamic action, frictional- and load carrying behaviour are in agreement with those of earlier published investigations. However, for low values of h/σ_t, say less than 1, the calculations become invalid.

Elrod (1979), Tonder (1980[a, b]), Teale and Lebeck (1980) and Tripp (1983) discuss the flow-factor method. However, they all find significant differences with regard to the magnitude of the flow factors for values of $h/\sigma_t < 3$. This is caused by numerical aspects, e.g. the boundary conditions chosen at the rectangular bearing element

and the number of points for describing the micro geometry.

Phan-Thien (1981[a,b]) studied roughness effects in hydrodynamic lubrication by using a perturbation expansion in the Stokes- and modified Reynolds equation. He found that, depending on the value of the product of the frequency of the corrugations and the mean film thickness (say > 1.9) the difference in load capacity between Stokes and Reynolds becomes significant and concludes that Reynolds is inadequate for these situations. Bush, et al. (1984) also used a perturbation approach to study the effects of roughness on friction and load capacity and included deformation of the geometry. The results are valid for values of $h/\sigma_t > 3$, i.e., no contact between the surfaces was assumed. The results are similar to those predicted by Patir and Cheng. The effect of deformable asperities has already received some attention in the past. Fein and Kreuz (1968) gave an analysis of a single elastic asperity sliding along a smooth rigid plane. Fowles (1969,1971[a,b]) firstly studied the collision between two asperities, each attached to rigid plane surfaces. Later, Fowles (1975) applied statistics to a model describing many colliding pairs of asperities. The calculated coefficient of friction, however, was much higher than the experimental results. Goglia et al. (1984[a,b]) presented an analysis for single irregularities and wavy surfaces in sliding line contacts. Recently, Lubrecht (1987) calculated the influence of longitudinal- and transversal sinusoidal roughness and a single isotropic bump on film thickness and pressure in a circular EHL contact. The stationary Reynolds equation was solved by using the multi-grid method. It is seen that all the EHL-features, pressure- and film shape, are also present in the asperity contacts.

The above mentioned studies provided some insight into the effects of roughness on the hydrodynamic action and its consequences for the friction. However, a complete analysis to calculate the friction in the ML-regime is still not available. Two serious attempts have been made to separate the normal force into the hydrodynamic part and that transmitted by interacting asperities, as a function of the operating conditions.

Johnson, et al. (1972) investigated the behaviour of an LCC in situations where most of the load is carried by the lubricant film. They considered a ML contact as a combination of non-linear springs.

2.12

The bulk deformation of the two solids is represented by a spring, connected in series with two parallel springs representing the stiffness of the interacting asperities and the lubricant film respectively. The stiffness of these non-linear springs is governed by well established theories, i.e. the Hertzian (1881) theory for the deformation of the solids, while the spring, representing the interacting asperities, is characterized by the theory of dry contact of rough surfaces developed by Greenwood and Williamson (1966). The stiffness of the lubricant film is obtained from the elastohydrodynamic theory of smooth surfaces by Dowson and Higginson (1966). In figure 2.4 the relation between $\bar{h}/\sigma$ and d_e/σ for the lubricant film- and asperity pressure respectively is shown. In this figure $\bar{h}/\sigma \sim d_e/\sigma$, where $\bar{h}$ or d_e is the mean separation of the surfaces, while h_0 is the film thickness which would be obtained assuming smooth surfaces under the same operating conditions.
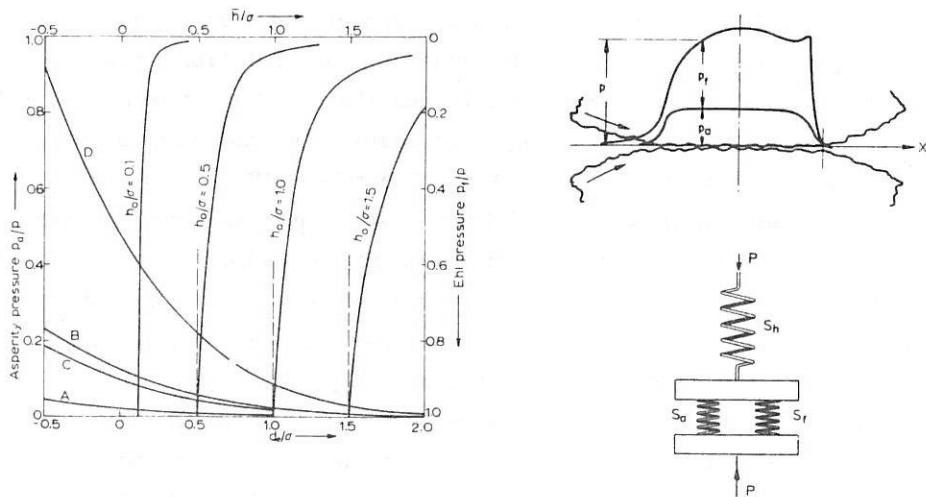

Fig. 2.4: Reproduced from Johnson et al. (1972).

A: $\sigma = 5 \cdot 10^{-8}$ m, $E_*/p = 660$. B: $\sigma = 5 \cdot 10^{-8}$ m, $E_*/p = 170$.
C: $\sigma = 25 \cdot 10^{-8}$ m, $E_*/p = 660$. D: $\sigma = 25 \cdot 10^{-8}$ m, $E_*/p = 170$.

It is found that;
- the lubricant film is very stiff compared to the asperities,

provided that the lubricant film carries an appreciable portion of the load.
- the mean separation of the surfaces is approximately equal to the film thickness which would be obtained assuming smooth surfaces.

Oh (1984, 1985) formulated the ML problem as a generalized non-linear complementary problem, i.e., the pressure acting on the load bearing surface is taken as the unknown and the lubricant flow and the gap between the surfaces are taken as its compliments. For an elastic deformable journal bearing the results of this method have been demonstrated.
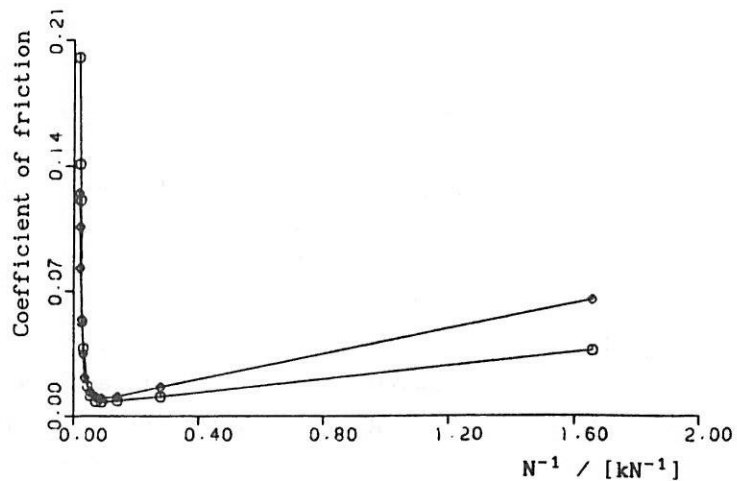

Fig. 2.5: Reproduced from Oh K.P. (1985).
O: n = 2000 r/min and ◊: n = 4000 r/min.

The solution of this method, however, strongly depends on the value of the permissible error used as criterion to decide if a local contact occurs or not.

2.4   SUMMARY

Literature shows that, in principle, two numbers are used to characterize the transition from full-film lubrication to mixed lubrication under HL- and EHL conditions. In HL the number $\eta \cdot \omega/p_{proj.}$, or rather $\eta \cdot V_+/\bar{p}$, is usual and for EHL conditions h/σ_t is commonly used. The essential difference between the numbers is that at HL the roughness is not taken into account.

In fact, there is not much difference between the use of h or $\eta \cdot V_+/\bar{p}$. In the case of EHL the relation between h and $\eta \cdot V_+/\bar{p}$ is (see section 3.4.4):

$$h \therefore c \cdot (\eta \cdot V_+/\bar{p})^{0.7} \tag{2.9}$$

Thus, $\eta \cdot V_+/(\bar{p} \cdot \sigma_t)$ might well be a suitable number for use under EHL conditions.

Experiments showed that viscosity, velocity and roughness are important parameters throughout the whole ML region.

Theoretical work with relation to ML resulted in modified Reynolds equations, (2.2) to (2.4) and (2.8) of Christensen et al. and Patir and Cheng respectively, which are now commonly in use for describing roughness effects on hydrodynamics. These theoretical investigations provide some qualitative insights of roughness effects on the hydrodynamic action. Isotropic roughness hardly affects the film thickness near the transition EHL-ML. On the other hand longitudinal- and transversal roughness decreases, respectively increases the film thickness. In general, friction near the EHL-ML transition increases with roughness. However, quantitative results differ between different authors.

Up to date, calculations concerning roughness effects on hydrodynamics are still doubtful due to numerical- and boundary aspects. The main problem in calculating a two-dimensional rough contact situation is calculation time. The necessary number of nodal points to accurately describe the problem numerically is enormous. Multigrid could provide a possible solution to this problem in future. However, at the moment the method is not powerful enough.

Applicability of the Reynolds equation becomes more and more doubtful

when the film thickness approaches the value of the surface roughness, especially when the slopes of the latter are relatively large. Another problem, arising with the use of the Reynolds- or Stokes equation and deformable roughness is that, theoretically, no contact can ever take place between the opposing surfaces. The criterion used for the minimum allowed local separation for (elasto) hydrodynamic lubrication determines the number of solid to solid contacts and with that the magnitude of the friction.

In this chapter friction and in particular the transitions have been studied. In the following chapter friction in the lubrication modes EHL, ML and BL will be outlined.

CHAPTER 3   LUBRICATION MODES

3.1   INTRODUCTION

All frictional features which are typical for an EHL contact are
expected to diminish slowly when an LCC enters more and more into the
ML regime. The more the BL regime is reached the more the frictional
behaviour of the LCC will be controlled by processes present in BL
contact situations. The next sections briefly outline the present
knowledge of EHL- and BL contact situations. It goes too far to
consider all aspects concerning EHL and BL; therefore, attention is
paid only to the frictional behaviour in these lubrication modes.

3.2   ELASTO HYDRODYNAMIC LUBRICATION

3.2.1   Introduction

Elastohydrodynamic lubrication is a relatively new topic in
tribology. The progress in theoretical and experimental knowledge
obtained in the last 30 years is significant. Most attention has been
paid to calculations concerning film thickness and pressure
distribution in a lubricated concentrated contact. The present
knowledge concerning prediction of friction in EHL-contacts is in a
state that can be called reasonable.

Many investigators have tried to understand how gear teeth could be
hydrodynamically lubricated, since the film thickness as calculated
with the classical hydrodynamic lubrication theory, was far to small
for a complete separation of the surfaces, when compared with the
surface roughness of the gear teeth. Grubin (1949) - also the name
Ertel (1939) is mentioned - recognized that both the elastic
deformation of the mating solids and the increase of the viscosity

with pressure were the answer to the question why highly loaded
contacts could be separated by a lubricant film. Grubin assumed in his
film thickness calculation that the shape of the gap between the
solids was Hertzian, see appendix C. He integrated the Reynolds
equation to determinate the separation of the Hertzian flats which
would allow the pressure to rise to infinity at the inlet to the
Hertzian zone. The calculated film thickness was one to two orders of
magnitude larger then the previously calculated film thicknesses.
However, no information about the film shape and pressure distribution
throughout the contact zone is found in this way. Petrusevich (1951),
Dowson & Higginson (1959) and later many others used numerical
procedures to obtain solutions for the whole EHL contact, by
simultaneously solving the equation for elastic deformation and the
Reynolds equation for hydrodynamic lubrication. Recently, Lubrecht
(1987) did the same for both line- and circular contacts using the
Multi-grid method. From these studies, detailed information about film
shape and pressure distribution became available. In figure 3.1 the
characteristic film shape and the pressure distribution in an EHL
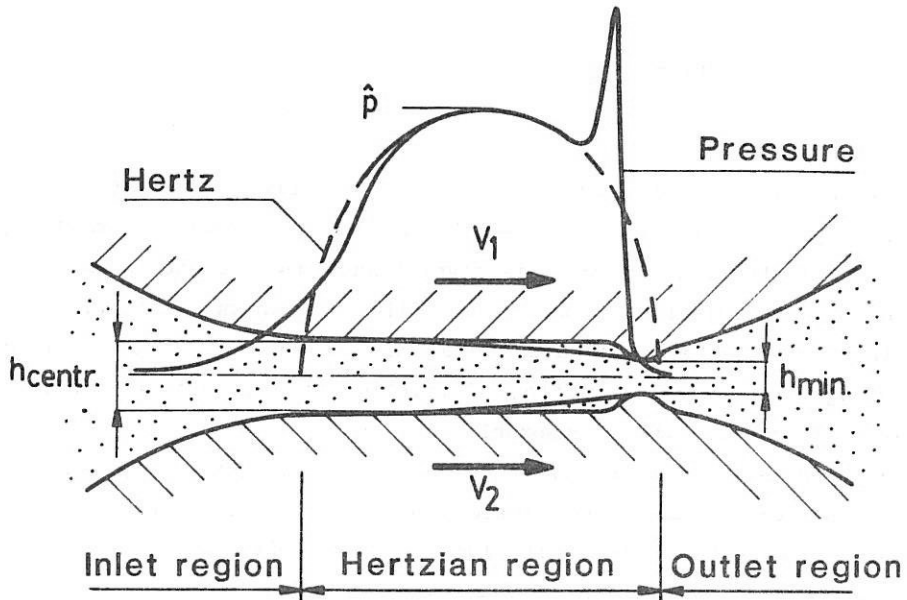contact are shown.

Fig. 3.1: Film shape and pressure distribution in an EHL contact.

It can be seen that the film has a nearly constant thickness over most of the Hertzian contact area and that a restriction, forming the minimum thickness, occurs near the outlet of the contact zone. Many research workers presented flim thickness formulas for EHL contacts, see appendix D. Characteristic for the lubricant-film in an EHL contact is that the film thickness is of the order of 1 μm or less and the length is two or three orders of magnitude larger. Also it was found that the film thickness is governed by the physical properties of the lubricant in the inlet region. The pressure distribution, apart from a sharp pressure peak toward the outlet of the main load transmitting region, is very similar to the semi-elliptical stress pattern of dry contact according to Hertz. This pressure peak is called the Petrusevich spike; it only occurs under certain load circumstances (Venner (1988)) and when the lubricant behaves like a liquid (section 3.2.3), see also the measurements of the pressure distribution in EHL contacts carried out by Safa (1982). A mean Hertzian pressure in an EHL-contact of 1 GPa or more is not unusual.

The prediction of friction under elastohydrodynamic conditions has been the subject of many discussions. The reason for this was that the lubricant properties, in the Hertzian contact region, were not very well understood and, therefore, received a lot of attention in the past. In the next sections a summary is given of the knowledge about friction in EHL-contacts and the behaviour of the lubricant under these extreme conditions.

3.2.2   Friction in EHL-contacts

Friction in EHL-contacts is usually studied on a disc machine. If the pressure, inlet temperature and rolling speed are maintained constant, then the friction versus slip relation (Crook (1963)) has the characteristic form as shown in fig. 3.2. The friction force can be divided into two parts; the rolling friction caused by velocity gradients in the inlet region and the sliding friction due to the shearing of the lubricant in the contact zone. Owing to the exponential behaviour of the shear properties of the lubricant with

pressure, the rolling friction is only a very small portion of the total friction. Therefore, in contrast to the film thickness which is mainly governed by the conditions in the inlet region, the friction force is mainly determined by the shear properties of the fluid and hence by the conditions in the Hertzian contact area.
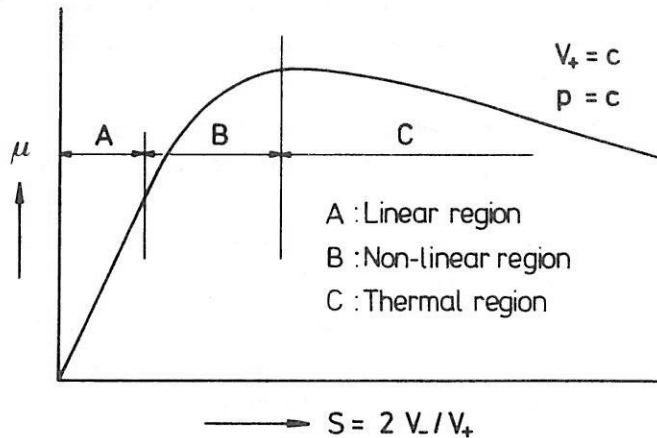

Fig. 3.2: Friction versus slip at constant sum velocity.

This friction curve can be divided into three separate regions. Region A is known as the linear small strain region where friction increases linearly with slip. The behaviour is entirely isothermal. Region B is the non-linear region where friction increases less rapidly with increasing slip. Towards the end of this region thermal effects become significant. Region C is known as the thermal region because the friction behaviour is dominated by shear heating. Consequently, in that region the friction falls with increasing slip rate. Each region has been investigated intensively by a great number of investigators. These investigations clearly showed that the usually assumed Newtonian behaviour of the lubricant, i.e. a linear relationship between shear (τ) and shear rate $(\dot{\gamma} = dV/dz$ or $V_-/h)$, represented by $\tau = \eta \cdot \dot{\gamma}$, is rarely present in EHL-contacts. The rheology of the lubricant plays a very important role in the determination of the friction. Figure 3.3 summarizes the types of friction curves that can be obtained for one liquid only by simply

changing the pressure in each experiment. This frictional behaviour will be discussed in more detail in the next section.
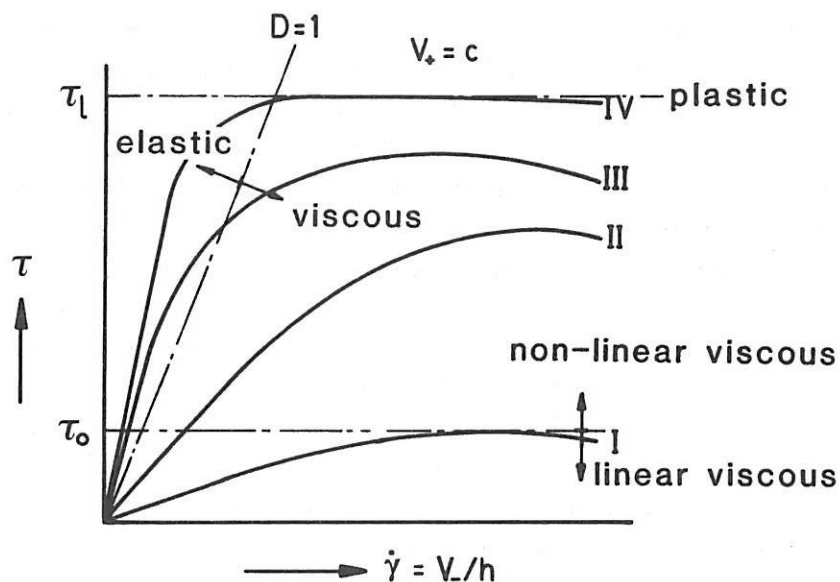

Fig. 3.3: Types of friction curves depending on the rheology of the lubricant.

    I : linear viscous - Newtonian-behaviour
    II : non linear viscous - Eyring-behaviour
    III: elastic - non linear viscous behaviour
    IV : elastic - plastic behaviour

3.2.3   Rheology of the lubricant under EHL-conditions

Based on his experiments Crook (1963) suggested that, in the linear small strain region of the friction curve, the behaviour of the lubricant could be of visco-elastic nature. He found that with rather low pressures the apparent viscosity, calculated with $\eta = \bar{\tau} / \dot{\gamma}$, was in agreement with other viscometrical data but for higher pressures there was a "break" in this apparent viscosity. This was also observed by Johnson and Cameron (1967). Johnson and Roberts (1974) used the Poon and Haines (1966/1967) apparatus with which it was possible to simultaneously study two different strain histories. In this way they

were able to discriminate between viscous- and elastic response of the lubricant. They found that the behaviour of the lubricant used was visco-elastic. The observed change from viscous- to elastic behaviour occurs when the time passage of a fluid element through the contact, a/V, is less than the relaxation time of the fluid, $\bar{\eta}/\bar{G}$. The ratio $D = (\bar{\eta}/\bar{G})/(a/V) = \bar{\eta} \cdot \bar{V}/(a \cdot \bar{G})$ is called the Deborah number. In fig. 3.3 the line $D = 1$ is drawn to discriminate between viscous and elastic behaviour. If $D \ll 1$ then the viscous behaviour is dominant, while for $D \gg 1$ mainly elastic behaviour is present.

The non-linear region, B, of the friction curve was studied intensively by Bell, et al. (1964), Cheng (1965), Dowson and Withaker (1965), etc. They calculated friction, with a complete thermal hydrodynamic analysis, assuming Newtonian properties for the lubricant. It turned out that their calculated friction was far too high compared with the observed friction in experiments and that the decrease of friction in this regime could not be attributed to thermal effects alone. From their observed frictional behaviour, that is linearity at low shear rates and non-linearity at higher shear rates, Bell et al. (1964) proposed the non-linear fluid model of Eyring as a base for the viscous behaviour of the fluid.

$$\text{Eyring:} \qquad \dot{\gamma} = \frac{\tau_0}{\eta} \sinh\left(\frac{\tau}{\tau_0}\right) \qquad\qquad (3.1)$$

In this fluid model a new parameter, τ_0, is introduced; this is a threshold parameter above which non-linearity occurs. There was still no good quantitative agreement with their experiments, however. Hirst and Moore (1974, '75, '78, '79 and '80) studied the non linear region of the friction curve, using the relation of Eyring. Much effort was put into τ_0 in relation with the size of the fluid molecules. From this work and from their own findings Johnson and Tevaarwerk (1977) formulated a constitutive equation which satisfies the experimental observations.

$$\dot{\gamma} = \dot{\gamma}_e + \dot{\gamma}_v$$

(3.2)

$$\dot{\gamma} = \frac{\dot{\tau}}{G} + \frac{\tau_0}{\eta} \sinh(\frac{\tau}{\tau_0})$$

It relates the shear stress τ, in uni-directional shear, to the shear rate $\dot{\gamma}$. The first term describes visco-elasticity and the second term expresses the non-linearity between τ and $\dot{\gamma}$, generally expressed by $f(\tau)$. Equation (3.2) in fact describes a non linear Maxwell liquid in which 3 lubricant parameters are involved; G, η and τ_0, which are depending on pressure and temperature.

Using $\dot{\tau} = d\tau/dt = (\overline{V}/a) \cdot d\tau/d(x/a)$, equation (3.2) can be rewritten as:

$$\eta \dot{\gamma} = D \frac{d\tau}{d(x/a)} + \tau_0 \sinh(\frac{\tau}{\tau_0})$$

(3.3)

Where $D = \eta \cdot \overline{V}/(G \cdot a)$ is the Deborah number as mentioned before. Relation (3.2) or (3.3) not only describes the elastic non linear viscous behaviour of the lubricant but it also incorporates Newtonian behaviour. If $D \ll 1$ and $\tau \ll \tau_0$ ($\sinh(\tau/\tau_0) \approx \tau/\tau_0$), equation (3.3) becomes $\eta \cdot \dot{\gamma} = \tau$, which describes Newtonian behaviour.

The disadvantage of the equation presented by Johnson and Tevaarwerk is that τ can increase without limitation; in reality, however, all materials have a limit, an ultimate strength. Smith (1959) already observed this and postulated that fluids posses a limiting shear stress beyond which they cannot increase their resistance to shear any more and, consequently, behave in a plastic manner. He found that the maximum friction coefficient $\overline{\tau}/\overline{p}$ of the friction curve was independent of pressure. Johnson and Cameron (1967) confirmed this and showed that this limiting shear stress is independent of the inlet temperature, rolling- and sliding speed. Working with a high pressure shear cell Bair and Winer (1979) proved the existence of a limiting shear stress for some lubricants. In these experiments shear heating effects were negligible. This was not the case in the experiments done by Smith (1959) and Johnson and Cameron

(1967). The existence of a limiting shear stress τ_1 sets a limit to the value of τ. Therefore, to equation (3.2) the next conditions are added, which describe an elastic/perfectly plastic solid, known as the Prandtl-Reuss equations.

For perfectly elastic behaviour, when $\tau < \tau_1$, then $f(\tau) = 0$

$$(3.4)$$

For perfectly plastic behaviour, when $\tau = \tau_1$, then $f(\tau) = \tau_1 \cdot \dot{\gamma}/\tau$

Thus, in principle, four parameters of the lubricant η, τ_0, G and τ_1 determine the friction in an EHL-contact. Evans and Johnson (1986[a,b]) intensively investigated the behaviour of these parameters as a function of temperature and pressure for three specially chosen lubricants. Using a two-disc machine with thermocontrolled discs, it was possible to measure under isothermal conditions. It was found that:
- $\bar{\eta}$ showed a logarithmic increase with increasing pressure and a logarithmic decrease with increasing temperature. The use of the simple exponential Barus equation, $\eta = \eta_0 \cdot e^{\alpha p}$, was shown to be inaccurate at high pressures.
- $\bar{\tau}_0$ showed an increase with absolute temperature and, depending on the lubricant, an increase or a decrease with pressure.
- $\bar{\tau}_1$ appeared to be directly proportional to the contact pressure but almost insensitive to temperature.
- $\bar{G}$ could not be obtained satisfactorily from the small strain region of the friction curve because of the tangential creep of the disc surfaces. In this respect it is better to use an oscillatory shear technique like Barlow et al. (1967), or use the approximation $\bar{G} = 30 \cdot \bar{\tau}_1$ as suggested by Tabor (1982[a]).

Coworkers of Winer experimentally demonstrated the existence of a glass transition temperature for lubricants under EHL-conditions by using techniques of light scattering and volume dilatometry methods. They studied this transition for lubricants, i.e. liquid like behaviour to a solid like behaviour, as a function of pressure and temperature. Alsaad et al. (1978) showed this transition for a great number of lubricants and called it the glass-transition. In figure 3.4
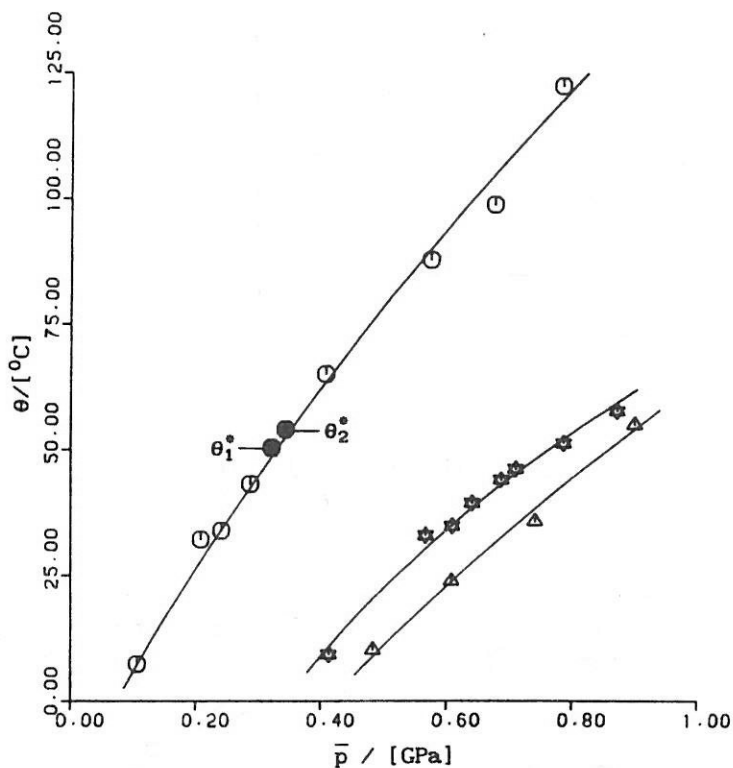
some liquid to solid transitions are given.

Fig. 3.4.: Liquid to solid transitions for 5P4E (O), Santotrac-50 (Δ)
and mineral oils (✿). Reproduced from Alsaad et al. (1978).
θ_1^* and θ_2^* are results from experiments described in 5.3.1.4

The area above each line represents the liquid state of the lubricant,
the area below it the solid state. For mineral based oils the
transition curves lie very close to each other within a difference of
± 10 °C. The position of the transition line for synthetic oils is
spread over the whole pressure range; compare 5P4E with Santotrac-50.

Evans and Johnson (1986[a,b]) constructed with fig. 3.3, equations
(3.2) and (3.4), and fig. 3.4 a regime chart in which different areas
of the chart correspond to different regimes of lubricant behaviour.
The coordinates chosen for the chart are the non dimensional pressure,
$\alpha_\theta \cdot \bar{p}$ and a parameter which is closely related to the film thickness,
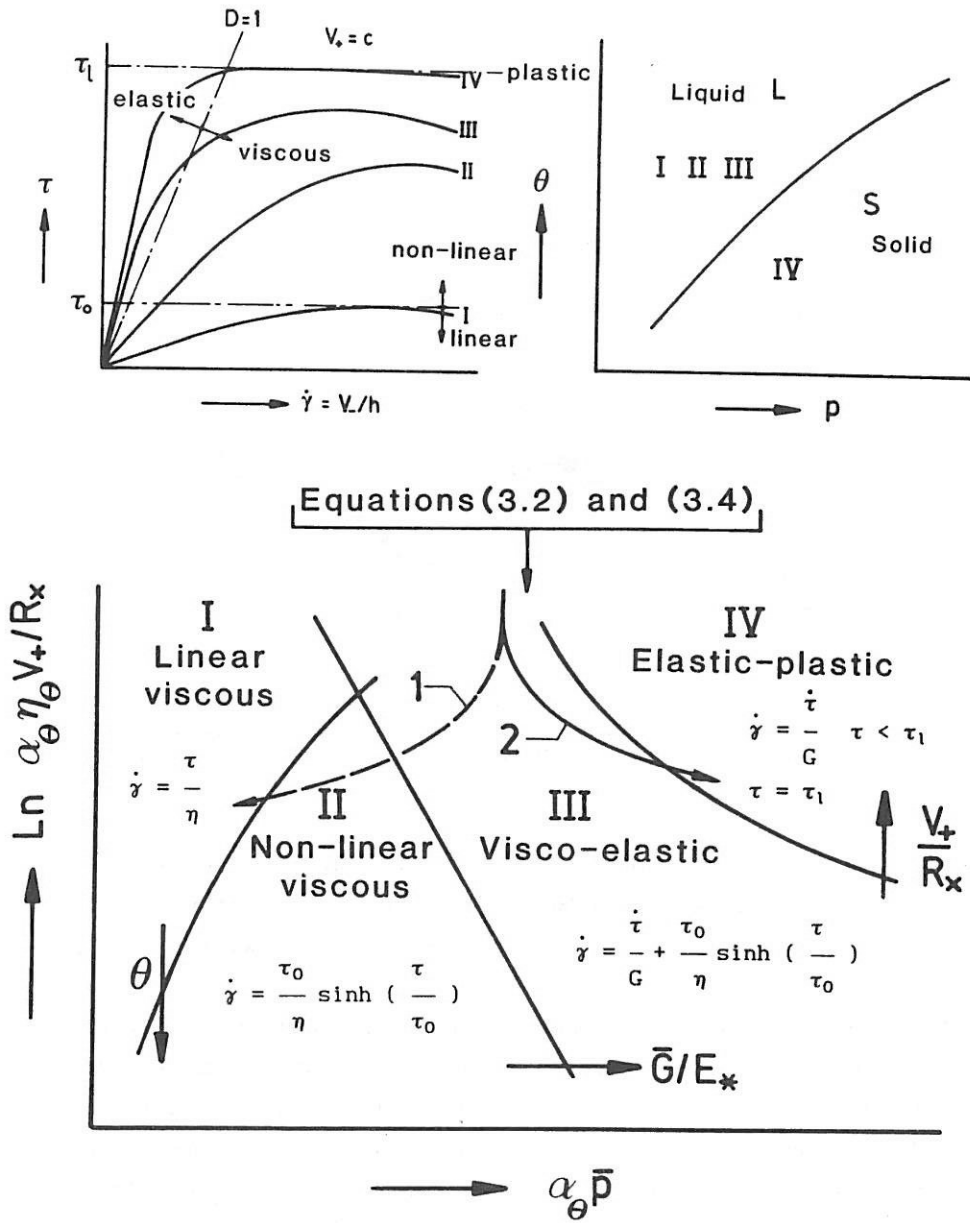$\alpha_\theta \cdot \eta_\theta \cdot \bar{V}/R_x$.

Fig. 3.5 Regime chart, reproduced from Evans (1983).

For each lubricant such a chart has to be made. The advantage of such
a chart is that it can be seen at once which rheological behaviour of

the lubricant is to be expected with a given load, velocity and temperature. The chart shows that pressure has an enormous influence on the rheological behaviour of the lubricant; by changing the pressure an LCC can enter all regimes. Temperature and velocity have much less influence on the lubricant behaviour in an EHL-contact; in general only 2 regimes can be covered.

3.2.4   EHL, summary

Formulas for film thickness for EHL-contacts are available. The validity of these formulas for circular- and elliptical contacts is limited to a part of the entire EHL-region, see appendix D. Also not taken into account is the rheological behaviour of the lubricant in determining these formulas.

Generally, in an EHL-contact a lubricant can behave linear viscous, non-linear viscous, elastic-non linear viscous or elastic-perfectly plastic depending on pressure, temperature and velocity, see fig. 3.5. With relation to friction four parameters of the lubricant are playing a role, i.e. η, τ_0, G and τ_1, each depending, in its own way, on temperature and pressure. To involve temperature the inclusion of the energy equation is needed.

Lubricant behaviour can be characterized by:

I   linear viscous behaviour   : $\tau < \tau_0$ and D < 1.
II   non linear viscous behaviour   : $\tau_1 > \tau > \tau_0$ and D < 1.
III elastic-non linear viscous behaviour : $\tau_1 > \tau > \tau_0$ and D > 1.
IV   elastic-perfectly plastic behaviour : $\tau \leq \tau_1$ and D > 1.

Friction for situations I and II (linear- and non linear viscous behaviour) can be predicted with a good reliability. For the elastic non linear viscous behaviour this is also the case but caution is needed at small shear rates, where the elasticity of the lubricant plays a role and G is not really known. In the elastic-perfectly plastic situation the same problem occurs at small shear rates as in the case of elastic non-linear behaviour. For the plastic shear only experimental data can be used.

3.3.   BOUNDARY LUBRICATION

3.3.1.   Introduction

The lubrication regime referred to as BL is a rather old topic in tribology. The amount of papers published, dealing with all kind of features with regard to BL is enormous. See the reviews of Bowden and Tabor (1950, 1964), Davies (1957), Rowe (1966), Godfrey (1968), Campbell (1969), Fein (1969), Rowe (1973) and Sakurai (1981).
Although very elegant techniques have been used to unravel the mechanisms involved in BL, see for instance Godfrey (1978) and Sakurai (1981), there is still no adequate theory describing BL yet, unlike the situation in EHL. This is caused by the lack of detailed knowledge of the chemical composition of the boundary films under sliding conditions and the physical properties of these films under conditions of high pressure, high temperatures and high shear rates. Therefore, it is to be expected that the understanding of friction becomes difficult when BL is involved, as is the case with ML.
The general findings of the published experiments concerning BL are collected and reviewed in the next sections.

3.3.2.   Surface film formation mechanisms

The fundamental mechanisms of interaction between lubricant and solid to produce a protective lubricant film are physical adsorption, chemical adsorption and chemical reaction, Godfrey (1968). Akhmatov (1966) discusses the film formation in detail and gives insight into the molecular physics involved in BL.

Physical adsorption occurs when lubricant molecules are bound to the solid surfaces by Van der Waal's forces. The bounding is relatively weak and no exchange of electrons takes place between the adsorbed molecules and the solid. Physical adsorption is characterized by reversibility and the formation of mono- or multimolecular layers. Polar molecules i.e. molecules which have a variation in electric charge along their length, such as long chain hydrocarbons, adsorb on

to the surface with vertical orientation. Many molecules pack in as closely as possible and strengthen the film with lateral cohesive forces. In figure 3.6[a] the physical adsorption of hexadecanol is represented.
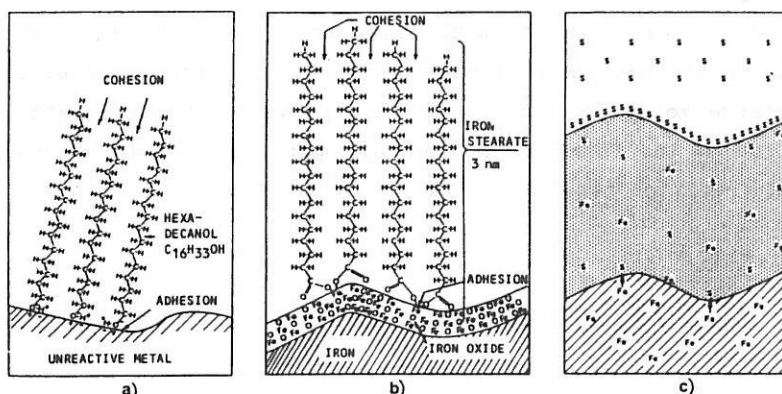

Fig. 3.6: Boundary lubrication films, Godfrey (1968).

    a. Physical adsorption of a long-chain alcohol to a metal surface.

    b. Chemical adsorption of stearic acid to an iron surface forms a soap, iron stearate.

    c. Chemical reaction of sulphur with iron forms an iron sulphide film.

Chemical adsorption occurs when the lubricant molecules are held to the surface by chemical bonds. The molecules first adsorb physically and then react chemically to form a new entity. The film is limited to a mono layer and the formation is characterized by irreversibility and strong binding energies. An example of the formation of a typical chemically adsorbed film is the reaction of stearic acid with iron oxide in the presence of water to form a metal soapfilm of ironstearate on the surface, figure 3.6[b].

Chemical reaction occurs when there is an exchange of valence electrons between lubricant and solid surfaces by which a new chemical compound is formed; the term will be used to describe the formation of films of organic salts on metals, figure 3.6[c]. In principle such lubricant films are unlimited in thickness and are characterized by

high bonding energies and irreversibility. The chemically reactive boundary lubricants usually contain sulphur, chloride or phosphorus atoms in the molecule and additionals like lead, zinc and selenium, Fein (1969). These reaction films are more stable than physically and chemically adsorbed films.

The above filmformation mechanisms are idealized. In practice a combination of these mechanisms will take place because of effects of for instance metallurgy of the solids, presence of oxygen and water, solubility of the film in the base oil and pressure, temperature and available reaction time.

3.3.3 Effect of operating conditions

3.3.3.1 Temperature

The temperature is a very important variable. With increasing temperature the strength of the bond of physically adsorbed films reduces. In case of chemically bonded films the rate of film formation increases, Sakurai (1981). The coefficient of friction is rather constant as function of temperature, but above a certain temperature friction always increases strongly with a corresponding increase in wear and therefore damage of the surfaces, Godfrey (1968).

For physically adsorbed films this critical temperature is well defined and occurs at the bulk meltingpoint of the lubricant film, because then the lateral bonds diminish. This transition is independent of the nature of the underlying metal and is reversible on cooling, the friction returns to its original low value, Campbell (1969).

Adsorbed films created by chemisorption have a transition tempera- ture which is much higher than the bulk meltingpoint of the lubricant itself, i.e. fatty acids. The protective film works effectively until the meltingpoint of the soap is reached. Bowden and Tabor (1950).
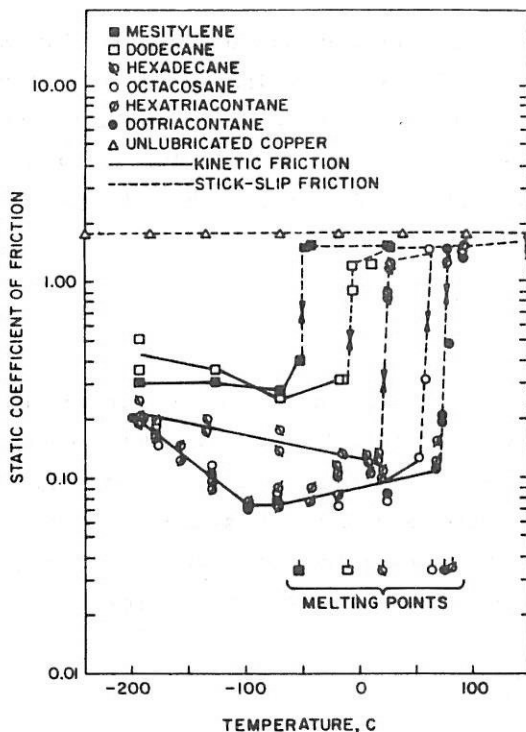
Fig. 3.7: Variation in friction with temperature for copper pairs
lubricated with hydrocarbons in dry Helium. Godfrey (1968)

The films formed by chemical reaction also lubricate effectively up
to their meltingpoint, but a good correlation has not been
established. This is due to effects such as decomposition, oxidation
or vaporizing, Godfrey (1968). Because of their characteristic strong
binding energies protection up to very high temperatures is possible,
Rowe (1966).

Thus, a high meltingpoint of lubricant, soap, or reaction film, and
a thermally stable film are necessary for a good BL film. A low shear
strength is needed for low friction. Unfortunately, however, a high
meltingpoint usually results in a high shear strength.

3.3.3.2 Normal load

Amontons (1699) law is obeyed over a wide range of normal forces,
that is, the coefficient of friction is independent of normal force.

3.16

This is found for both flat and curved surfaces. For very low normal forces, smaller then 0.1 N, μ is increasing with decreasing normal force. This was first observed by Hardy and Bircumshaw (1925) and later confirmed by Bowden and Tabor (1950). This phenomenon is attributed to the effect of Van der Waal forces relative to the applied normal force.

3.3.3.3 Velocity

The coefficient of friction is nearly independent of sliding velocity over a range of more then two decades, Beeck et al. (1940), Forester (1946). Also it is found that at relatively low velocities, below 10^{-3} m/s, there are two types of relations between μ and velocity. For mineral oils μ increases with decreasing velocity, for fatty acids μ decreases with decreasing velocity.

3.3.3.4 Atmosphere

The two components of principle importance are watervapour and oxygen. Both enter into BL, often supplementing each other. Several studies, reviewed by Campbell (1969) and others, showed that water vapour increases friction.

In organic lubricants the solubility of oxygen is low, nevertheless it has an enormous influence on BL. The dissolved amounts are sufficient to enable the film on a surface to reform when it is removed by rubbing. In general, friction rises in the absence of oxygen. Some reservations with regard to this statement have to be made. The effectiveness of additives in their interaction with the surface may depend on oxygen and the formed oxides have a large influence on the coefficient of friction.

Because of the variety of features involved in BL, Sakurai (1981), it is not surprising that the results of various BL studies are often confusing and conflicting.

3.3.4   Shear strength of the films

The bonding of the films is of interest for the protection of the
surfaces against penetrating asperities, but the shear strength of the
formed films determines the friction, induced between the two
relatively moving surfaces. This shear strength of the boundary film
depends on how the film is formed. In figure 3.8 the shear strength
across the film of the idealized formed films is presented
schematically.
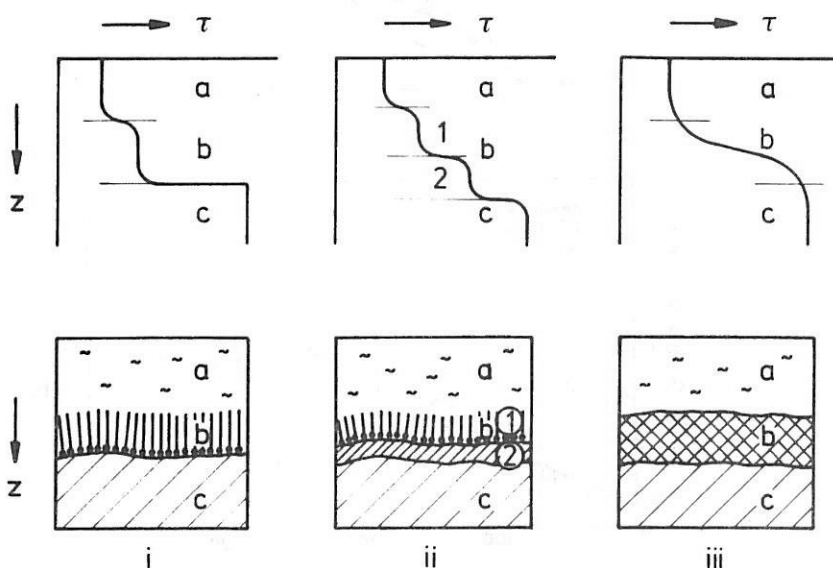

fig. 3.8: Variation of shear strength across idealized
          formed films, Holmberg (1984).
          i   : Physical adsorption.
          ii : Chemical adsorption.
          iii : Chemical reaction.

Briscoe et al. (1973) and Amuzu et al. (1977) succeeded in measu-
ring the shear strength of organic solids and inorganic crystalline
materials such as paraffin wax, metallic soaps and oriented mono
layers of fatty acids, for pressures up to 3 GPa without extrusion or
rupture of the boundary film. Briscoe et al. (1973) and Tabor (1982[a])
proposed the relation between shear strength and pressure as:

$$\tau_{bl} = \alpha \cdot p \qquad\qquad (3.5)$$

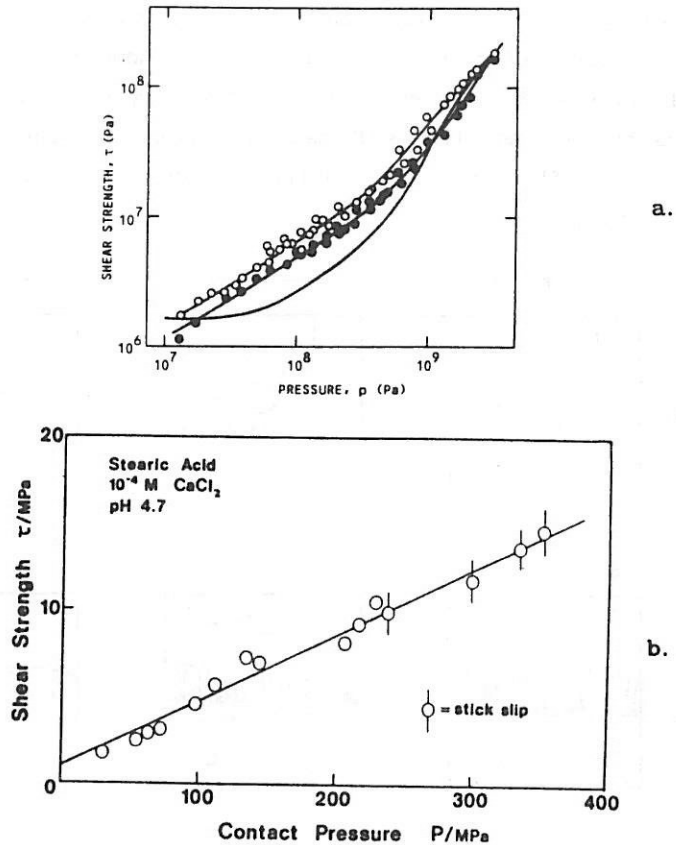where α is a constant, depending on the type of surface layer.

a.

b.

Fig. 3.9: Variation of shear strength with contact pressure
for surface films of stearic acid.
a. Briscoe (1973).
b. Tabor (1982[a]).

For some of the tested films the dependence of the shear strength on temperature in the range of 20 to 140 $^\circ$C is negligible and for others there is a decrease in the shear strength by a factor of two.

The consequence of relation (3.5) is that the real area of contact does not necessarily have to be proportional with N to yield a coefficient of friction which is independent of N.

3.3.5 Friction model

Bowden and Tabor (1950) proposed the next relation for the friction in a BL contact, as shown in figure 3.10.

$$F = A \{ \varepsilon \tau_m + (1-\varepsilon)\tau_{bl}\} \qquad (3.6)$$

where: A = the area which supports the applied normal force,

ε = the fraction of this area over which the boundary layer is penetrated,

τ_m = the shear strength of the junctions at the metal-metal contact,

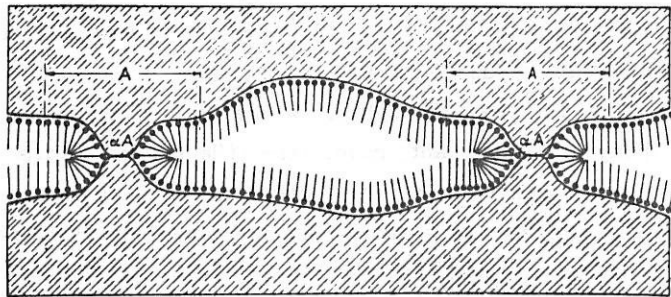τ_{bl} = the shear strength of the boundary layer.

Fig. 3.10: Contact between solids, Bowden and Tabor (1950).

They rejected Hardy's (1936) well known friction model because BL experiments showed that there is always some wear and Hardy's model did not allow contact between the solid surfaces. Tamai and Rightmore (1965) evaluated equation (3.6) and concluded that ε and τ_{bl} are independent of each other.

Summarizing, the formation of solid surface films is essential for effective lubrication in the BL regime. The shear strength of these films determines the friction. The coefficient of friction lies between approximately 0.1 and 0.4. If these protecting layers are not present, coefficients of friction of 1 or higher can be expected.

The melting point of the film appears to be the one unifying physical property which determines the film performance, and which correlates well with the "failure temperature criterion" of Blok (1937).

However, many factors do mask the basic mechanisms involved in BL and make this type of lubrication far from easy to understand.

3.4   MIXED LUBRICATION

3.4.1   Introduction

The sections 3.2 and 3.3 discussed in general the two "asymptotic" lubrication modes EHL and BL of the ML-regime. This study resulted in the determination of the variables involved in these lubrication modes and that may be of influence in the ML-regime.

For friction in the ML-regime, where interactions between the asperities play an important role, the (Hertzian) contact area is split up into two parts, i.e., the micro-contact area formed by the interacting asperities and a macro-contact area, schematically shown in figure 3.11 and visualized in figure 3.12. Greenwood and Tripp (1970) made clear that the total area of the micro-contacts is small compared to that of the Hertzian macro-contact area. In these micro contacts, the frictional behaviour at the interfaces of the interacting asperities can be divided in DF, BL and EHL. For the macro-contact, EHL i.e. liquid/solid behaviour of the lubricant, determines the friction.
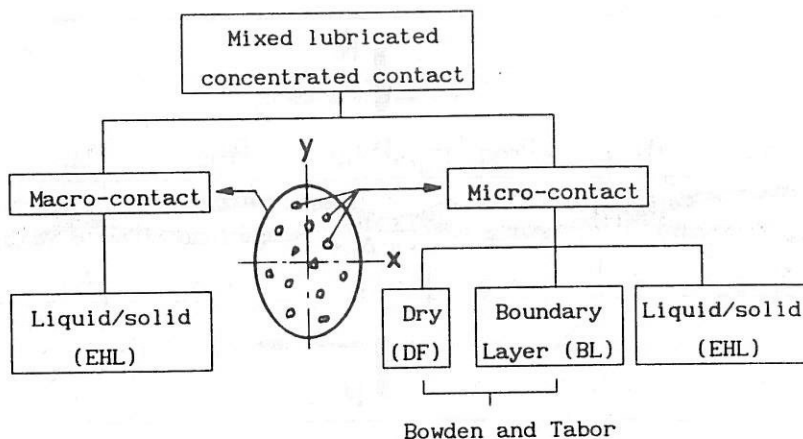
Fig. 3.11: Lubrication in macro- and micro-contact.

Besides the lubrication modes for interacting asperities introduced by Bowden and Tabor, the EHL mode is added as a possible lubrication mode. When an LCC is operating in the BL regime, the average pressure in the micro-contacts is much higher than the mean pressure in a contact operating in the EHL-regime with the same normal force, Greenwood et al. (1966, 1970). In the ML-regime there are asperity contacts and it is expected that the pressures in these contacts are high. Locally, the lubricant can transform from liquid-state behaviour into solid state behaviour and vise versa, section 3.2.3. When liquid/solid behaviour between the interacting asperities governs friction then this is referreed to as micro-EHL.

3.4.2   Friction model

The contact between the two opposing surfaces of an LCC operating in the ML-regime is illustrated in figure 3.12.
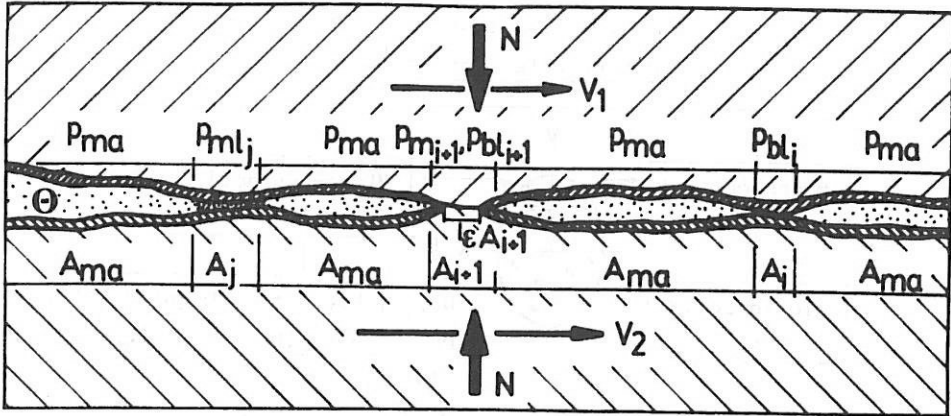
Fig. 3.12: Impression of contact situation in the ML-regime.

The momentary resistance to sliding can be expressed by:

$$F = \sum_{i=1}^{n} \left\{ \varepsilon_i \iint_{A_i} \tau_{m_i} dA_i + (1 - \varepsilon_i) \iint_{A_i} \tau_{bl_i} dA_i \right\} +$$

$$\sum_{j=1}^{m} \iint_{A_j} \tau_{ml_j} dA_j + \iint_{A_{ma}} \tau_{ma} \, dA_{ma} \qquad (3.7)$$

The normal force is given by:

$$N = \sum_{i=1}^{n} \left\{ \varepsilon_i \iint_{A_i} p_{m_i} dA_i + (1 - \varepsilon_i) \iint_{A_i} p_{bl_i} dA_i \right\} +$$

$$\sum_{j=1}^{m} \iint_{A_j} p_{ml_j} dA_j + \iint_{A_{ma}} p_{ma} \, dA_{ma} \qquad (3.8)$$

where: n = number of BL micro-contacts.

m = number of EHL micro-contacts.

ε_i = fraction of penetrated boundary layer in i^{th} micro-contact.

A_i = i^{th} BL contact area.

A_j = j^{th} micro-EHL contact area.

A_{ma} = macro-EHL contact area.

τ_{m_i} = shear strength of the ith solid-solid (DF) junction.

τ_{bl_i} = shear strength of the boundary film in i^{th} contact.

τ_{ml_j} = shear strength of the jth micro-EHL contact.

τ_{ma}^{j} = shear strength of the macro-EHL lubricant film.

p_{m_i} = pressure of the ith solid-solid (DF) junction.

p_{bl_i} = pressure in the ith boundary layer.

p_{ml_j} = pressure at the jth micro-EHL contact.

p_{ma}^{j} = pressure in the lubricant film.

The first term of (3.7) represents Bowden and Tabor's friction model for BL and the second term micro-EHL, respectively. Friction, due to the lubricant in the macro-contact, is described by the third term. The dependence of the shear strengths, directly and indirectly, of pressure and temperature has been outlined in the previous sections. At sliding over a small distance at constant operating conditions, the contact situation changes due to the micro-geometry and, therefore, the value of the variables mentioned in (3.7) changes. The frictional force will fluctuate with sliding distance about a certain mean value depending on mean values of the different variables which control friction. If micro-geometry changes with time (sliding distance) due to wear then, in general, the mean value of the frictional force also changes with time.

The complexity of equation (3.7) is enormous, since the variables depend on other variables such as the local pressure, which in turn depends on micro-geometry and local properties, etc. Therefore, the friction of an LCC operating in the ML-regime is considered by means of the mean values of the variables involved in friction. Equation (3.7) is rewritten into:

$$\bar{F}^{(a,b,c)} = \sum_{i=1}^{n} \bar{\tau}_{bl_i} A_i + \sum_{j=1}^{m} \bar{\tau}_{ml_j} A_j + \iint_{A_{ma}} \tau_{ma} \, dA_{ma}$$

$$\bar{F}^{(d,e)} = \bar{\tau}_{bl} A_{bl} + \bar{\tau}_{ml} A_{ml} + \bar{\tau}_{ma} A_{ma} \tag{3.9}$$

with:
$$A_{bl} = \sum_{i=1}^{n} A_i \quad , \quad A_{ml} = \sum_{j=1}^{m} A_j$$

$$A_{ma} = A_{Hertz} - (A_{bl} + A_{ml}) = A_{Hertz} - A_c \approx A_{Hertz}$$

The assumptions made are:

a. DF does not occur, $\varepsilon_i = 0$ (for all BL micro-contacts).

b. Elastic-plastic behaviour of the lubricant in the micro-EHL contacts.

c. The shear stresses (and pressures) are constant in the ith and j^{th} micro-contact, and equal to $\bar{\tau}_{bl_i}$ and $\bar{\tau}_{ml_j}$ respectively. The shear stresses are linearly related to pressure.

d. The shear stresses are constant for each ith and j^{th} micro-contact and equal to $\bar{\tau}_{bl}$ and $\bar{\tau}_{ml}$ respectively. Greenwood et al. (1966, 1970) showed that the total mean pressure in the micro-contacts is constant and independent of normal force and the real area of contact is proportional with the normal force. This, together with the linear relationship of shearstress with pressure this assumption can be made.

e. $\bar{\tau}_{ma}$ represents the mean shearstress in the lubricant for the macro-contact.

Equation (3.8) for the normal force is rewritten into:

$$N = \bar{p}_{bl} \cdot A_{bl} + \bar{p}_{ml} \cdot A_{ml} + \bar{p}_{ma} \cdot A_{ma} = \bar{p}_{Hertz} \cdot A_{Hertz} \qquad (3.10)$$

Using the results of Greenwood et al. (1966, 1970), i.e., $\bar{p}_{ml}$ and $\bar{p}_{bl}$ are equal to $\bar{p}_c$ and $A_{ma} = A_{Hertz} - A_c$, equation (3.10) transforms into:

$$N = \bar{p}_c \cdot A_c + \bar{p}_{ma} \cdot (A_{Hertz} - A_c) = \bar{p}_{Hertz} \cdot A_{hertz} \qquad (3.11)$$

This friction model is limited, because the values of the different variables at certain operational conditions are unknown. Equation (3.9) gives an impression of the variables involved, from which numbers can be obtained which characterize the friction in the ML-regime.

3.4.3   Dimensional analysis

According to equation (3.9), the friction is a function of:

$$\bar{F} = \Phi \ (A_{bl}, \ A_{ml}, \ A_{ma}, \ \bar{\tau}_{bl}, \ \bar{\tau}_{ml}, \ \bar{\tau}_{ma}) \qquad (3.12)$$

The relationships between the variables in (3.12) and other variables are given by:

-       Hertz (1881)

$$A_{Hertz} = \Phi_1 \ (R_*, \ N, \ E_*) \qquad (3.13)$$

-       Greenwood et al. (1966, 1970)

$$A_c = A_{bl} + A_{ml} = \Phi_2 \ (s, \ \sigma_t, \ \beta, \ n_t, \ A_{Hertz}, \ E_*) \qquad (3.14)$$

–   Tabor (1982[a]) and Briscoe et al. (1973)

$$\bar{\tau}_{bl} = \Phi_3 \ (\bar{p}_{bl}, \ \theta) = \Phi_3 \ (\bar{p}_c, \ \theta) \qquad\qquad (3.15)$$

–   Bair and Winer (1979), Evans (1983)

$$\bar{\tau}_{ml} = \bar{\tau}_l = \Phi_4 \ (\bar{p}_{ml}, \ \theta) = \Phi_4 \ (\bar{p}_c, \ \theta) \qquad\qquad (3.16)$$

–   Johnson et al. (1977), Evans (1983)

$$\bar{\tau}_{ma} = \Phi_5 \ (s, \ \bar{p}_{ma}, \ \theta, \ \alpha, \ \eta_1, \ \tau_1, \ \tau_0, \ V_+, \ V_-) \qquad\qquad (3.17)$$

in which

s = separation of the surfaces

n_t = number of summits per unit area

β = mean radius of the asperity summits

Substitution of (3.13) to (3.14) in (3.12) gives:

$$\bar{F} = \Phi \ (s, \ \bar{p}_{ma}, \ \theta, \ \alpha, \ \eta_1, \ \bar{G}, \ \bar{\tau}_1, \ \bar{\tau}_0, \ V_+, \ V_-,$$

$$\bar{p}_c, \ \sigma_t, \ \beta, \ n_t, \ R_*, \ N, \ E_*) \qquad (3.18)$$

In (3.18), $\bar{F}$ is a function of some variables which are not known. Using equation (3.11), $\bar{p}_{ma}$ or $\bar{p}_c$ can be eliminated. Therefore:

$$\bar{F} = \Phi \ (s, \ \bar{p}_{Hertz}, \ \theta, \ \alpha, \ \eta_1, \ \bar{G}, \ \bar{\tau}_1, \ \bar{\tau}_0, \ V_+, \ V_-,$$

$$\bar{p}_c, \ \sigma_t, \ \beta, \ n_t, \ R_*, \ N, \ E_*) \qquad (3.19)$$

The coefficient of friction is now governed by:

$$\mu = \Phi \ (s, \ \bar{p}_{Hertz}, \ \theta, \ \alpha, \ \eta_1, \ \bar{G}, \ \bar{\tau}_1, \ \bar{\tau}_0, \ V_+, \ V_-,$$

$$\bar{p}_c, \ \sigma_t, \ \beta, \ n_t, \ R_*, \ N, \ E_*) \qquad (3.20)$$

For the isothermal situation, under the assumptions made in the previous section, friction depends on n=15 variables. There are k=3 dimensional units involved, namely, kilogram, meter and second. Following Buckinghams Π theorem (1914, 1915) then n-k = 12 independent dimensionless numbers can be created. Taking for instance s, η_1 and V_+ (chapter 2) as mean variables, equation (3.20) can be rewritten into:

$$\mu = \Phi \left[\left(\frac{\eta_1 \cdot V_+}{P_{Hertz} \cdot s}\right)^{c_1} \cdot \left(\frac{\alpha \cdot \eta_1 \cdot V_+}{s}\right)^{c_2} \cdot \left(\frac{\eta_1 \cdot V_+}{G \cdot s}\right)^{c_3} \cdot \left(\frac{\eta_1 \cdot V_+}{\tau_1 \cdot s}\right)^{c_4} \cdot \left(\frac{\eta_1 \cdot V_+}{\tau_0 \cdot s}\right)^{c_5} \cdot \right.$$

$$\left(\frac{V_-}{V_+}\right)^{c_6} \cdot \left(\frac{\eta_1 \cdot V_+}{P_c \cdot s}\right)^{c_7} \cdot \left(\frac{s}{\sigma_t}\right)^{c_8} \cdot \left(\frac{s}{\beta}\right)^{c_9} \cdot \left(s^2 \cdot n_t\right)^{c_{10}} \cdot \left(\frac{s}{R_*}\right)^{c_{11}} \cdot \left(\frac{\eta_1 \cdot V_+}{E_* \cdot s}\right)^{c_{12}}$$

$$(3.21)$$

The powers of the numbers are often characteristic (-1, 1/2, 1, 2, etc.) and the numbers in (3.21) may be replaced by a number consisting of the product of the original number with others. For instance, the product of the 2th and 11th term with c_2 = 1 and c_{11} = 1 gives $\alpha \cdot \eta_1 \cdot V_+/R_*$ the number of figure 3.5.

Rearranging of equation (3.21) gives:

$$\mu = \Phi \left[\left(\frac{\eta_1 \cdot V_+}{P_{Hertz} \cdot \sigma_t}\right)^{c_1} \cdot \left(\frac{\alpha \cdot \eta_1 \cdot V_+}{R_*}\right)^{c_2} \cdot \left(\frac{\bar{\tau}_1}{G}\right)^{c_3} \cdot \left(\frac{\bar{\tau}_1}{P_{Hertz}}\right)^{c_4} \cdot \left(\alpha \cdot \bar{\tau}_0\right)^{c_5} \cdot \right.$$

$$\left(\frac{V_-}{V_+}\right)^{c_6} \cdot \left(\frac{\bar{P}_c}{P_{Hertz}}\right)^{c_7} \cdot \left(\frac{s}{\sigma_t}\right)^{c_8} \cdot \left(\frac{\sigma_t}{\beta}\right)^{c_9} \cdot \left(\beta \cdot \sigma_t \cdot n_t\right)^{c_{10}} \cdot$$

$$\left(\alpha \cdot P_{Hertz}\right)^{c_{11}} \cdot \left(\frac{R_* \cdot P_{Hertz}^2}{\sigma_t \cdot E_*^2}\right)^{c_{12}} \qquad (3.22)$$

By this exercise many known numbers given in the literature with relation to full-film lubrication (2, 3, 4, 5, 6 and 11) and rough surface contact (7, 9, 10 and 12) are found. The first term $\eta_1 \cdot V_+/(\bar{p}_{Hertz} \cdot \sigma_t)$ and the eighth term s/σ_t (= h/σ_t) were already discussed in chapter 2 and will be outlined in the next section.

3.4.4. Comparison of $\eta_1 V_+/\bar{p}$ and film thickness h

h/σ_t is often used as the parameter which expresses the operational conditions of an EHL contact. However, the use of the film thickness as a variable for the whole ML-region is somewhat doubtful.

- Film thickness equations are derived for the EHL-regime. In appendix D it is outlined that for LCC's the calculation of film thickness for circular and elliptical contacts is still not reliable for the whole EHL-regime. This is particularly true for high values of M., the operating area for LCC's near the ML-regime, i.e., at high normal forces and/or low velocities and/or high temperatures (low viscosities).

- Also in the case of flat contacts, or other contact situations for which no film thickness formulas are available, a parameter is needed which represents the severity of the operational conditions of these contacts.

- The use of the variable α has some practical problems because for most of the lubricants its value is not known.

Also taking the recommendations found in literature into account, the relation $\eta_1 \cdot V_+/\bar{p}$ is proposed instead of the film thickness h. Further, there is not much difference between $\eta_1 \cdot V_+/\bar{p}$ and the film thickness h, as shown in the next part.

The film thickness formula for circular contacts given by Moes et al.(1972) reads:

$$h \therefore \alpha^{0.55} \quad \eta_1^{0.7} \quad E_*^{-0.067} \quad N^{-0.083} \quad R_x^{0.467} \quad V_+^{0.7} \qquad (3.23)$$

Mean pressure in an EHL-contact:

$$\bar{p} \therefore N^{0.333} \quad R_*^{-0.667} \quad E_*^{0.667} \qquad (3.24)$$

Rearranging of (3.23) and (3.24) yields:

$$h \therefore \alpha^{0.55} \quad E_*^{0.40} \quad N^{0.15} \quad (\eta_1 \cdot V_+/\bar{p})^{0.70} \qquad (3.25)$$

The same analysis can be made for line- and elliptical contacts, with nearly the same relation between h and $\eta_1 \cdot V_+/\bar{p}$. Equation (3.25) shows the main difference between $\eta_1 \cdot V_+/\bar{p}$ and h. The value of α differs for different lubricants by a factor of 2 to 3. Likewise, the difference in E for metals used in EHL-contacts may amount to a factor of 3. Thus, because of the low powers for α, E_* and N, the operational conditions of an LCC can safely be characterized by $\eta_1 \cdot V_+/\bar{p}$. The advantage of using $\eta_1 \cdot V_+/\bar{p}$ instead of h is that the operational variables can easily be expressed into $\eta_1 \cdot V_+/\bar{p}$ for all kind of contact situations. $\eta_1 \cdot V_+/\bar{p}$ will be referred to in the next sections as the operational number H.

3.4.5 Summary

Study of friction in the EHL- and BL mode resulted in a friction model for the ML-regime. However, the values of most of the variables involved in this model are not known and even a simplification of this model did not give the desired result, i.e., calculation of friction in the ML-regime and of the transitions EHL-ML and ML-BL. A dimensional analysis applied to the variables of the simplified model resulted in a lubrication number $\eta_1 \cdot V_+/(\bar{p} \cdot \sigma_t) = H/\sigma_t$ which can be used to represent friction in an LCC.

CHAPTER 4   EXPERIMENTAL PROCEDURE

4.1   SYSTEMS APPROACH

4.1.1   Introduction

From the previous chapter it is clear that the present level of theoretical knowledge does not enable us to predict the different modes of lubrication of an LCC as a function of the operational variables and the element properties. Thus, it was decided to investigate the different lubrication regimes by tribometry.

A systematic approach of tribological contact situations is given by Czichos (1978). He showed that all possible contact situations in tribology can be regarded as tribo-systems.

A system is defined as a set of elements interconnected, by its structure and function. This means that studying a tribo-system is analysing its structure and function. The structure consists of the elements of the system, their relevant properties and the interrelations between these elements. Function is connected to the conversion of the system inputs into the system outputs taking into account the possible disturbances. The above conversion can be divided into the conversion of motion and work, generation or reproduction of information and the transportation or forming of materials. The loss outputs - frictional losses and wear products for tribosystems in particular - which result from this conversion, are of interest. They determine the tribo systems' function and structure. In fig. 4.1 the above mentioned description of tribosystems is shown schematically.
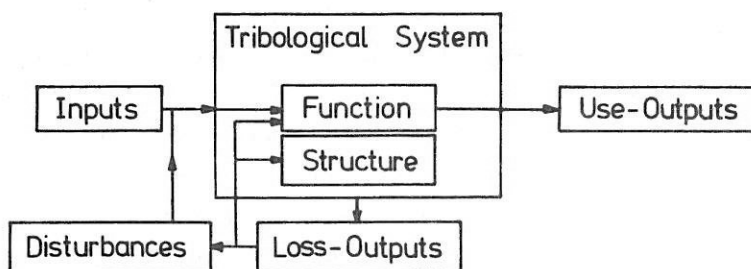

Fig. 4.1: Model for tribo-systems, reproduced from Czichos (1974[c]).

The advantage of this approach is that, both theoretically and experimentally, the knowledge obtained in this way can be applied to practical situations. Caution is needed in this transfer. If even one element property or interrelation is different in comparison to the practical situation, the wrong conclusions may be drawn.

In the next section LCC's are analysed using this systems concept.

4.1.2   Structure and function

The structure of all LCC's can be reduced to the following elements, i.e. two elastically deformable solid surfaces (1) and (2), between them a lubricant (3) and the atmosphere (4) in which the contact is operating. See fig. 4.2. The properties of the elements, which are relevant for friction- and wear processes, can be divided into geometrical-, structural-, mechanical- and thermal properties. These are listed in table 4.1. These properties should be known, not only for the bulk of the elements but also for the surface or the boundary area, because it is there that the interactions between the elements take place. Thus, both the "macro"- and "micro" properties are of importance. However, in literature little is known about the "micro"-properties, Sakurai (1981) and Godfrey (1978).

In fig. 4.3 the interrelations of physical- and chemical nature between the four elements of a lubricated system are presented schematically. Depending on the mode of lubrication these interrelations play a more or less important role in LCC's. The same applies to the properties of the elements. For instance, the diffusion of atmospheric oxygen into the lubricant, followed by oxidation processes between lubricant and the solid elements, are of great importance for the frictional behaviour in the case of ML and BL, whilst for EHL this is of no importance. Bearing this in mind, it is not feasible to study all the possible influences by tribometry, that is, properties of and interrelations between the elements at the same time. A choice must be made under which conditions LCC's are studied and this is outlined in section 4.1.4.
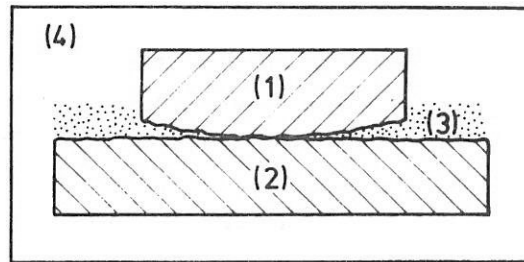
Fig. 4.2: Structure elements of tribosystems.

Table 4.1: Element properties.

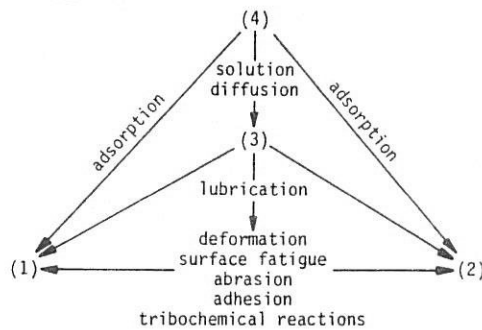| Element	Main properties of interest
1 and 2	Geometry: R∗, surface roughness. Mechanical: E∗, Hardness Metallurgical structure. Thermal conductivity.
3	η, τ_0, τ_1 and G as a function of p and θ. Chemical composition and thermal properties
4	Chemical composition, amount of its components.

Fig. 4.3: Interrelations between the elements of a lubricated system.

The function of an LCC depends upon the system (read construction) in which it is operating. Unless are interested in one LCC application in particular, the study by tribometry of the function in general is the study of the loss outputs friction and wear, represented by the coefficient of friction μ and the specific wear rate k, under known operating conditions. The specific wear rate k is defined as; $k = V/(N \cdot s)$, where V is the wear volume, N the normal force and s the distance of sliding.

4.1.3   Input - Output variables

As suggested above, a quantitative description of the tribological behaviour of a tribosystem should be possible using the coefficient of friction μ and the specific wear rate k. These system-dependent variables, i.e. nonintrisic material properties, can be seen as the response of a tribosystem to the operating variables, caused by different friction- and wear processes within the system. Both are characterized by the relevant properties of the elements involved in these processes. The variables μ and k are also called tribological operators.

These "response" variables μ and k are the outputs of the investigated tribosystem. As already indicated, the inputs are the operational variables; they are defined by the quantities:
- Type of relative motion between the elements (1) and (2). This relative motion can be a superposition of the basic types of motion, i.e. sliding, rolling, spin and impact. These movements can be continuous, oscillating, reciprocating or intermittent.
- Velocity of the elements (1) and (2).
- Normal force applied to the elements (1) and (2).
- Temperature at which the contact is operating.
- Operating time, which determines (together with the velocity) the distance of sliding.

For more detailed information about the operational variables the reader is referred to Czichos (1978).

4.1.4 <u>Summary</u>

For several reasons, as mentioned above, it is clear that the number of possible variables which have influence on friction, is enormous. Therefore, to study LCC's by tribometry it is necessary, as a start, to make choices as to how and under which operating conditions LCC's will be investigated.

The choices made are:

1: Estimation of the transitions EHL-ML and ML-BL as a function of the operational variables. The other operating conditions, i.e. element properties, are kept as constant as possible, at least the initial properties.

2: After these experiments, the influences of different element properties on the transitions are to be examined.

3: The chosen elements:

- Solid elements (1) and (2);

  In practice, in most applications with heavily loaded LCC's the solid elements are made of hardened steel. Therefore, steel used for roller bearings was chosen. Later Aluminum was selected to study the effects of elasticity on the transitions.

- Lubricant (3);

  The use of practical fluids has the disadvantage that they usually contain unknown additives and that the bulk properties are also known insufficiently. Hence, pure fluids with known properties were chosen. In a later stage more practical fluids were tested.

- Atmosphere (4);

  All tests were carried out in laboratory environment, i.e. in air of approximately 60 % relative humidity.

4.2   TRIBOMETERS

Friction measurements were carried out on the following tribometers:

    S-tribometer
    Pin-disc machine
    Two-disc machine

S-tribometer :

   The S-tribometer, shown in fig. 4.7 page 4.15, consists of a
reciprocating pin, sliding on a stationary plate. The plate is held in
a holder, mounted on a heat exchanger, which in turn is supported by
two steel blade springs which only allow parallel movement in the
sliding direction. The heat exchanger is thermostatically controlled.
The pin is fixed in a loading arm, which is connected to the support.
The pivot of this loading arm with support lies in the plane of the
sliding contact. The support, guided by two cylindrical bars,
supported by a system of 4 roll-blocks, is driven by a crank
mechanism, by which the support, and therefore the pin, gets a
sinusoidal motion with an amplitude A = 23 mm. The maximum velocity
is; $\hat{V} = 2\pi \cdot A \cdot f$, in which f is the frequency of the moving support. At
the other end of the loading arm a mechanical lift has been mounted on
the frame. This lift makes it possible to control the length of
contact between pin and plate during one cycle and the minimum sliding
velocity between pin and plate during contact. In this way the sliding
velocity can be held almost constant during the period of contact.
   By pressurizing the bellows on top of the support, the pin is
loaded against the plate. The pressure is kept constant in the bellows
by using a big air-accumulator, which is connected to the bellows. The
normal load is specified by $N = C \cdot (p_b - p_0)$ where C is the conversion
constant (pressure to force) of the bellows, p_b the bellows pressure
and p_0 the bellows pressure needed to touch the pin against the plate.
The bellows pressure is measured by a manometer or a piezo-electric
resistive transducer. With the signal from an electro-magnetic pickup
both the frequency of the moving support is measured by means of a
frequency meter and the number of cycles by an electro mechanical

counter. The temperature of the lubricant is measured with a Ni-CrNi thermocouple.

The frictional force, induced between pin and plate, is measured by the piezo-electric force transducer and recorded, using a digital oscilloscope. In fig. 4.4 the friction force and the velocity as a function of time are schematically shown. It shows that friction is zero during a part of one cycle and rises steeply when the roll does not make contact with the lift anymore; contact is then made between pin and plate. The frictional force decreases very fast when the roll on the loading arm is lifted.
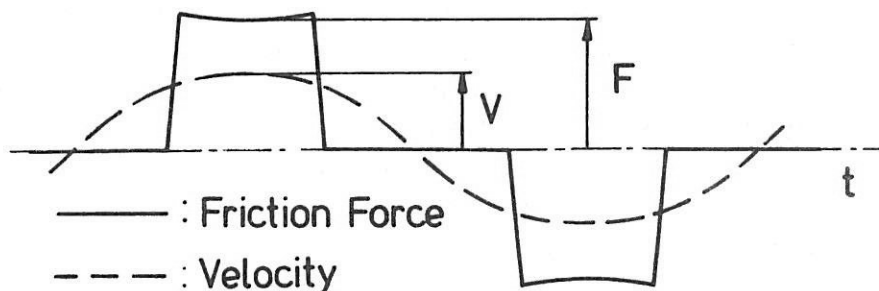
Fig. 4.4: S-tribometer; friction and velocity.

The frictional force during contact is measured at $V = \hat{V}$. Also it is seen that the velocity during contact is almost constant.

Pin-disc machine :

In fig. 4.8 page 4.16, the pin on disc machine is shown. Here a rotating disc is sliding against a stationary pin. This pin and disc combination is placed on a plate, which can deflect around an elastic hinge.

The disc is mounted on the shaft of an aero-static bearing. This shaft is connected to a shaft with a flywheel which, in turn, is driven by a belt from a motor with a continuously variable speed transmission. The connection between the driving shaft and the shaft carrying the disc is realized by a coupling, which is very stiff only in the tangential direction. For a quick disconnection between drive and disc shaft, an

electro-magnetic coupling is placed near the flywheel.

The pin is fixed onto a holder which is suspended in a system of piezo-electric force transducers. This unit, mounted on top of the aero-static bearing can move in a horizontal plane, its pivot lies in the plane of sliding contact. The pin is loaded against the disc by pressurizing the bellows and the pressure is kept constant, as is the case in the S-tribometer. From a thermostatically controlled bath, through a 3 micron filter element, lubricant is supplied on top of the contact between pin and disc with a flow rate $Q \approx 1.2$ l/min.

The principle of this tribometer is as follows: To maintain the rotation of the disc, a torque is needed in the shaft equal to the frictional force, induced between pin and disc, multiplied by the mean radius r of the wear track ($r \gg r_{contact}$). This torque tends to hinge the plate with the pin-disc combination, but the force transducer below the plate prevents this. The stationary friction force can be calculated with $F = F_t \cdot l/r$, where F_t is the measured transducer force and l/r the arm ratio. With the piezo-electric force transducers the variations of the frictional force and normal force under constant operating conditions are measured.

Besides the frictional force, the operational variables N, V and θ are measured. The normal force is $N = C \cdot (p_b - p_0)$, as in the S-tribometer, and is specified by measuring the pressure in the bellows with a manometer or a piezo-electric resistive transducer. With a grooved disc, mounted on the driving shaft and an electrical-optical pulse device the speed of the shaft is measured with a frequency meter. The temperature of the lubricant is measured with a Ni-CrNi thermocouple in the inlet of the contact.

Two-disc machine :

The two-disc machine, described by Lammers (1986), is shown schematically in fig. 4.9 page 4.17. The discs are mounted on shafts and supported on both sides in ball bearings. The left hand shaft-disc combination is mounted in a static housing, the right hand one is mounted in a movable housing, pivoting around a fixed axis. The discs are driven independently by electronically controlled motors through a gearbox and belt. On each shaft an electrical-optical encoder device

is placed; their output signals are converted into speeds, in rpm, by means of a frequency meter or procescomputer.

The discs are loaded together by applying dead weights, suspended on a lever arm with a ratio of 10. The normal force is specified by $N = 10 \cdot (m \cdot g + N_*)$ where N_* is the force due to the mass of the leverarm and pan measured at the pan and m is the added mass. From a thermostatically controlled bath, through a 3 micron filter element, the lubricant is supplied on top of the contact at a rate of $Q \approx 2$ l/min. Four Ni-CrNi thermocouples are placed at the inlet and outlet of the contact to measure the temperatures of the lubricant and of the discs, see fig. 4.9[c]. The frictional torque is equal to $F \cdot D/2$, where D is the diameter of the disc and F the friction; it is measured in the left hand shaft by means of a straingauged torque transducer.

The advantage of this machine, compared to the two other tribometers, is the possibility to investigate the influence of rolling and sliding, sum velocity V_+ and sliding velocity V_-, on friction.

Summarizing, three tribometers have been used to investigate the frictional behaviour of LCC's as a function of the operational variables. In table 4.2 the ranges of these tribometers with regard to the operational variables N, V and θ are given.

Table 4.2: Specifications.

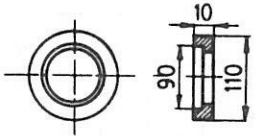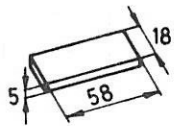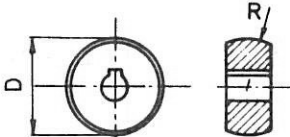|	N (N)	V_+ (m/s)	θ (°C)	Type of motion
S-tribometer	25 - 1000	10^{-3} - 0.5	15 - 100	reciprocating sliding
Pin-disc	25 - 150	10^{-3} - 1.5	20 - 100	continuously sliding
Two-disc	500 - 5000	10^{-2} - 10	15 - 100	continuously rolling and sliding

4.10

With these tribometers the whole or a part of the mixed lubrication regime can be studied. The use of three different tribometers has the additional advantage that possible effects of machine dependant disturbances on the experimental results can be recognized.

The coefficient of friction measurements carried out on these tribometers were found to be consistent to better than $\pm 2 \cdot 10^{-3}$ under the most favourable conditions. The operational number H consisting of the velocity, viscosity (temperature) and pressure (normal force) is found to have a relative error of less than 4%.

4.3   SPECIMENS

The specimens used in the experiments were made of hardened steel AISI-52100 and Aluminum AL 7075-T651; for some material properties see appendix E. In table 4.3 the dimensions of the steel specimen are given, and visualized in figure 4.5.

Table 4.3: Specimen.

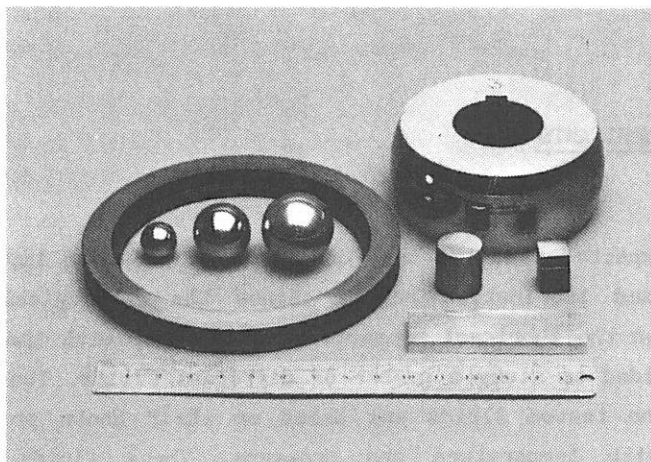|	Pin-disc machine	S-tribometer
Pin	R = 3.175 and 6.35 mm	R = 3.175 , 6.35 and 12.5 mm
	R = 50 and 195 mm	R = 50 and 90 mm.
Counter specimen		
Two-disc machine:		R = 474, 190 and D/2 mm D = 76.2 mm

Fig. 4.5: Specimens

Balls from ball-bearings and rollers from roller-bearings, with a crownradius of 195 mm, were used as pins. Specimens with R = 50 mm were spark eroded out of a sphere of 100 mm diameter. The counter specimens were made from a AISI-52100 tube and hardened by SKF in the same way as their bearing elements. For the two-disc machine, discs with a crownradius of R = D/2, for circular contact measurements, were spark eroded out of steel balls. The other discs with crownradii of R = 474 and 190 mm, for elliptical contact measurements, were made by turning, hardening, grinding and polishing, performed in that order. Aluminum specimens were only tested on the S-tribometer. The pins were made on a computer-controlled lathe with radii of R = 3, 6, 10, 50, 100 and 250 mm respectively.

Most surfaces used in lubrication practice are prepared using a finishing technique, involving the random contact between grits and the surface. Therefore, specimens from standard elements did not receive any extra surface treatment. On the contrary, the "self made" specimens were grinded and polished to also establish a random structure. Depending on the desired roughness, abrasive paper with grit sizes "240", "320", "400" and "600" respectively and for polishing 15, 7, 5 and 1 μm diamond paste was used.

Before each experiment the specimens were rinsed in an ultrasonic cleaner with ethanol and/or carbon tetrachloride and subsequently dried in hot air.

4.12

4.4   LUBRICANTS

It is expected that the type of lubricant plays an important role in the mixed lubrication regime. Since the rheological behaviour depends upon the lubricant properties, which vary with the lubricant, it was decided to study a number of different fluids. The choice for 50 % of the tested fluids was based on their known properties in relation with temperature and pressure. These fluids have been investigated intensively by others under conditions which were expected to provide some form of comparison. The rest of the fluids were chosen because of their use in practice. In appendix B some relevant properties of the fluids are given. From the tables it is clear that the chosen fluids cover a wide range of property values. In section 3.2.3 the influences of temperature and pressure on the rheological parameters is mentioned.

The viscosity versus temperature/pressure relationship, according to Roelands (1966), reads:

$$\eta(p,\theta) = e^{\left\{\left[9.67 + \ln \eta_0\right]\left[1 + \frac{p}{1.962\cdot10^8}\right]^Z \left[\frac{\theta_0 + 135}{\theta + 135}\right]^{s_0} - 9.67\right\}} \quad (4.1)$$

where Z and s_0 are the Roelands pressure- and temperature index respectively. (In appendix B values of s_0 and Z are given).

For the limiting shear stress, which is directly proportional to pressure and almost insensitive to temperature, the ratio of τ_l/p for some liquids are given.

Values of τ_0 and G are not given; their behaviour as a function of temperature and pressure is not well known. According to Hirst and Moore (1980) and Evans (1983) the value of τ_0 changes with temperature according to $\tau_0 = A + B\cdot T$, where T is the absolute temperature. A and B are constants depending on the lubricant. The relation of τ_0 with pressure is still not clear. For G the approximation by Tabor (1982[a]) is used, i.e., $G \approx 30\cdot\tau_l$.

4.5   TEST PROCEDURE

In the above paragraphs it is outlined under which operating conditions the LCC's were investigated. The test procedure was as follows.

Before each experiment to determine a Stribeck curve for LCC's was started, the tribometer specimens and lubricant were warmed up until the desired temperature was reached.

Each measuring point for the Stribeck curve was obtained two to five minutes after applying the normal force, i.e. when a constant coefficient of friction was observed, section 5.2.5. During the experiments, the velocity was changed at constant pressure and temperature. The reason for this proceeding was the desire to carry out experiments in the ML-regime under nearly isothermal conditions. If we assume an idealized Stribeck curve, as drawn in figure 4.6 then, with an experiment under constant contact pressure and temperature, the heat generated in the contact (which is equal to $\mu \cdot N \cdot V_-$) will yield a curve (1) as shown in figure 4.6.
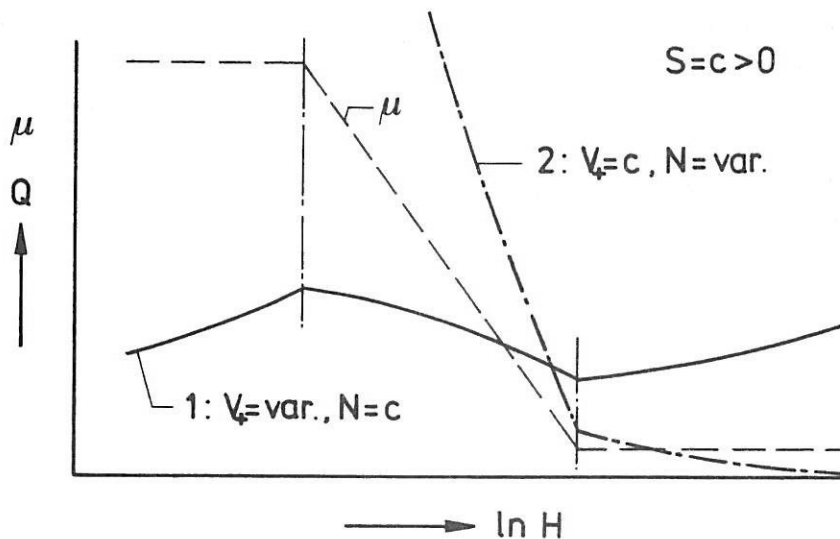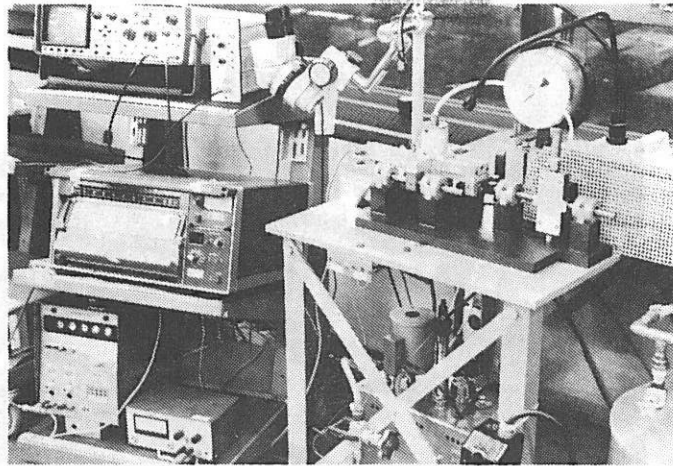

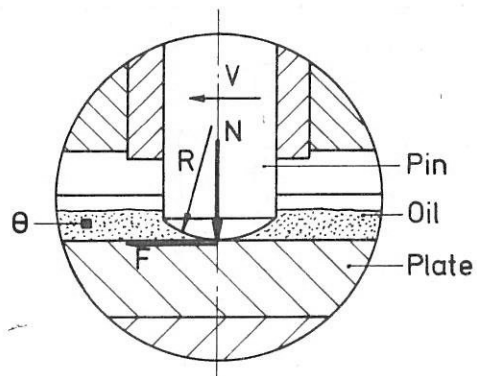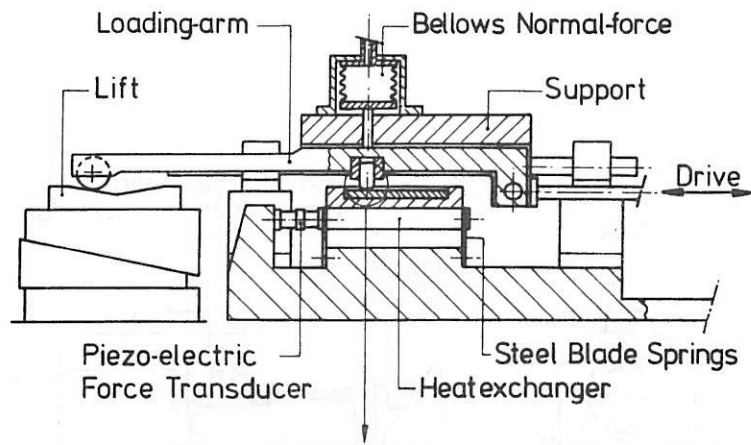Fig. 4.6: Heat generation in the contact during experiment.

In reality this curve will flatten out because the Stribeck curve has smooth transitions from one lubrication mode to the other. If the pressure would have been changed and the velocity and temperature would have been kept constant during the experiments, the generated heat would have risen extremely, see the dotted line (2) in figure 4.6. This is because the normal force has to increase with a factor of eight in order to change the pressure with a factor of two. Changing only the temperature, then the heat generated in the contact varies with the coefficient of friction. Another reason for changing the velocity instead of pressure or temperature is that the Stribeck curve is measured in one point of figure 3.4. Some experiments were carried out by changing the temperature to look for effects on the friction curve when the solid-liquid transition is passed, section 5.3.1.4.

The electrical conductivity of the LCC was measured on the S-tribometer to check if there was any contact between the two opposing surfaces. In appendix F the electrical circuit is given. When a good electrical contact is formed, no potential difference will be observed; the electrical contact resistance is zero. However, when the surfaces are separated by a lubricant film, the difference in potential is that of the full applied value; the resistance is nearly infinite. These measurements were performed with the objective to get a first indication whether there is any contact or not.

After each experiment the test specimens were observed with an optical microscope and roughness values in sliding direction were measured, with a cut-off length of 0.8 mm, on the Talysurf 5T-120-3a or on the Taly-Form surf.

a.

Loading-arm — ┌ Bellows Normal-force
Lift
Support
Drive
Piezo-electric Force Transducer
Heat exchanger
Steel Blade Springs

V
N
R
Pin
Oil
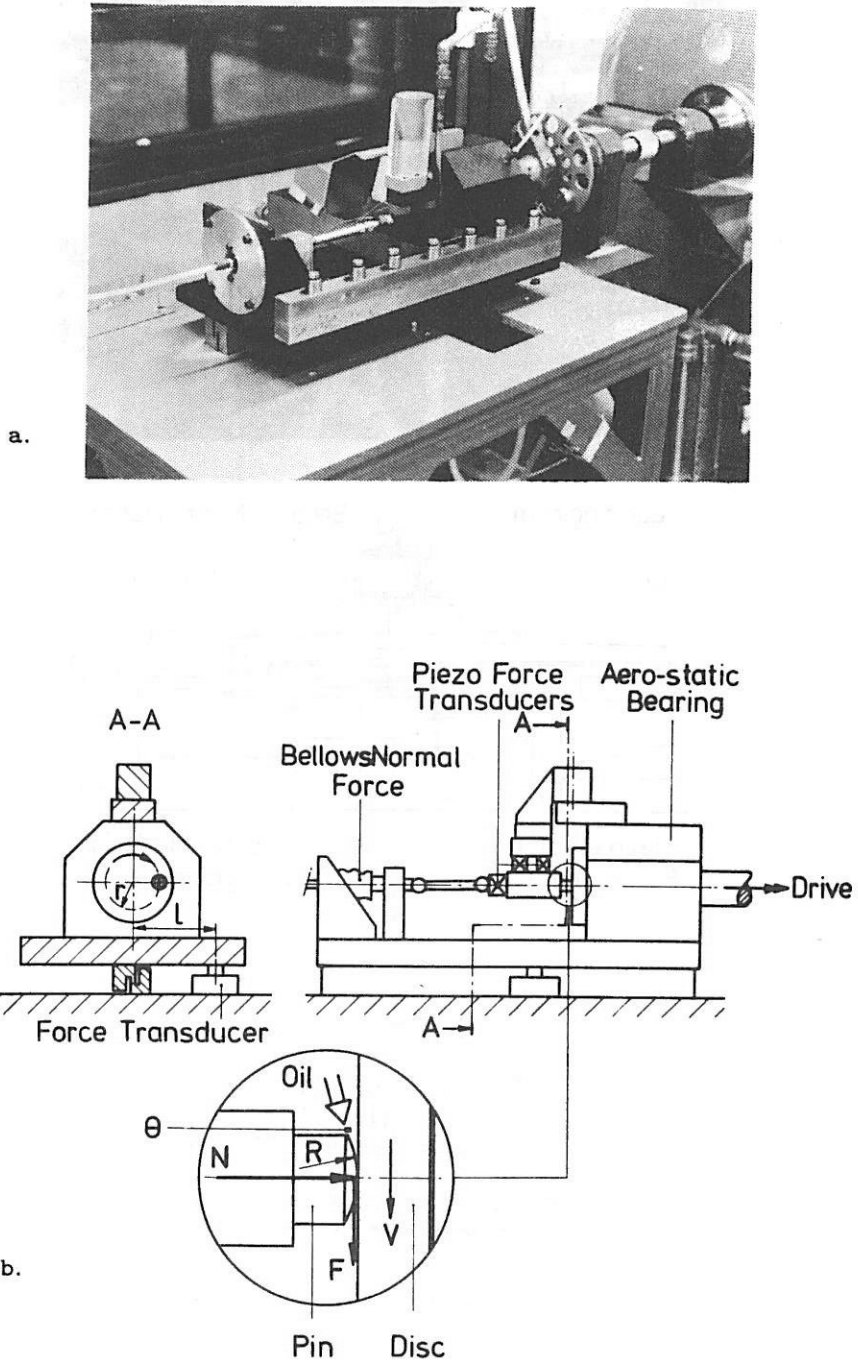θ
F
Plate

b.

Fig. 4.7: a. S-tribometer
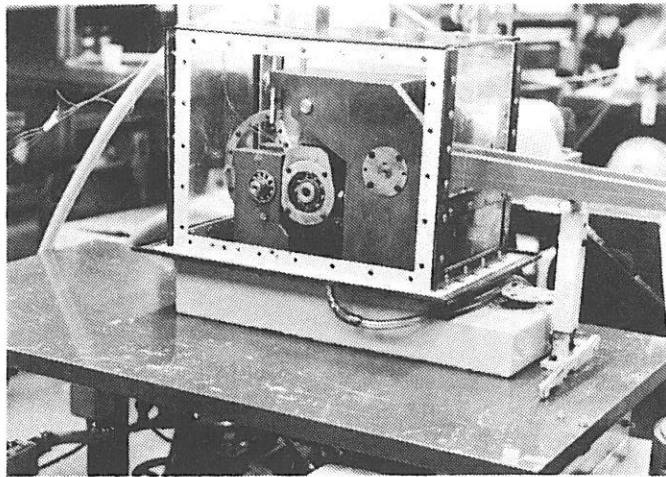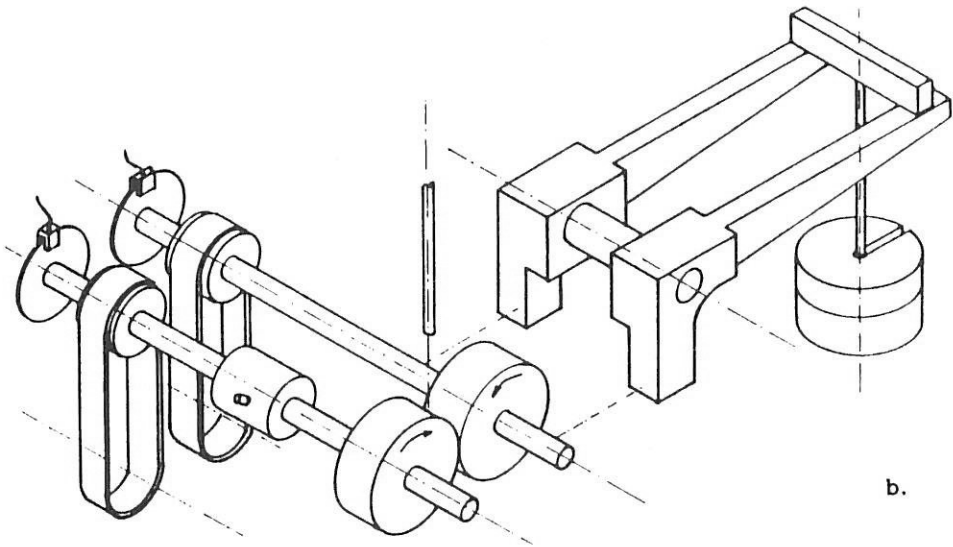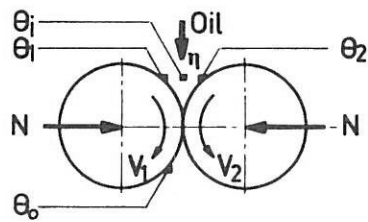   b. General layout

Fig. 4.8: a. Pin-disc machine
b. General layout

a.

b.

c.

Fig. 4.9: a. Two-disc machine

b. General layout

c. Temperature measurement

CHAPTER 5   EXPERIMENTAL RESULTS

5.1.   INTRODUCTION

In this chapter results are presented of experiments carried out on the test rigs described in section 4.2. They are divided into two main parts.

Firstly, experiments in which the influences of the operational variables on friction and the transitions EHL-ML and ML-BL of LCC's have been studied. These experiments include effects of:

- Velocity; with a distinction in sliding- and sum velocity (sliding and rolling as type of motion).
- Temperature; controlling the viscosity of the lubricant.
- Normal force; together with geometry and elasticity modulus, it controls pressure.
- Time or sliding distance; these are mutually related through sliding velocity.

The results of these experiments are outlined in section 5.2.

Secondly, experiments in which the influence of element properties on friction and the transitions is studied. Attention is paid to the effects of lubricant, surface roughness and material on friction and on the transitions. The results of these experiments are presented in section 5.3.

The above experiments result in frictional curves, of the Stribeck type, from which the frictional behaviour in the different lubrication modes and the transitions between these modes as a function of the operational variables and element properties can be studied.

A remark concerning the transitions is of interest. The transitions are defined by the intersections obtained by extrapolating the curves representing the coefficients of friction of the EHL-regime and BL-regime respectively with the tangent of the ML-regime as shown in figure 5.1. The reason for this approach is twofold:

Firstly, in EHL a minimum in the coefficient of friction usually does

not occur, as presented in section 5.2.

Secondly, when for the position of the transition EHL-ML point A* is chosen, see fig. 5.1, then this transition is governed by the highest roughness summit present at one of the rough surfaces. Also this position depends on the arbitrarily chosen difference between the measured friction and the calculated hydrodynamic friction for smooth surfaces at these operating conditions. The latter argumentation is also applicable for point B*, however now for the measured coefficient of friction and the coefficient of friction representing BL.

Thus, points A and B are regarded as the transitions of EHL-ML and ML-BL, respectively.

5.2   OPERATIONAL VARIABLES

5.2.1   Introduction

The experiments described in this section are carried out on run-in AISI-52100 specimens, section 5.2.5, and with Sebacate as a lubricant. Attention is focused on the influences of the operational variables velocity, type of motion (sliding and rolling), temperature (viscosity), normal force (pressure) and the test duration on friction in the different lubrication modes. The other operational conditions like atmosphere (laboratory environment) roughness ($Ra_t \sim 2.5 \cdot 10^{-8}$ m), etc. have been kept constant as much as possible.

5.2.2   Velocity

From the HL- and EHL theory it is known that the velocities of the surfaces play a major role in the hydrodynamic action of the liquid between them. In simple sliding experiments, i.e. keeping one surface stationary, the friction of an LCC at constant normal load and temperature is measured at decreasing- or increasing velocity. The influence of velocity on the coefficient of friction is shown in figure 5.1.
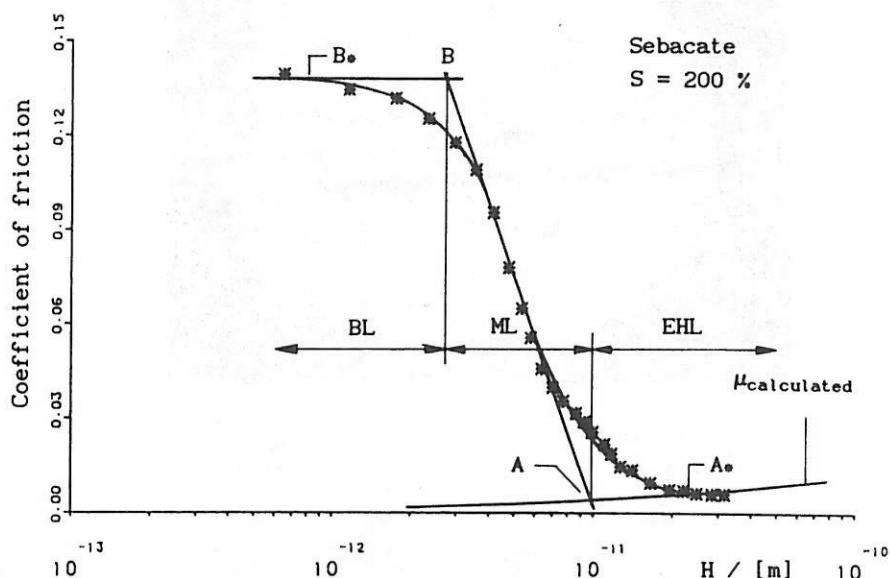
Fig. 5.1: μ as a function of ln H, obtained at constant pressure
($\bar{p}$ = 0.12 GPa) and temperature (θ = 54 $^{\circ}$C) by changing
velocity.

This curve, measured at a low pressure of 0.12 GPa, shows the same
characteristic features as those reported in literature, i.e. low
friction, characteristic of full-film lubrication at the right hand
side, high friction, characteristic of boundary lubrication at the
left hand side of the curve and in between a medium friction,
characteristic of the mixed lubrication regime. The friction curve
which represents the (calculated) hydrodynamic friction of this
contact (if it is assumed that there is no asperity interaction), has
also been drawn. The measurements of the electrical contact resistance
showed the same results as those reported by others, e.g. Czichos
(1977). For H (= $\eta_1 \cdot V_+/\bar{p}$) values greater then H_{A*} the contact
resistance is high, at H values below H_A the contact resistance
becomes very low.

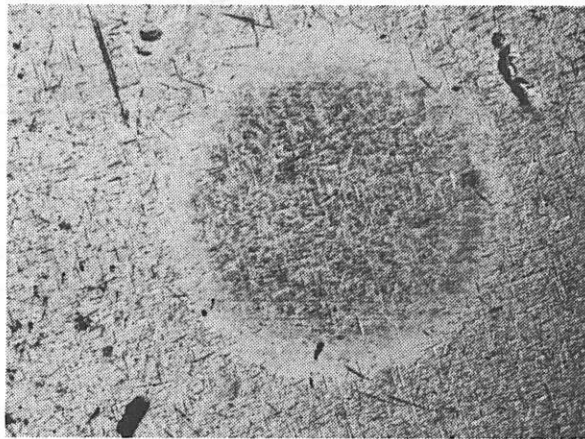Photographs of the wear surfaces on the spheres, taken after the
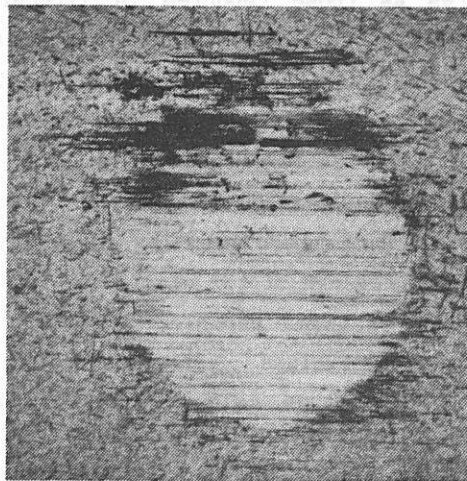
5.4

a.
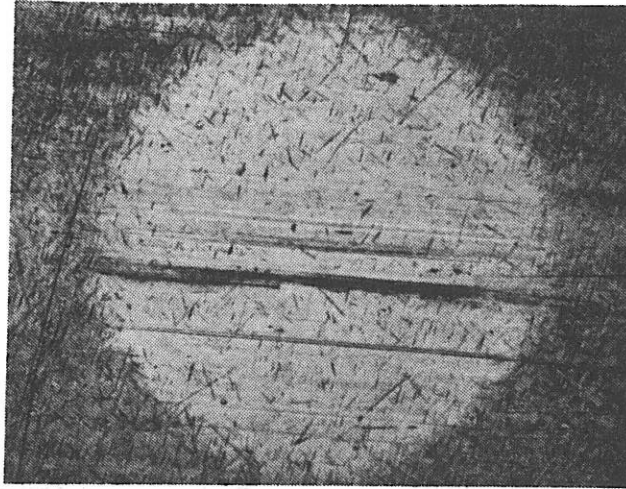
100 μm

b.

100 μm

c.

200 μm

Fig. 5.2: Photographs of the contact region after ML-experiments.

experiments, usually have an appearance as shown in figure 5.2[a]. In this case the radius of the contact area is equal to the Hertzian contact radius. The initial roughness structure has nearly disappeared in the whole contact area. The random roughness structure has changed into a longitudinal structure. Other observed contact spots are presented in the figures 5.2[b] and 5.2[c]. An interesting picture is figure 5.2[b], which shows that the roughness inside the contact is nearly unaffected. The original roughness structure is only wiped off in a ring shaped area. The outer radius conforms to the Hertzian contact radius. Such contact types have frequently been observed, especially at higher pressures. Some experiments resulted into a contact area as shown in figure 5.2[c]. Here the wear radius is larger then the Hertzian contact radius. The wear scar indicates that adhesive wear, probably resulting in abrasive effects, took place. However, most of the contacts showed a contact area as illustrated in figure 5.2[a].

With simple sliding experiments no distinction can be made between the influence of sum- and sliding velocity, $V_+ = V_-$. To determine which of them is the controlling parameter in relation to the transitions, experiments are carried out on the two-disc machine.

In figure 5.3[a] it is shown that the velocity field for the two moving surfaces in a contact, can be regarded as a superposition of a pure rolling- and a pure sliding motion. Figure 5.3[b] shows a diagram with the surface velocities V_1 and V_2, the sum velocity $V_+ = V_1 + V_2$ and the sliding velocity $V_- = |V_1 - V_2|$.

Also lines of constant sum velocity, sliding velocity and constant slip value have been drawn. The slip is defined as:

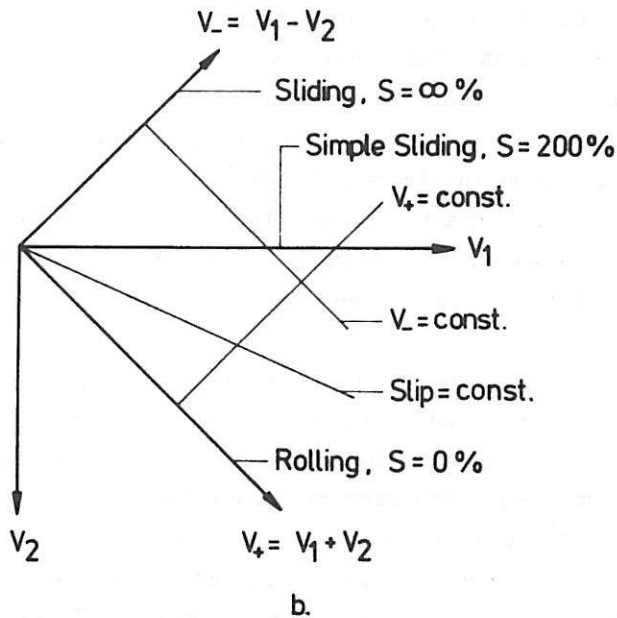$$S = \frac{V_-}{V_+} \, 200 \, \% = \frac{|V_1 - V_2|}{V_1 + V_2} \, 200 \, \% \qquad (5.1)$$
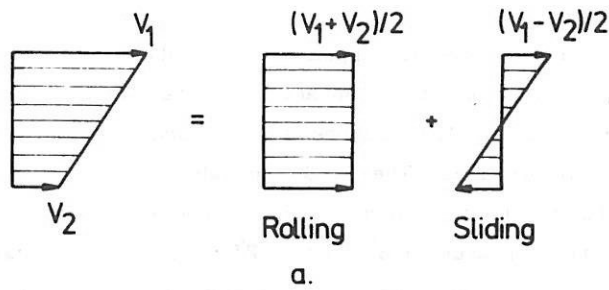
Fig. 5.3: a. Rolling and sliding.
b. Velocity field.

Results from experiments carried out on the two-disc machine are presented in figures 5.4, 5.5 and 5.6. In figure 5.4 the friction curves at constant sum velocities are shown for an elliptical- and for a circular contact. These friction curves, where μ is depicted as a function of slip, illustrate the following features. At high sum velocities (EHL) a typical friction curve as presented in figure 3.2, is obtained. With decreasing sum velocity the influence of the sliding velocity (resulting in heat dissipation) on friction becomes less and less pronounced. At very low sum velocities no significant influence

of the slip, i.e. sliding velocity, has been found. Only at low slip values an increase in friction with increasing slip is found. In figure 5.5 constant slip measurements are presented for an elliptical- and for a circular contact situation in terms of Stribeck-like curves. For the elliptical contact situation a transition EHL-ML occurs, whilst for the circular contact situation both transitions EHL-ML and BL-ML are visible. Note that at the abscissa $\eta_1 \cdot (V_1 + V_2)/\bar{p}$ is used, and (with constant η_1 and $\bar{p}$) in fact the effect of V_+ is shown. Figure 5.5 does not show a minimum for the coefficient of friction at the transition EHL-ML. The coefficient of friction in the EHL-regime decreases with increasing V_+. Figure 5.6 is a 3-dimensional plot of figures 5.4 and 5.5 for the elliptical and circular contact situation. Returning back to figures 5.4 and 5.5, it appears that the sum velocity merely determines the transitions EHL-ML and ML-BL. The sliding velocity only plays a significant role with regard to friction if there is mainly hydrodynamic action or when only a low slip is present.
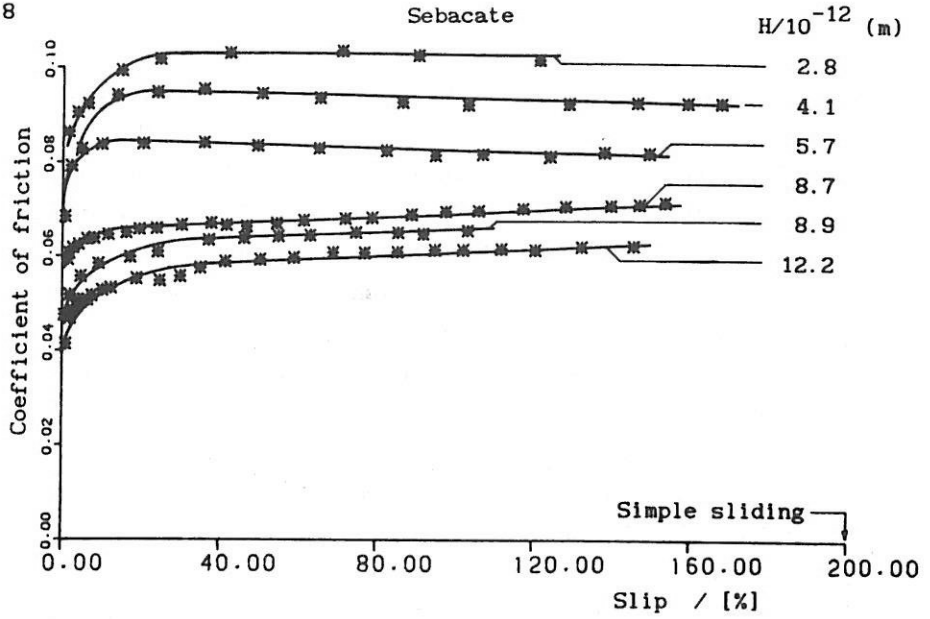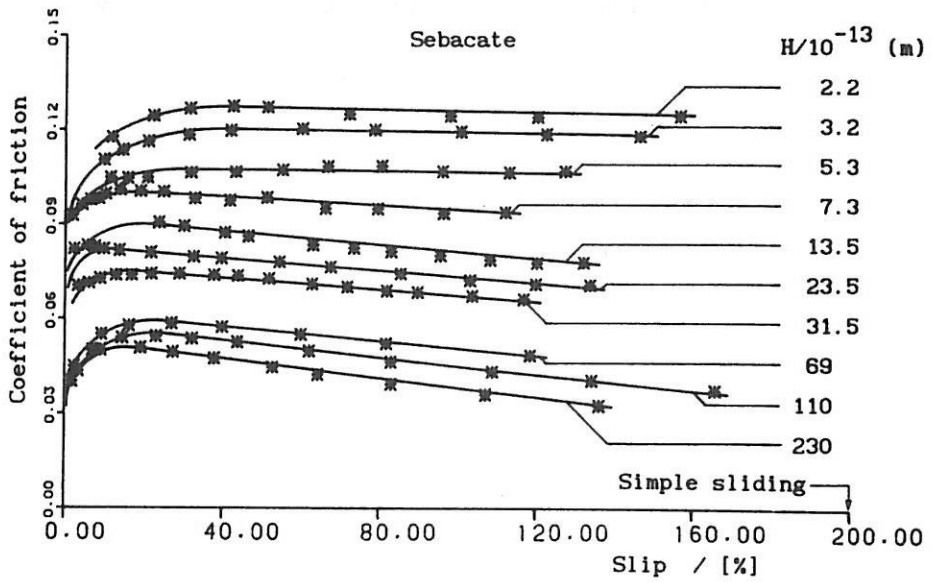
Fig. 5.4: Coefficient of friction as a function of
slip at constant $H = \eta_1 \cdot V_+ / \bar{p}$ values.

a: elliptical contact, $\bar{p} = 0.57$ GPa and $\theta = 21$ $^{\circ}$C.

b: circular contact, $\bar{p} = 1.34$ GPa and $\theta = 24$ $^{\circ}$C.

Fig. 5.5: Coefficient of friction as a function of

$H = \eta_1 V_+ / \bar{p}$ at constant slipvalues.

a: elliptical contact, $\bar{p} = 0.57$ GPa and $\theta = 21$ °C.

b: circular contact, $\bar{p} = 1.34$ GPa and $\theta = 24$ °C.
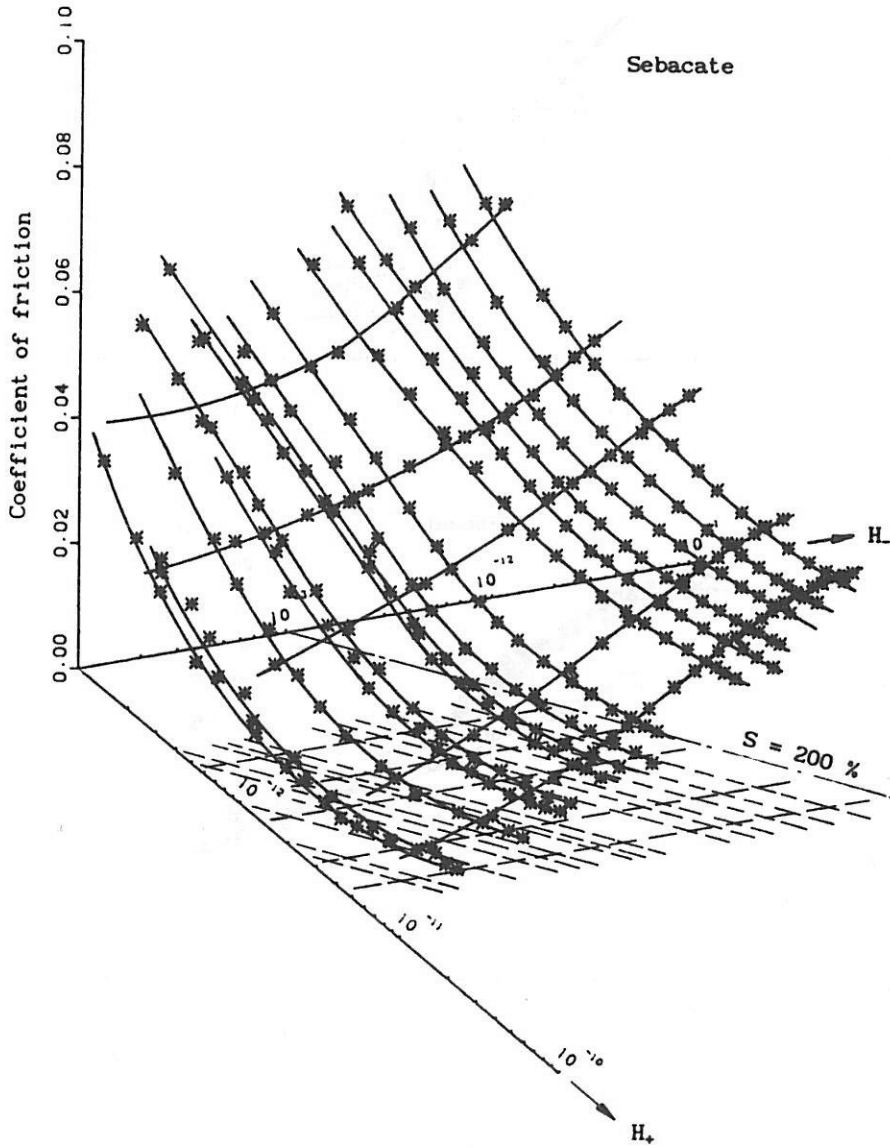
Fig. 5.6^a Three dimensional representation of the coef-
ficient of friction as a function of H_- and H_+,
where $H_- = \eta_1 \cdot V_-/\bar{p}$ and $H_+ = \eta_1 \cdot V_+/\bar{p}$.
Elliptical contact, $\bar{p}$ = 0.57 GPa and θ = 21 ^{o}C.
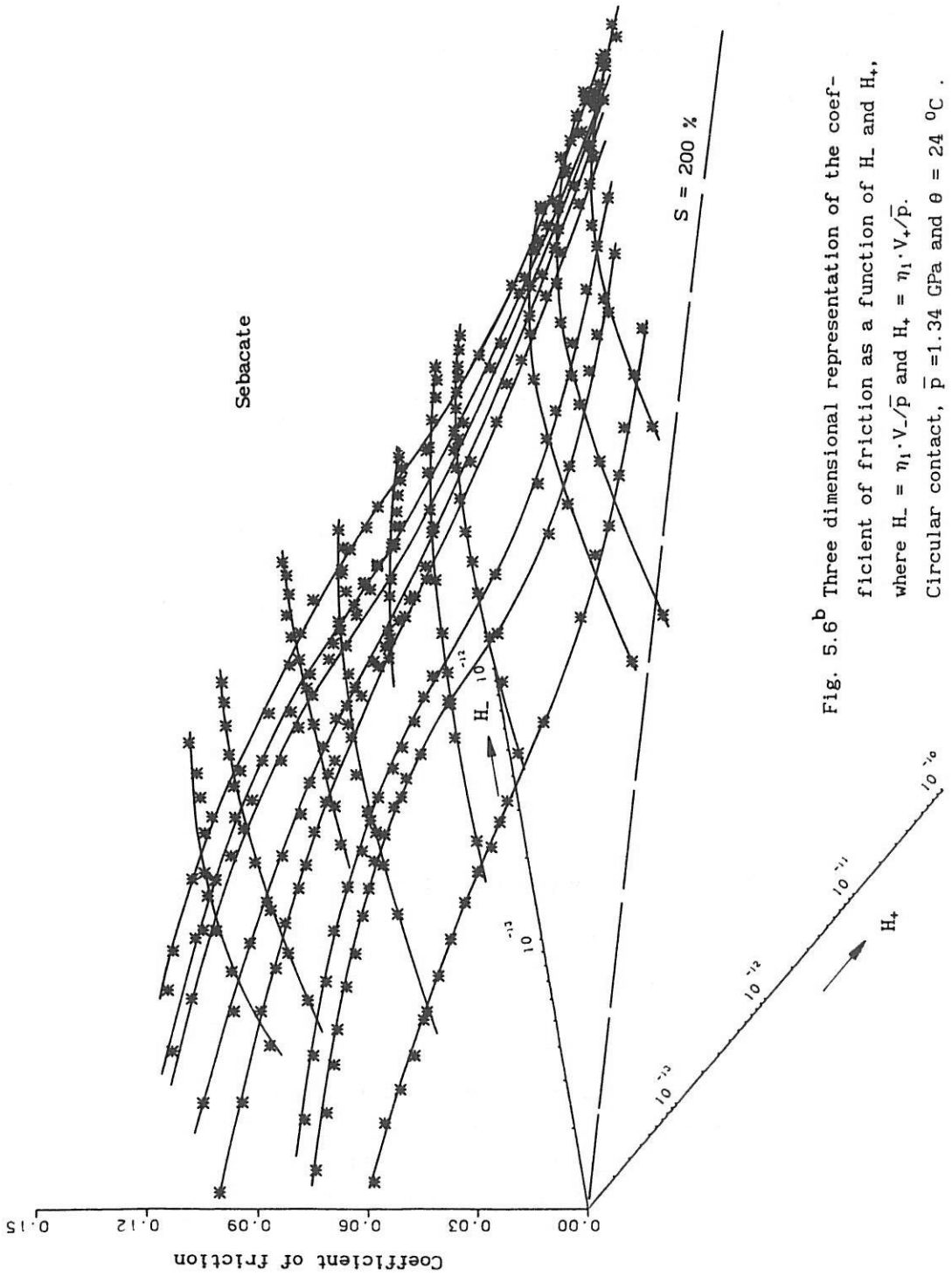
Fig. 5.6^b Three dimensional representation of the coefficient of friction as a function of H_ and H_+, where H_ = $\eta_1 \cdot V_- \sqrt{\bar{p}}$ and H_+ = $\eta_1 \cdot V_+ \sqrt{\bar{p}}$. Circular contact, $\bar{p}$ =1.34 GPa and θ = 24 ^{o}C .
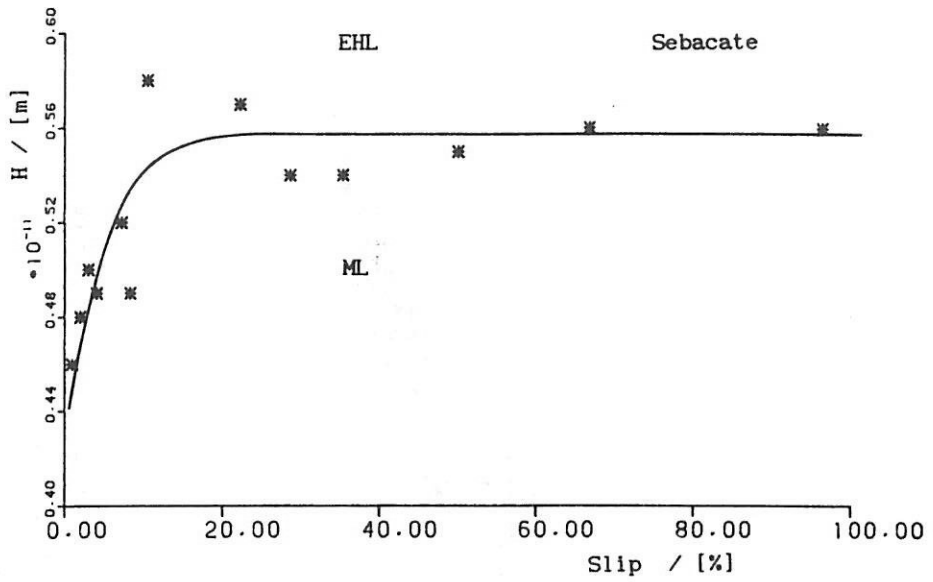
a.
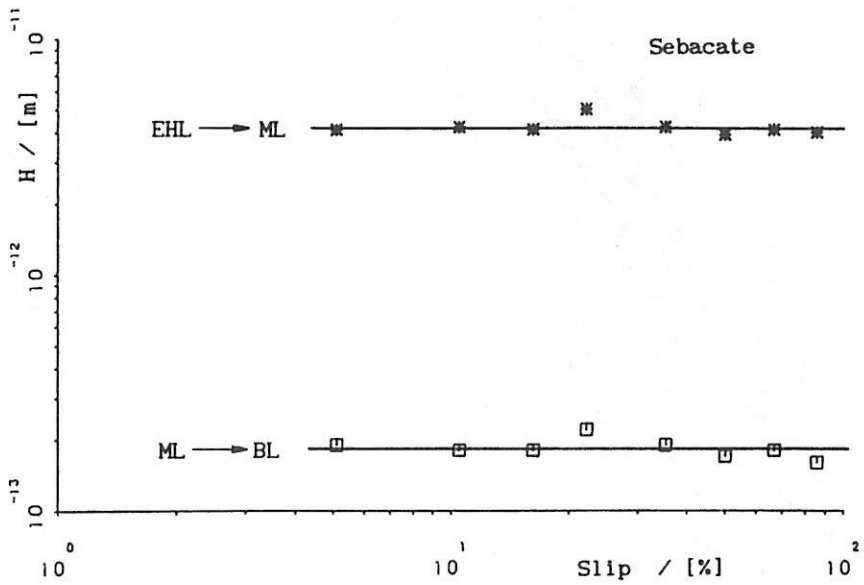
b.

Fig. 5.7: Transitions EHL-ML and ML-BL as a function of
slip at constant pressure and temperature.
a: elliptical contact, $\bar{p}$ = 0.57 GPa and θ = 21 $^{\circ}$C.
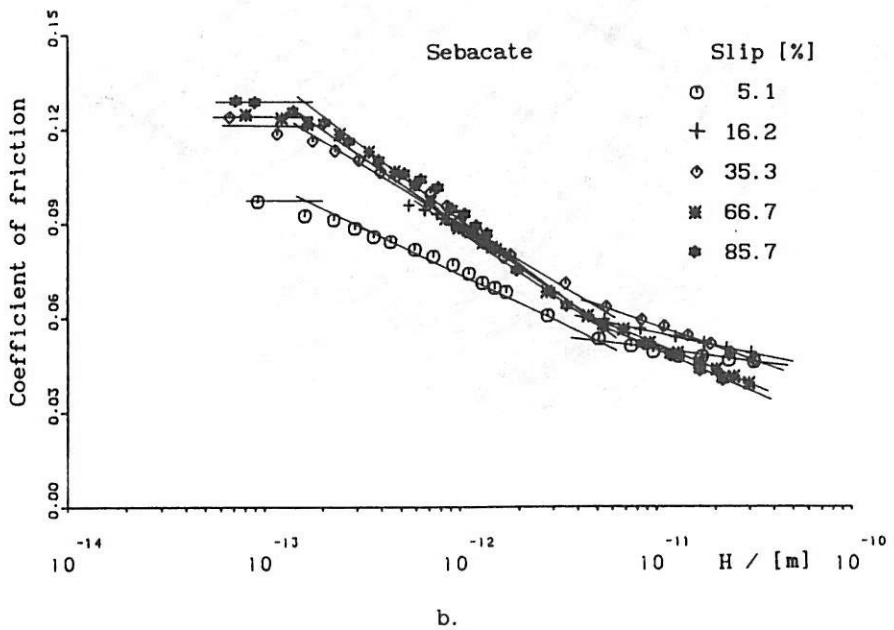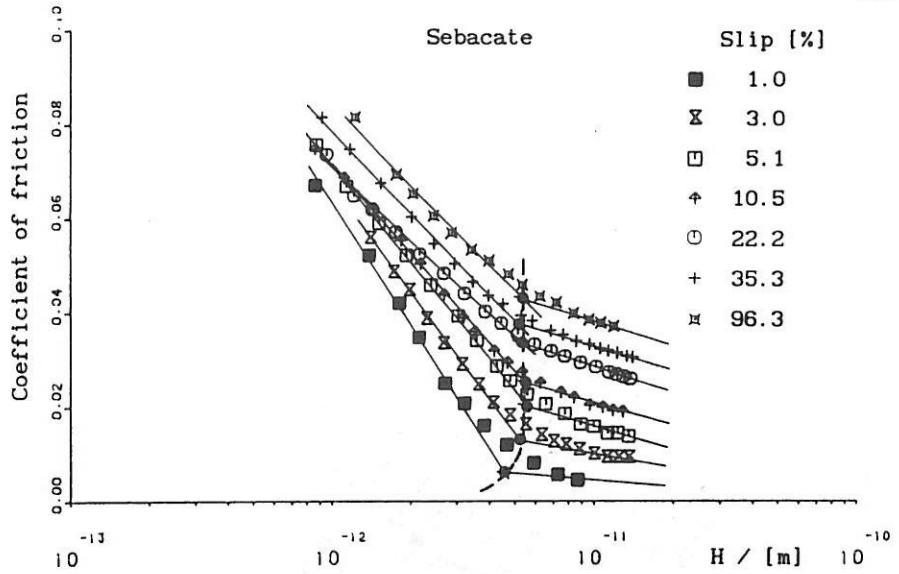b: circular contact, $\bar{p}$ = 1.34 GPa and θ = 24 $^{\circ}$C.

Using the method as mentioned in section 5.1 to determine the transitions EHL-ML and ML-BL at different slip values, figure 5.7 has been obtained where $\eta_1 \cdot V_+/\bar{p}$ is depicted as a function of slip. It shows that both the transitions EHL-ML and ML-BL are mainly controlled by the sum velocity and not by the sliding velocity as is often suggested in literature. Only at small slip values the transitions EHL-ML and ML-BL shift to lower values of H, i.e, sum velocities, as illustrated in figure 5.7[a] for the transition EHL-ML. This is not surprising, since in the pure rolling situation only rolling friction occurs, no sliding friction is present. Obviously ML and BL does not manifests itself in friction in the pure rolling contact situation. Although some micro-slip (Heathcote, Reynolds) in the contact is present and therefore some sliding friction, still a shift of the transitions to lower values of H (V_+) occurs. In figure 5.8 the transitions EHL-ML and ML-BL are presented schematically as a function of V_- and V_+.
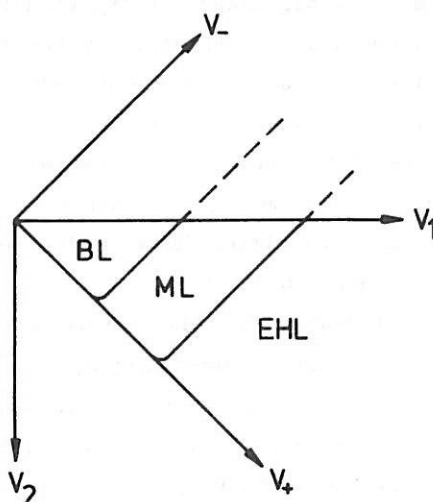

Fig. 5.8: Transitions EHL-ML and ML-BL as a function of V_- and V_+ at constant pressure, temperature and element properties.

Knowing that the sum velocity is the controlling parameter for both transitions it can be concluded that results concerning these transitions, which are obtained from simple sliding experiments, can be used for nearly the entire slip region.

5.2.3   Temperature

The influence of temperature and with that the influence of the
lubricant's viscosity on friction, has been studied at low- and at
high pressures using run-in circular contacts. The low pressure
measurements were carried out under conditions of simple sliding, the
high pressure contact situation at a slip value of 50 %. In figures
5.9 and 5.10 the friction curves at different temperatures are given.
At a pressure of 0.12 GPa, figure 5.9, the temperature was changed
from 17.5°C to 90°C, whereby the viscosity changed with a factor of
approximately 7. Apart from some minor differences all friction curves
coincide. For the calculation of H the inlet viscosity is used. Figure
5.10 shows results of a temperature change from 20°C to 63°C at a
pressure of 1.34 GPa. The viscosity changed by a factor of 3.5. These
friction curves show a clear difference in friction in the EHL-regime,
in accordance with the rheological behaviour of the lubricant at these
conditions as pointed out in sections 3.2.2 and 3.2.3. Because the
lubricant significantly contributes to friction (which is not the case
at low pressures), the friction curves converge in the ML-regime
towards the BL-regime. If μ is depicted as a function of $H = \eta_i \cdot V_* / \bar{p}$,
they converge to the same transition ML-BL and diverge in the other
direction to the same transition EHL-ML.

Thus, by using H as a parameter, the transitions from EHL-ML and
ML-BL are maintained at different temperatures, for both the low- and
the high pressure situation. These measurements show that both the
transitions EHL-ML and ML-BL are controlled by the viscosity of the
lubricant at the inlet of the contact.
If the heat production in an LCC is high, resulting in a temperature
rise of the elements, then the viscosity in the inlet will decrease,
compared to the viscosity present in an iso-thermal situation. This
results in a decrease of H and therefore in an increase in friction,
etc. This continues until a stationary situation or failure occurs. In
these experiments no shear heating effects have been observed.
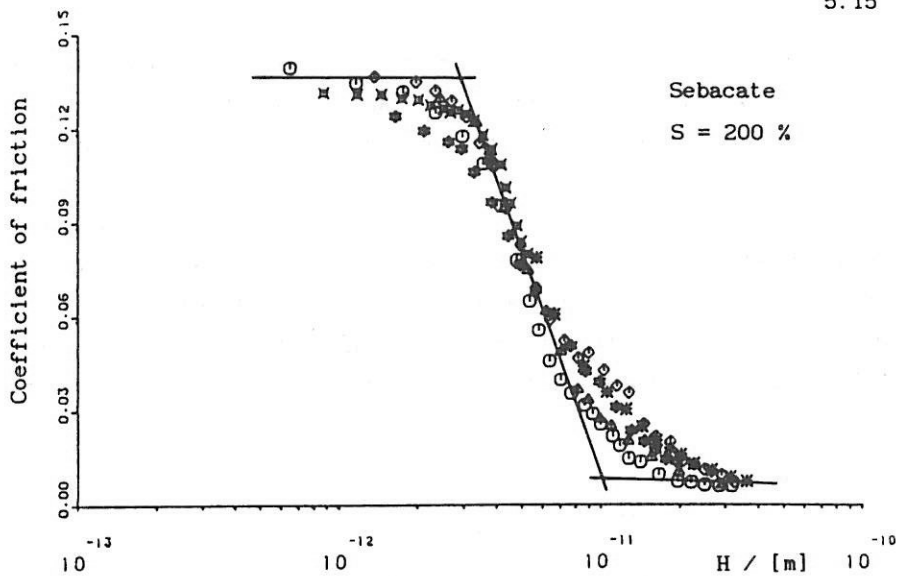
Fig. 5.9: μ - ln H curves for different temperatures at a pressure of 0.12 GPa. ✳ = 17.5 ^{O}C, ▲ = 37.5 ^{O}C, ① = 54 ^{O}C, ◇ = 69 ^{O}C, ✿ = 80 ^{O}C and ✕ = 90 ^{O}C.
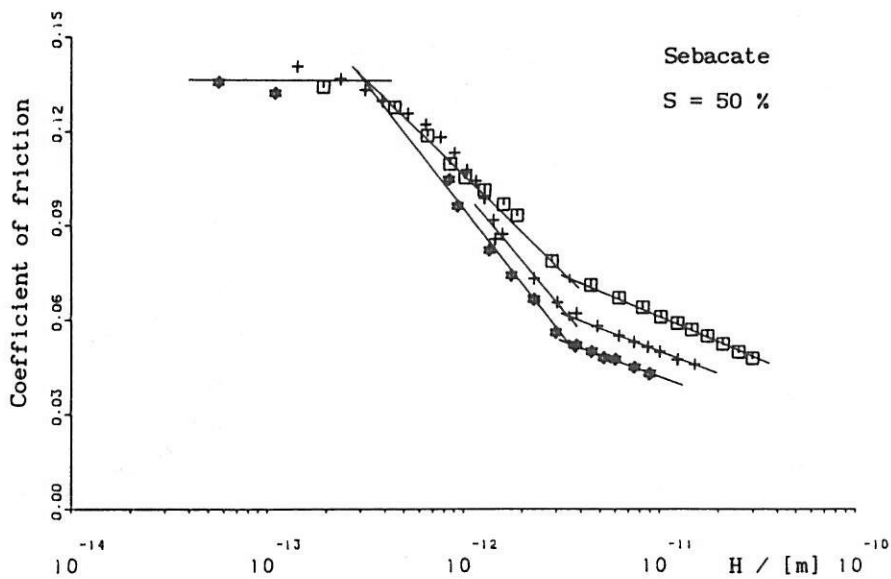
Fig. 5.10 μ - ln H curves for different temperatures at a pressure of 1.34 GPa. □ = 20 ^{O}C, + = 41 ^{O}C and ✿ = 63 ^{O}C.

The observation that the inlet viscosity and the sum velocity are controlling both the transitions EHL-ML and ML-BL, confirms that hydrodynamic action in the inlet region of an LCC is important.

Again it is seen, figures 5.9 and 5.10, that at higher pressures the friction curve shifts to lower values of H and also that the curve does not show a minimum in the coefficient of friction at the EHL-ML transition, as in the case of low pressures (Stribeck). This is caused by the behaviour of the lubricant at high pressures, figure 3.5. From this it is clear that the minimum friction concept for estimating the transition EHL-ML is not applicable to LCC's.

5.2.4   Normal force/pressure

In the previous experiments it was found that pressure influences the position and the shape of the friction curves if μ is related to the parameter H. Figure 5.11 shows the effect of pressure on the μ – ln H curve.
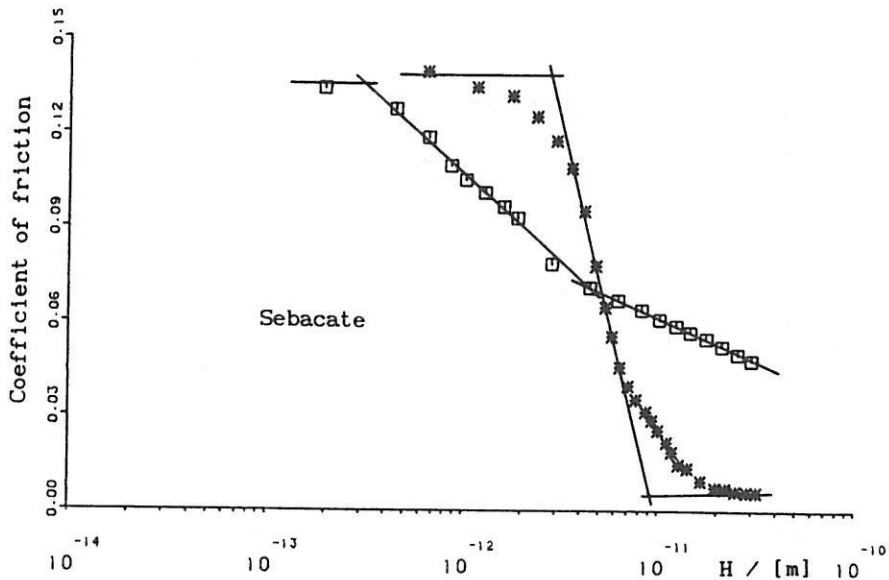
Fig. 5.11: Influence of pressure on the μ – ln H friction curve.

    ✳ : $\bar{p}$ = 0.12 GPa, θ = 20 $^{\circ}$C and S = 200 %.

    □ : $\bar{p}$ = 1.34 GPa, θ = 20 $^{\circ}$C and S = 50 %.

With increasing pressure, the transitions EHL-ML and ML-BL shift to lower values of H and the slope of the tangent of the ML friction regime decreases. The coefficient of friction near the transition EHL-ML strongly increases with pressure, whilst the coefficient of friction in the BL-regime is almost unaffected by pressure. In figure 5.12 the transitions EHL-ML and ML-BL, represented by the appropriate H-values, are given as a function of $\bar{p}_{Hertz}$.
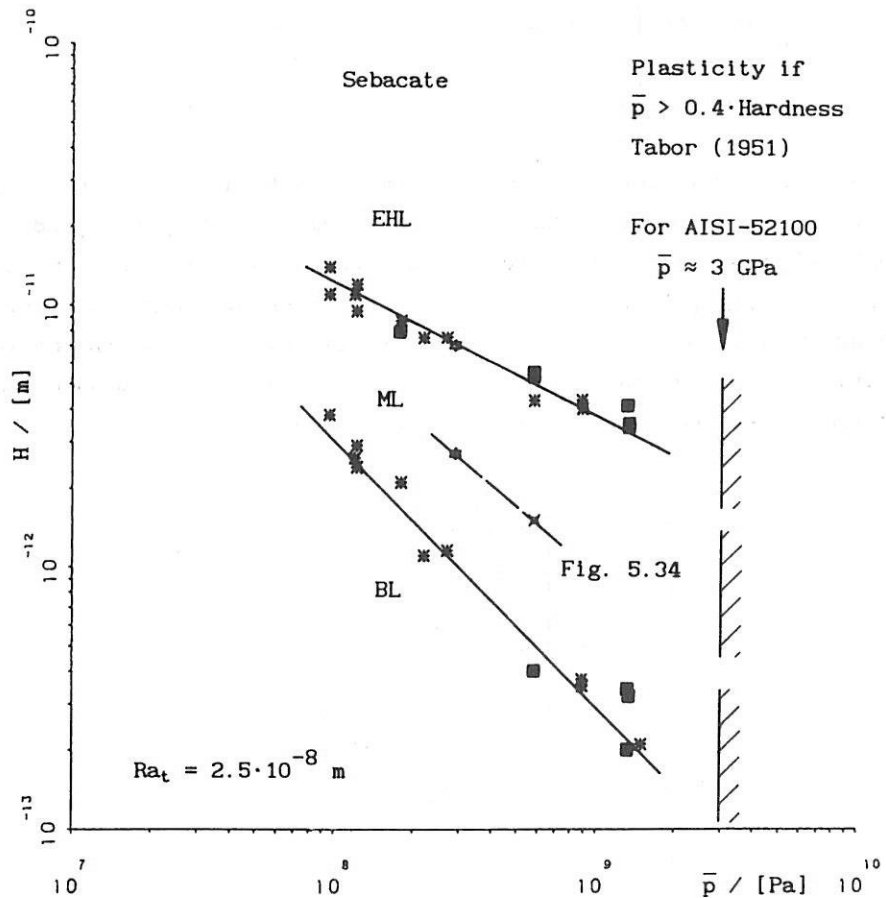
Fig. 5.12: Transitions EHL-ML and ML-BL represented by H as a function of the mean Hertzian contact pressure $\bar{p}_{Hertz}$. The ✽ and ✖ marked results are discussed in section 5.4.

Figure 5.12 clearly shows a dependence of the transitions on pressure. The transitions EHL-ML and ML-BL can be described by the relation:

$$H = c_1 \cdot \bar{p}_H^{c_2} \qquad \text{or} \qquad \eta_1 \cdot V_+ \cdot \bar{p}_H^{-(1 + c_2)} = c_1 \qquad (5.2)$$

where:

	c_1	c_2
EHL - ML	$1.25 \cdot 10^{-7}$	- 0.5
ML - BL	$3.1 \cdot 10^{-4}$	- 1

A remarkable result for the transition ML-BL is found, i.e., for this transition equation (5.2) shows that it is controlled by the product of $\eta_1 V_+$ at constant element properties. That means that, as long as $\eta_1 \cdot V_+ > \eta_1 \cdot V_+|_{\text{ML-BL}}$, an LCC can not enter the BL-regime by only raising the pressure. Obviously, this assumes that the temperature in the inlet is not raised by shear heating. If shear heating does occur then the dotted curve in figure 5.13 will be followed.
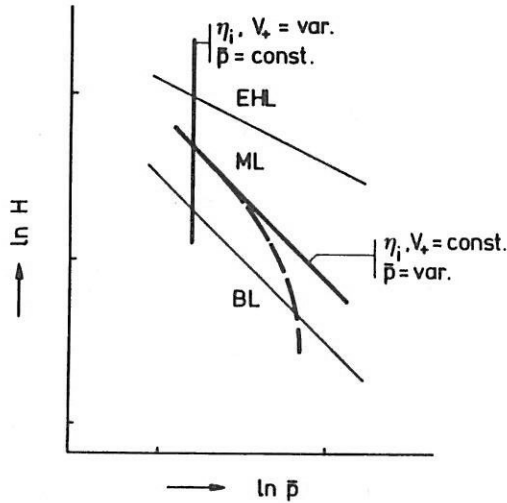
Fig. 5.13: Changing viscosity, velocity and pressure in the
ln H - ln $\bar{p}$ graph at constant micro-geometry.

The influence of pressure on the transition EHL-ML, has the following consequence. In section 3.4.4 is was shown that the relation between the film thickness h and the operating parameter H is given by h = $0.32 \cdot \alpha^{0.55} \cdot E_0^{0.40} \cdot N^{0.15} \cdot H^{0.70}$. These experiments were carried out with the same lubricant and with run-in AISI-52100 specimen with the same surface roughness, $Ra_t \sim 2.5 \ 10^{-8}$ m. The (■) dotted data-points of figure 5.12 represent experiments performed at the same normal force and temperature. Thus, for these experiments the relation h = $c \cdot H^{0.7}$ is valid. On the basis of these results it can be concluded that the commonly used h/σ_t ratio, to characterize the transition EHL-ML, is pressure dependent and, thus, is not a constant as suggested in literature.

5.2.5   Time – Running in effects

The fourth important operational variable is sliding distance or time. Several investigators, Ku et al. (1978[a,b]) Carper et al. (1973, 1975), Bell et al. (1972[a,b], 1975) showed that LCC's were failing after a certain operating time, when working with a constant normal force, velocity and temperature of the supplied oil. Mostly this failure in time is caused by a temperature rise (heat dissipation) which was not controlled in the tribosystem as shown schematically in figure 5.14. For an LCC the temperature rise at the inlet is of importance with respect to the pressure generation and the film thickness respectively.

Wear and the processes involved in it, change the properties of the elements in time. One of the most changing properties due to wear is geometry. At first sight, macro-geometry increases with wear (if possible) and generally as a consequence, the load capacity also increases. However, not only the macro-geometry, but also the micro-geometry changes, even when macro-geometry wear is not present. This change in micro-geometry either increases or decreases the hydrodynamic action. It is worth noting that this change in micro-geometry is not only affected by wear but also occurs
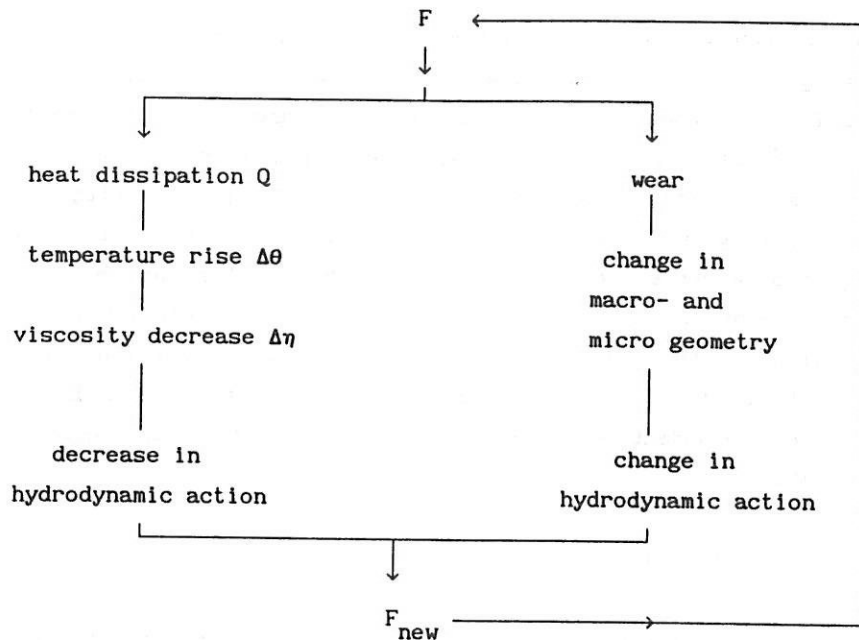
Fig. 5.14: Change in friction of an LCC at constant
operational variables.

when plastic deformation of the asperities takes place.* Thus, in
general, wear increases or decreases friction depending on the change
in micro- and macro-geometry. In practice the term running-in is used
if the load carrying capacity increases, i.e. the hydrodynamic action
increases, resulting in a decrease in the friction at constant
operational variables.

---

* This plastic deformation is related to the hardness of the material.
In the dimensional analysis of section 3.4.3 the hardness H is not
taken into account because run-in elastic deformable surfaces were
considered. If H is added to equation (3.18), a term in equation
(3.21) appears in the form $(\eta_1 \cdot V_* / H \cdot s)^{c_{13}}$. Together with the 8th,
9th and 12th term, the Greenwood's plasticity index ϕ =
$E_* / H \cdot (\sigma/\beta)^{1/2}$ is found (c_8 = -1/2, c_9 = 1/4 and c_{12} = -1).
Plasticity of the asperities occurs at values of $\phi > 1$ and they
deform elastically if $\phi < 0.6$.

To avoid influences of time or sliding distance and herewith errors in interpretation in determining the transitions EHL-ML and ML-BL, this effect was studied in more detail. Two methods were used to measure friction in time. Firstly, a quick friction measurement after a change in velocity at constant operating temperature and pressure. Secondly, after a few minutes, i.e. after a certain sliding distance, the value of the friction was measured when the recorded friction almost did not change any more at these operating variables. Using the first method of friction measurement, the surfaces hardly got the chance to conform or accommodate to each other under the applied operating conditions. With the second method, the surfaces had ample time to properly accommodate to each other at each operating contact situation, i.e., a quasi-stationary friction situation developed. The difference between the results obtained with these two methods is illustrated by the μ - ln H curves shown in figure 5.15. By using the method of "quick friction measurement" a steeper friction curve for the ML-regime was obtained.

5.22
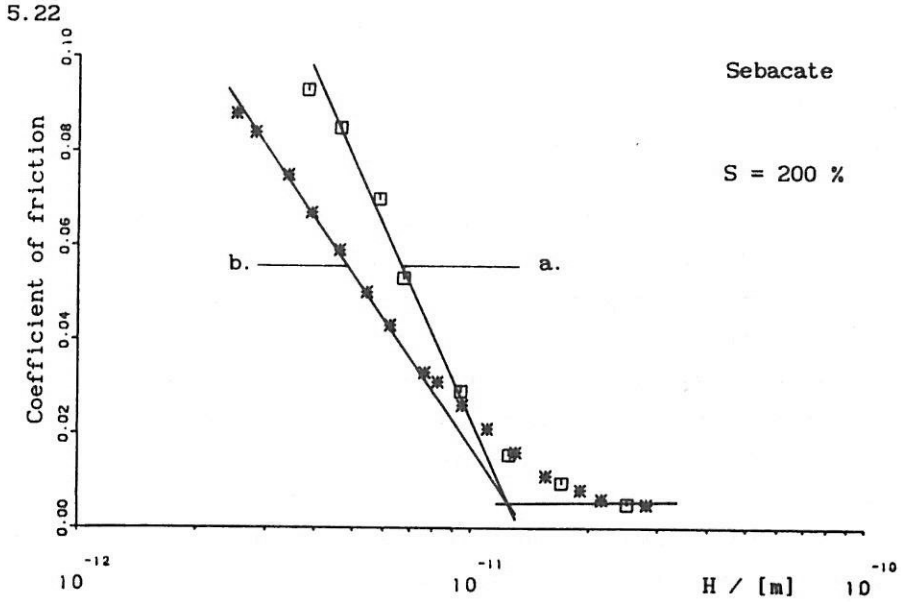
Fig. 5.15: μ–ln H curves obtained at $\bar{p}$ = 0.12 GPa and θ = 31 °C
using: a. the quick friction measurement (□).
b. the quasi-stationary friction measurement (✳).
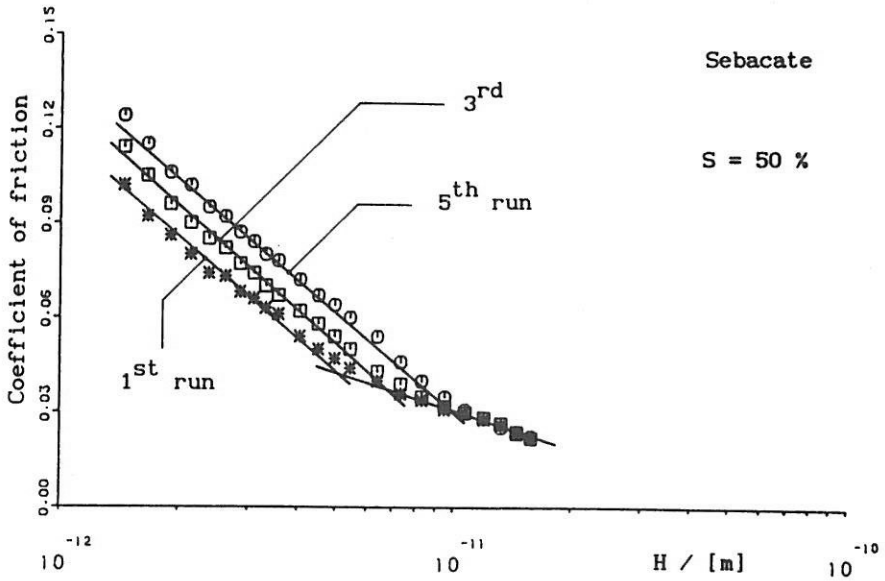
Fig. 5.16: μ–ln H curves obtained by quick friction measurement
for several runs into the ML-regime with the same
contact at $\bar{p}$ = 0.58 GPa, θ = 18 °C and S = 50 %.
✳ = 1st run, □ = 3rd run and ◉ = 5th run.
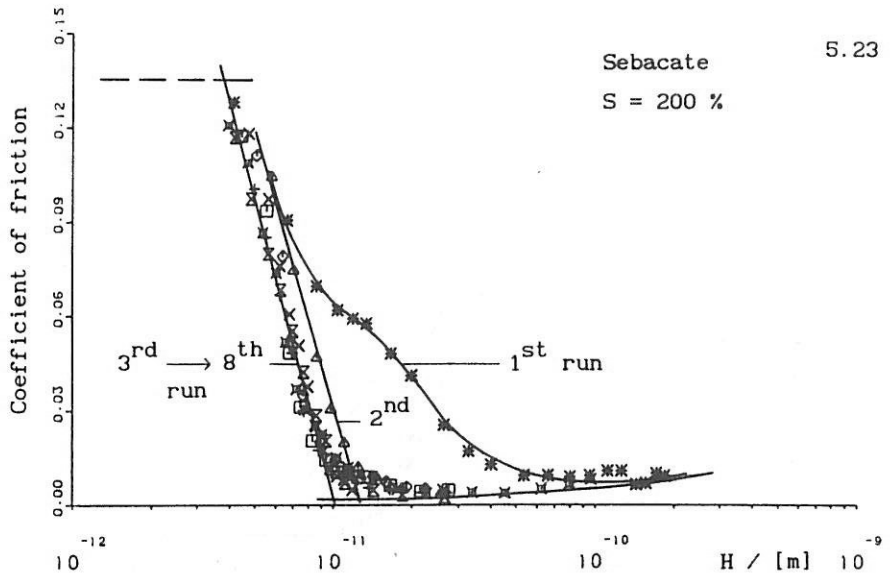
Fig. 5.17: μ-ln H curves obtained by quasi-stationary friction measurement for several runs through the ML-regime with the same contact at $\bar{p} = 0.1$ GPa, $\theta = 22$ $^{\circ}$C and S = 200 %.. Run no: $\ast$ = 1, $\triangle$ = 2, $\diamondsuit$ = 3, + = 4, $\square$ = 5, $\times$ = 6, $\mathbb{X}$ = 7 and $\bowtie$ = 8.
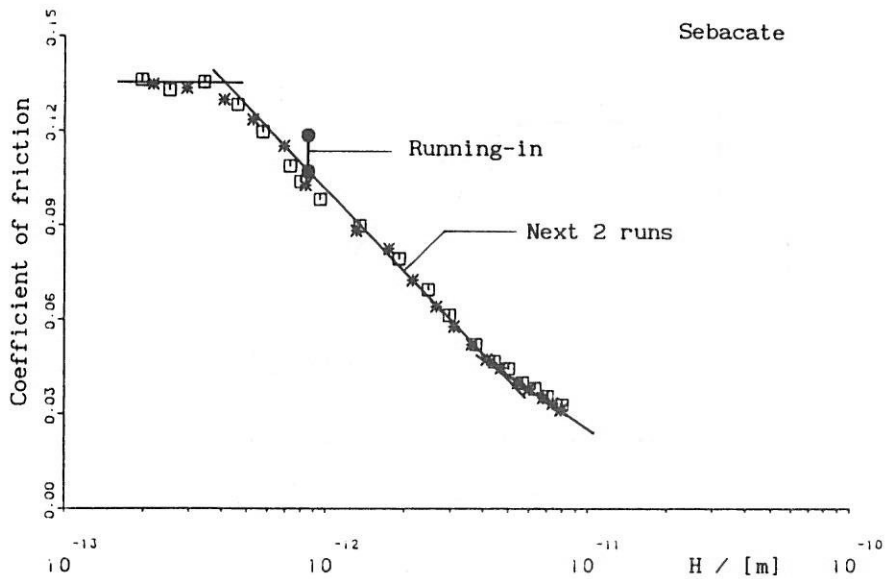
Fig. 5.18: Running-in at constant $\eta_1 \cdot V_+/\bar{p}$, followed by two runs governed with the quasi-stationary friction measurements at $\bar{p} = 0.57$ GPa, $\theta = 20$ $^{\circ}$C and S = 50 %.

a.

b.
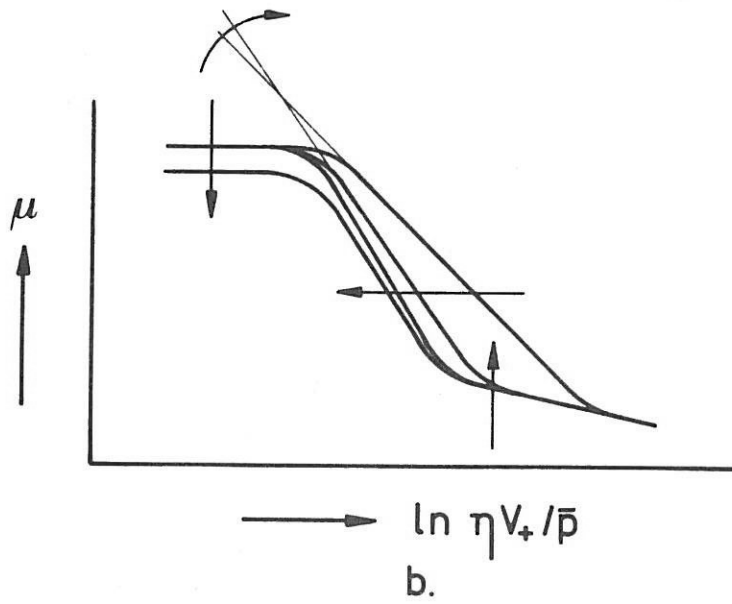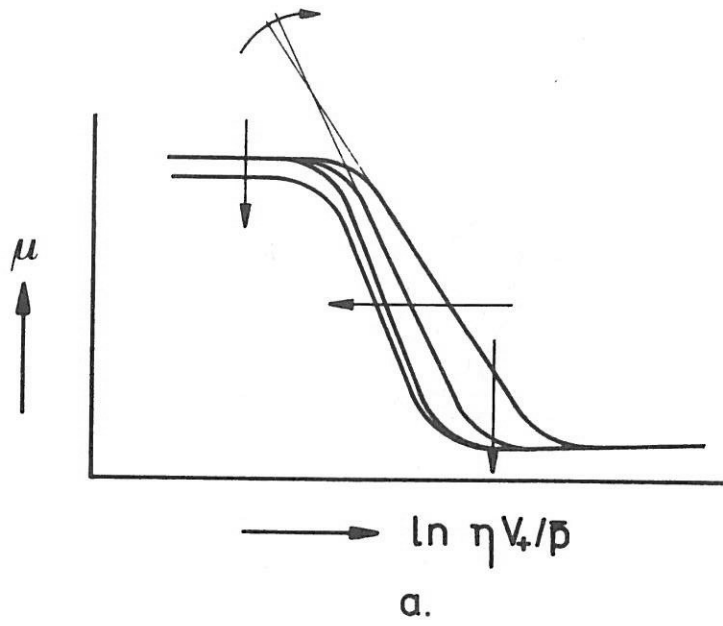
Fig. 5.19: Running-in effects at:

a. low pressure

b. high pressure

On the two-disc machine several runs from the EHL- into the ML-regime were made, using the "quick friction measurement" method, see figure 5.16. From these measurements it became clear that μ increases with increasing run number, i.e. running-in does not take place with this friction measurement method and no stable transitions can be achieved. After a few runs the surfaces showed some damage, which was growing after each run. Using the second method, by which each data point is obtained after a few minutes of sliding, for a contact which enters the mixed lubrication regime several times, μ - ln H curves as shown in figure 5.17 are obtained. These measurements show that after only two runs almost no further shift in the position of the friction curve occurs. Also almost no further change in micro-geometry with sliding distance or time during a friction curve measurement takes place. The rate of change in micro-geometry with sliding distance (for instance due to corrosive wear) is low compared to the time needed for measuring a total friction curve. This running-in continues until the surfaces in the sliding direction are totally conformal. In principle, this results in a continuous shift of the friction curve to lower values of H with sliding distance until this conformal situation has been reached. The same "stationary" friction curve can be obtained if the system is run-in at constant operational variables during appr. 1 to 2 hours near the transition ML-BL; all asperities involved in the contact processes run in. The friction curve hardly changes in the next runs, with the second friction measurement method, see figure 5.18. This running-in method, i.e. the quasi-stationary friction measurement, produces changes in the friction curves as illustrated in figure 5.19.

Running-in manifests itself for the low pressure situations by a shift of the ML-regime to lower values of H, a decreasing value for the minimum coefficient of friction, a steeper curve for the ML-regime and sometimes a decrease of the coefficient of friction for boundary lubrication. In the BL-regime the shift of the coefficient of friction to lower values is a result of micro geometry effects, i.e., hydrodynamic effects are still present between the interacting

asperities, see section 5.3.1.2 and 5.3.2.2. Thus, micro-EHL occurs in the regime where BL is expected; in this respect the term quasi-"BL" may be introduced. For the high pressure situations the same shifts are found, except that now the minimum coefficient of friction does not exist. At the transition EHL-ML, μ shifts to higher values.

Results presented in the previous sections were obtained from surfaces which were run in by the method given in figure 5.17 or 5.18.

5.2.6   Summary of measurements on Sebacate/AISI-52100

With surfaces, run in with a procedure as explained in section 5.2.5, experiments were carried out to determine the influences of the operational variables: normal force N, velocity V and temperature θ on the lubrication of concentrated contacts. The lubricant was Sebacate and the specimens, having a roughness $Ra_t \sim 2.5 \; 10^{-8}$ m, were made of AISI-52100 steel. Results of these experiments are:

- Friction curves measured under conditions of EHL showed a shape, different from that of the traditional generalized Stribeck curve near the transition EHL-ML.
- Contrary to the situation in low pressure contacts, in the EHL high pressure case it is not permissible to neglect the hydrodynamic component of the friction in the calculation of friction in the ML-regime.
- Not the sliding velocity (as suggested by many authors) but the sum velocity is the predominantly controlling parameter with regard to the transitions EHL-ML and ML-BL.
- For the whole ML-region viscosity plays an important role. The inlet viscosity is the controlling parameter for the transition EHL-ML as well as for the transition ML-BL.
- The transitions are mainly controlled by the product of viscosity and sum velocity. The Hertzian contact pressure has almost no influence on the transition ML-BL. On the contrary, the transition EHL-ML and the ratio h/σ_t are pressure dependent.

5.3   ELEMENT PROPERTIES IN RELATION TO MIXED LUBRICATION

Friction in the ML-regime is governed by the behaviour of the
lubricant and the interacting asperities. Now that the influences of
the operational variables at certain constant element properties on
the transitions are known, it is interesting to pay attention to the
effects of the element properties: lubricant, surface roughness and
material of the surfaces on friction and on the transitions EHL-ML and
ML-BL. In the following sections these variables are outlined with
relation to ML.

5.3.1   Lubricant

5.3.1.1.   Introduction

The lubricant Sebacate used in the previous tests, section 5.2, is
a special liquid in comparison to the common lubricants used in
mechanical applications. Apart from the synthetic nature of Sebacate
and other specific properties, for Sebacate no solid-state behaviour
could be measured up to pressures of 1.1 GPa and temperatures down to
$-3°C$, Alsaad et al. (1978). All the experiments with Sebacate were
carried out in the liquid-state regime of the lubricant, see figure
3.4. By choosing lubricants with known transitions from liquid- to
solid state behaviour this change with relation to the frictional
behaviour of an LCC can be studied. In figure 5.20 the results of two
measurements with HVI-650 as lubricant are given.
Curve 1 represents the frictional response of an LCC performed in the
liquid-state area of the lubricant. Curve 2, however, depicts the
friction in the solid state area. This shows that a distinction should
be made between experiments, performed in the area of liquid-state
behaviour of the lubricant and experiments performed under conditions
where solid-state behaviour can be expected. In the literature
concerning the study of LCC's with respect to ML this distinction is
not often made, which may lead to the wrong conclusions about the
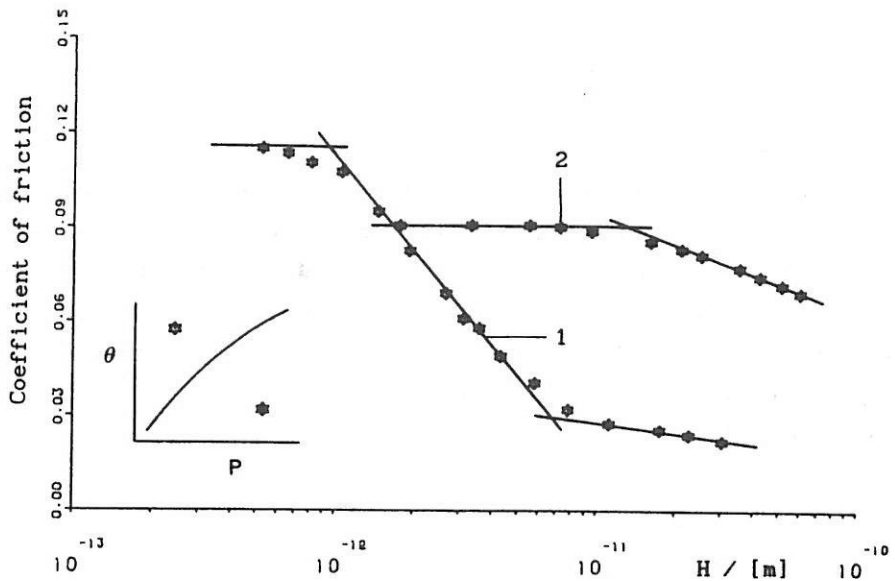
Fig. 5.20: Friction curves obtained in the liquid- and solid
state behaviour regime of the lubricant (HVI-650).

❋ : $\bar{p}$ = 1.60 GPa, θ = 42 °C and $R_\bullet$ = 3.18·10^{-3} m

❋ : $\bar{p}$ = 0.24 GPa, θ = 81 °C and $R_\bullet$ = 97.5·10^{-3} m

parameters involved in ML and in the failure of LCC's.

The measurements reported in this section (5.3.1) were all carried
out with AISI-52100 steel specimen, all having the same surface
roughness, Ra_t ~ 2.5·10^{-8} m.

5.3.1.2   Liquid-state behaviour

For the different lubricants given in appendix B the transitions
EHL-ML and ML-BL were obtained from measured μ – ln H curves at
different pressures and at temperatures of 40°C and 80°C respectively.
The results are given in figure 5.21.
These measurements show that the type of lubricant does not
significantly influence the EHL-ML and ML-BL transitions. The role of
α becomes doubtful. The value of α for the different lubricants
differs in these experiments by a factor of 2. One would expect that a
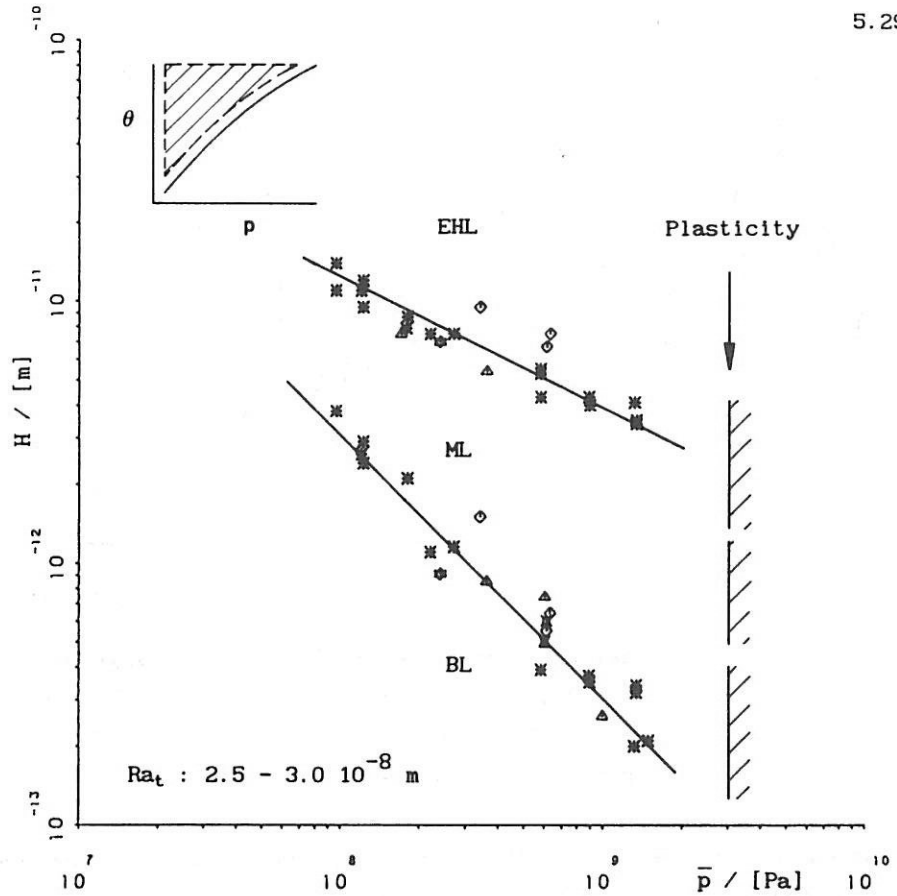
Fig. 5.21: Transitions EHL-ML and ML-BL performed in the
lubricants liquid-state behaviour regime.
※ : Sebacate, △ : Santotrac-50, ⋈ : HVI-160S,
◇ : Gadenia-30 and ✿: HVI-650.

rise in α, i.e. a larger film thickness, would decrease H, which has
not been observed. α is introduced in EHL by using the Barus equation
to express the dependence of viscosity on pressure. When using the
Roelands equation to describe the viscosity-pressure relation Z
becomes the important parameter. For several fluids Z varies by a
factor of say, 1.2.

Measurements with a liquid-state behaviour of the lubricant showed
three kinds of friction curves; these are presented in figure 5.22.
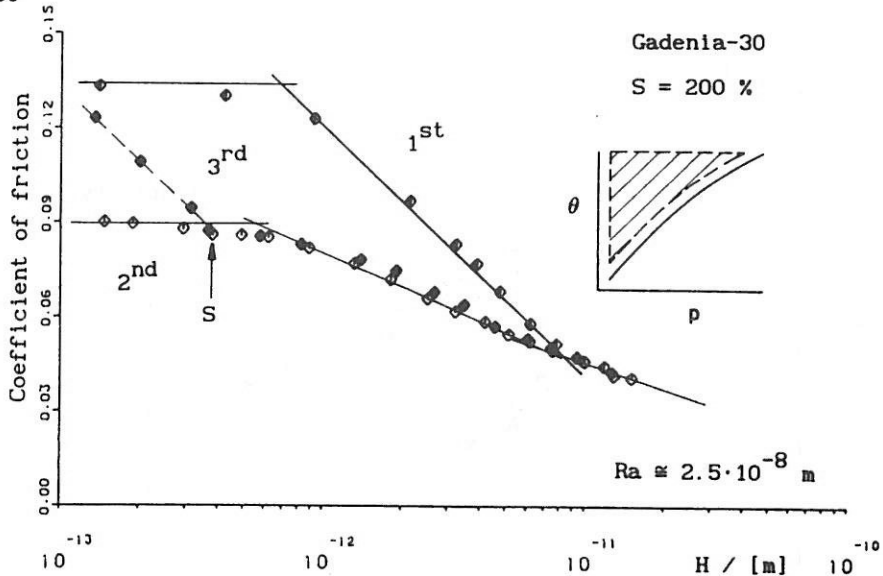
Fig. 5.22: Typical friction curves at liquid-state behaviour.

◇ : $\bar{p}$ = 0.62 GPa, θ = 72.5 °C and R_* = 25·10^{-3} m

◆ : $\bar{p}$ = 0.62 GPa, θ = 70.5 °C and R_* = 25·10^{-3} m

◈ : $\bar{p}$ = 0.62 GPa, θ = 98 °C   and R_* = 25·10^{-3} m

These curves were measured with different specimens at nearly the same operational variables and initial element properties.

Curve 1 is the most frequently measured friction curve, i.e. the coefficient of friction in the EHL-regime rises steeply to a coefficient of friction in the BL-regime of appr. 0.12 to 0.15.

Friction curve 2 has been measured several times. It shows a typical low value for the coefficient of friction in the quasi "BL"-regime. In this regime the value for the coefficient of friction depends on the type of lubricant and lies between ~ 0.08 and ~ 0.11. With the contact resistance measurement no contact was recorded, which is not the case for friction curve 1. Photographs from the contact region are similar to figure 5.2[b] and 5.27.

Friction curve 3 is an intermediate situation, in which the friction grows from the lower level (point S) to the higher coefficient of friction. This change-over from one friction level to the other, which has been observed for all lubricants, could be induced by simply reducing the velocity. Point S sometimes lies between the transitions

EHL-ML and ML-BL. However, no relation could be found between point S and the operational variables; presumably its location depends entirely upon local micro-geometry effects. This assumption becomes more conceivable if the lower friction level is studied in more detail and by the results presented in section 5.3.2.2.

Comparing the measured shear stress $\bar{\tau}$ (= $\bar{F}/A_{Hertz}$) in the quasi "BL"-regime, obtained from friction curves like no. 2 of figure 5.22, with the limiting shear stress of the lubricant, or comparing the ratio $\bar{\tau}_l/\bar{p}_{Hertz}$ with the coefficient of friction gives a striking result, see figures 5.23[a] to 5.23[d]. To complete this, comparison measurements have also been included in the lubricants' solid-state area, section 5.3.1.3. The ratio $\bar{\tau}/\bar{p}_{Hertz}$ in the quasi "BL"-regime for a specific lubricant agrees very well with the ratio $\bar{\tau}_l/\bar{p}_{Hertz}$ of that lubricant.
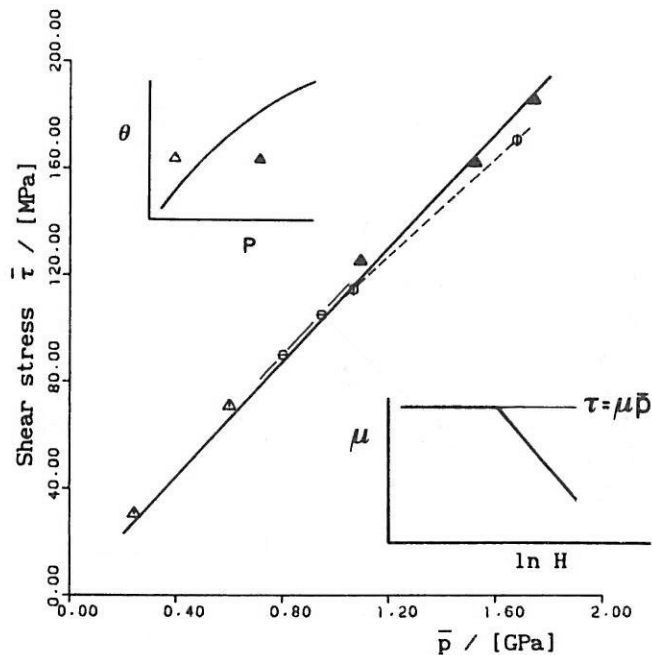
Fig. 5.23[a]: $\bar{\tau}$ measured in the quasi "BL"-regime as a function of $\bar{p}$ for Santotrac-50 at θ = 63 °C, compared with limiting shear stress results from literature.

θ : Bair and Winer (1978).

φ : Evans - line contact (1983).
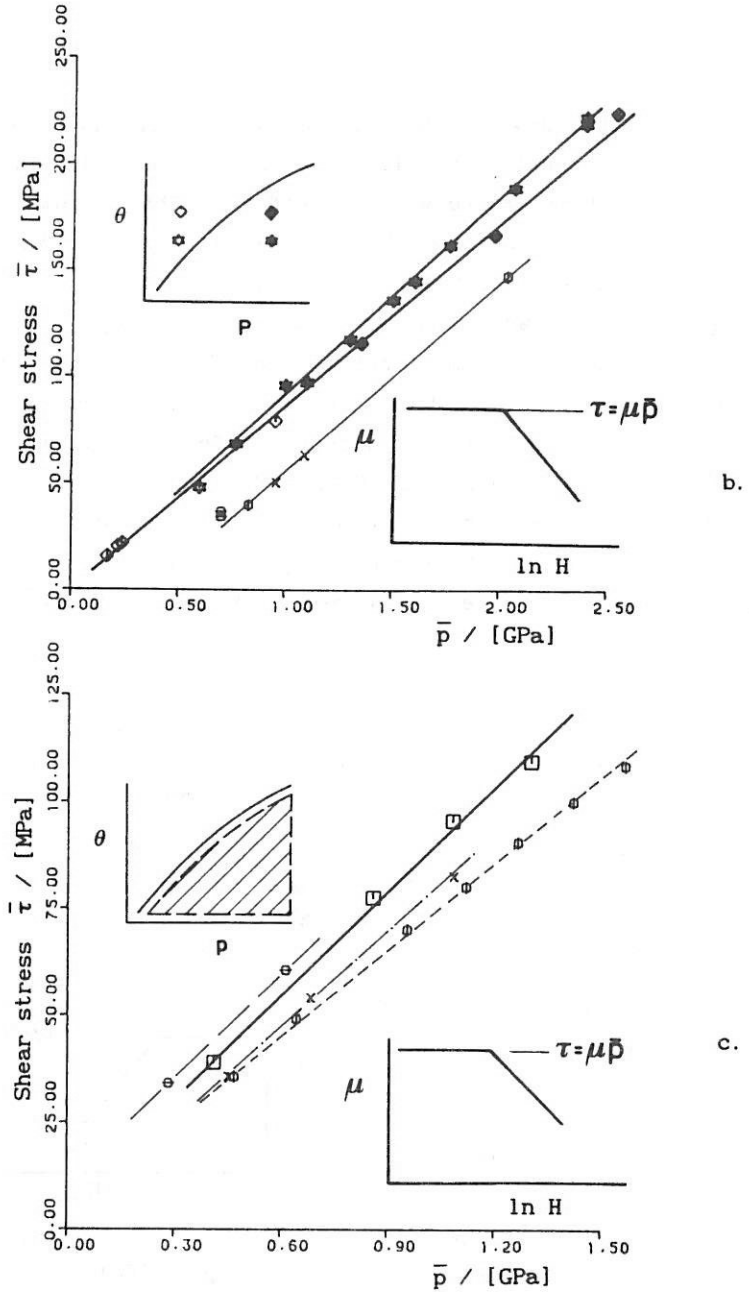
Fig. 5.23^{b,c}: $\bar{\tau}$ measured in the quasi "BL"-regime as a function of $\bar{p}$.
b) HVI-650 at θ = 42 $^{\circ}$C and 80 $^{\circ}$C. c) 5P4E at θ = 41 $^{\circ}$C.
Compared with limiting shear stress values from
literature. $\ominus$: Bair and Winer (1979).
Φ : Evans - line contact (1983).
X : Tevaarwerk - circular contact (1976).
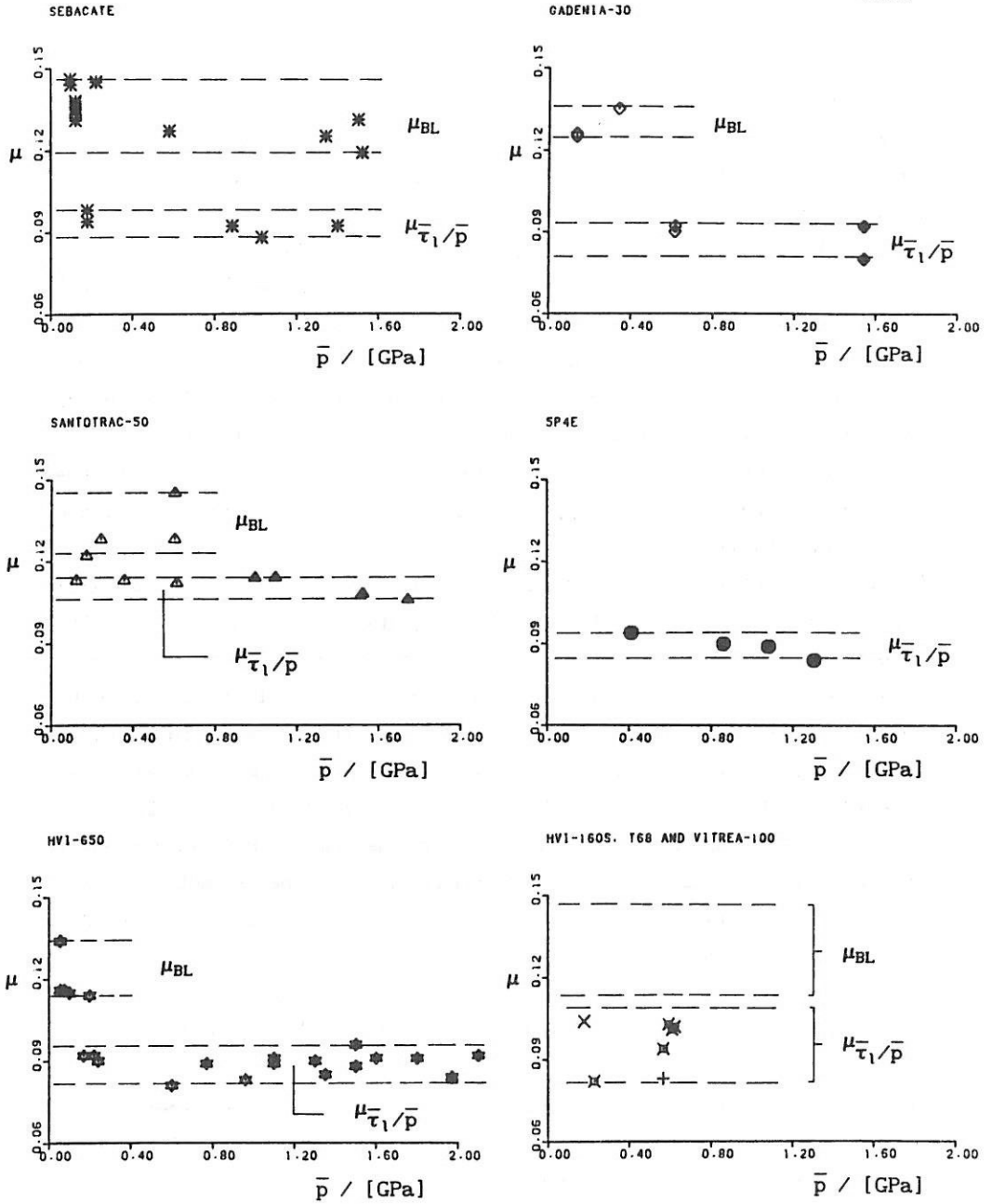
Fig. 5.23$^{\text{d}}$: Coefficient of friction in the BL- or quasi "BL"-regime as a function of $\bar{p}$. The black marked results are obtained in the lubricants solid-state regime.

It should be pointed out here that in fact not the mean Hertzian pressure and mean shear-stress should be used for the quasi "BL"-regime in figure 5.23, but instead the much higher mean real pressure and mean shear stress in the micro contacts; These, however, are not known. Because of the linear relationship between $\bar{\tau}_l$ and $\bar{p}$ the ratio is of interest. It is concluded from the figures 5.23^a to 5.23^d that friction in the quasi "BL"-regime is controlled by the solid-state properties of the lubricant in the micro-contacts. Thus, in these situations micro-EHL is present between the interacting asperities. All the features known for the macro contact situation are also applicable to the micro-contact; unfortunately most of the operating conditions ($\dot{\gamma}$, p, θ, etc.) are not known for these micro-contacts in particular.

Returning to curve 2 of figure 5.22, it is supposed that in the quasi "BL"-regime (micro-EHL) the entire load is carried by interacting asperities, which are separated by a lubricant film, behaving like a solid. The existence of a change-over from micro-EHL to BL at reducing velocity in this regime (mainly the same asperities remain in contact) supposes that the hydrodynamic action in the inlet region of at least some of the interacting asperities starts to fail and real BL occurs locally. Curves 2 and 3 are obtained in the quasi "BL"-regime under the same operational variables. For this reason the geometry of the interacting asperities is becoming of interest. The curvatures and/or the slopes of the interacting asperities are assumed to play an important role. It should be noted that the observed change-over cannot be due to thermal effects, since the heat generation in the micro-contacts decreases with decreasing velocity.

Some final remarks on these "liquid-state behaviour" measurements are:

- Micro-EHL becomes more pronounced when the mean Hertzian pressure increases at the same element properties.
- With 5P4E as the lubricant no ML-regime was measured. At the moment of entering the ML-regime the coefficient of friction abruptly increased to a value of appr. 0.3 and the surfaces were completely damaged, see figure 5.2^c and section 5.3.1.4.

5.3.1.3   Solid-state behaviour

Measurements under conditions of solid-state or plastic behaviour of the lubricant yielded friction curves as presented in figure 5.24. One would expect horizontal lines with a coefficient of friction equal to $\bar{\tau}_1/\bar{p}$, the dotted line. The friction curves, however, show a horizontal part at low H values and a decreasing coefficient of friction for higher H values. From figure 5.24 it is clear that neither $H = \eta_1 \cdot V_+/\bar{p}$ nor the film thickness h are the right parameters to discriminate between the conditions under which an LCC can be operating if solid-state behaviour of the lubricant is present for the whole macro-contact.
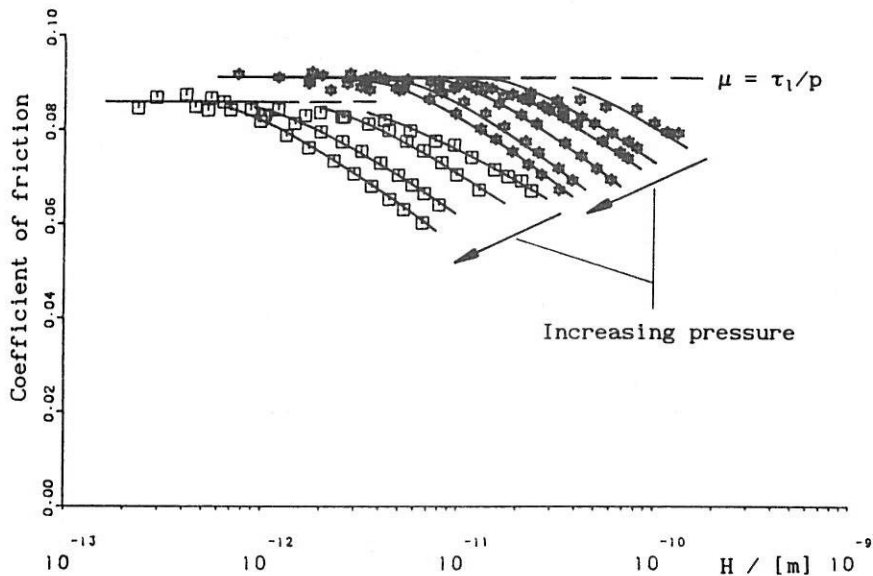
Fig. 5.24: Solid-state behaviour measurements of HVI-650 at
42°C (✿) and 80°C (□) and different pressures.
$R_* = 3.18 \cdot 10^{-3}$ m and S = 200 %.
□ : $\bar{p} = 0.96 - 1.35 - 1.97$ and 2.53 GPa.
✿ : $\bar{p} = 0.77 - 1.10 - 1.30 - 1.60 - 2.06$ and 2.40 GPa

Figures 5.24, 5.25 and 5.26 show that both R_* and the pressure
influence the position of the friction curve and that in this case
(solid-state behaviour) not the sum velocity but the sliding velocity
is an important variable with respect to friction.

The measurements of contact resistance indicated that there is no
contact between the opposing surfaces. Photographs from the contact
region, as shown in figure 5.27, also show that there has been no
change in the roughness structure.
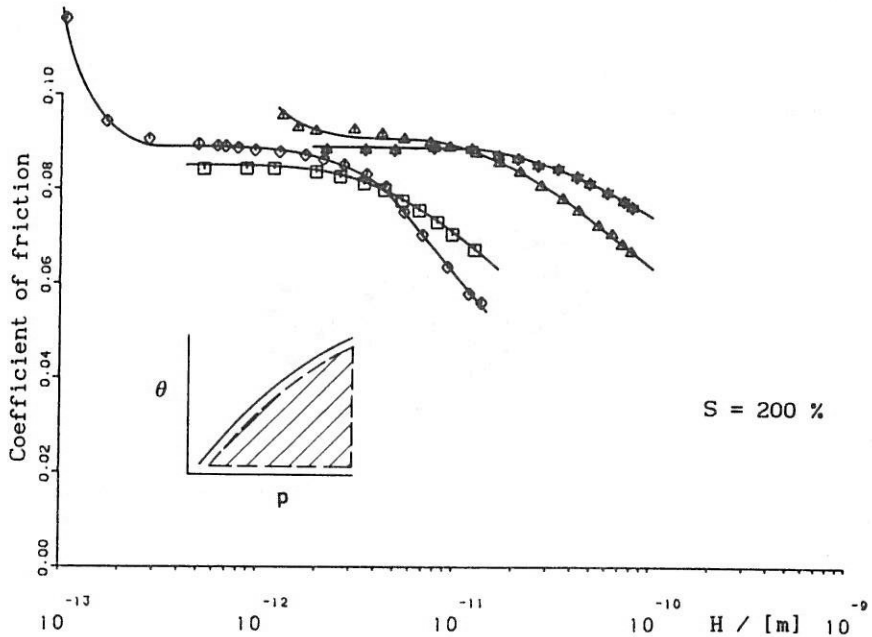
Fig. 5.25: Solid-state measurements of HVI-650. Influence of R_*.

    ✿ : $R_* = 3.175$ mm, $\theta = 42\,^\circ$C and $\bar{p} = 1.10$ GPa.

    ▲ : $R_* = 6.25$ mm, $\theta = 42\,^\circ$C and $\bar{p} = 1.00$ GPa.

    □ : $R_* = 3.175$ mm, $\theta = 80\,^\circ$C and $\bar{p} = 1.35$ GPa.

    ◊ : $R_* = 6.25$ mm, $\theta = 80\,^\circ$C and $\bar{p} = 1.50$ GPa.
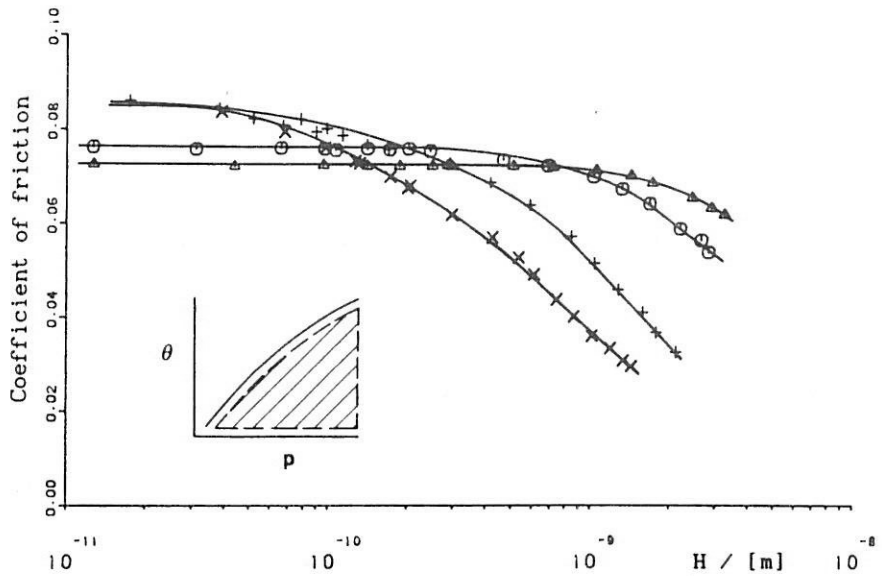
Fig. 5.26: Solid state measurements of HVI-650 at θ = 27°C
and p̄ = 1.3 GPa with different slip values of:
△ = 5, ⊕ = 10, + = 50 and ✕ = 100 %.
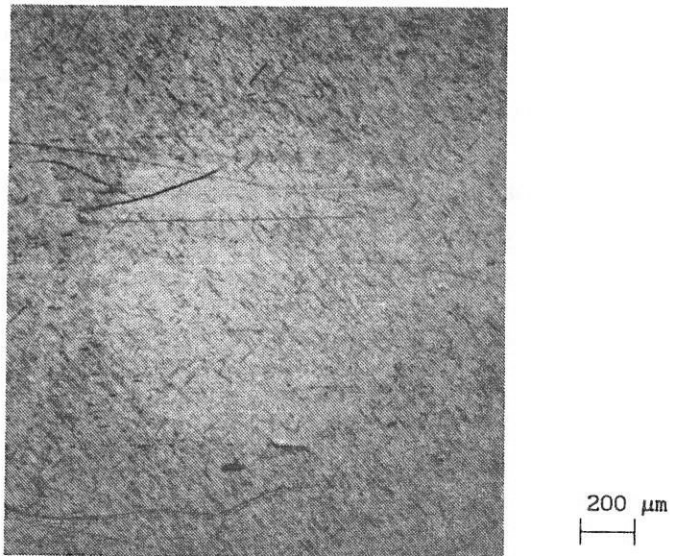
Fig. 5.27: Photograph of the contact region after a
solid - state behaviour measurement.

In figure 5.25 two friction curves (Δ) and ($\diamond$) show an increase in friction at low values of H. Here the lubrication of the macro contact starts to fail. The pressure generation in the inlet region is insufficient to create a solid lubricant film and contact between the highest roughness summits takes place. Photographs from these contact regions are similar to the one of fig. 5.2[a].

By defining the transition in these friction curves (figures 5.24 to 5.26) by the intersection of the extrapolated straight parts of these curves and by rearranging the variables involved in this transition, figure 5.28 is obtained for the different lubricants. The transition in the "solid-state" friction curve is governed by the relationship $V_- \cdot \bar{p} \cdot R_* \approx 4 \cdot 10^5$.

Smith (1958/1959) studied a mineral oil at a constant pressure of 2.68 GPa and at different R_* as a function of the sliding velocity to show the existence of plastic behaviour. These plastic shear experiments showed a transition at $V_- \cdot R_* \approx 1.5 \cdot 10^{-4}$, with $\bar{p} = 2.68$ GPa this yields for $V_- \cdot \bar{p} \cdot R_*$ a value of appr. $4 \cdot 10^5$, which agrees very well with the above result $V_- \cdot \bar{p} \cdot R_* \approx 4 \cdot 10^5$. The decrease in μ for values of $V_- \cdot \bar{p} \cdot R_* > 4 \cdot 10^5$ is probably due to temperature rise from heat dissipation in the contact, caused by (plastic) shear. Smith assumed that the temperature rise is determined by the rate at which heat can be conducted through the lubricant film, as is usual in thermal-EHL, Johnson et al. (1980). Based on this assumption a Nusselt number can be defined, which characterizes this type of systems with respect to heat transfer.

$$Nu = \frac{\alpha \cdot R_*}{\lambda} = \frac{Q \cdot R_*}{\lambda \cdot \Delta\theta} \qquad (5.1)$$

in which: α = coefficient of heat transfer = $Q/\Delta\theta$

R_* = characteristic length, is reduced radius

λ = coefficient of heat conductivity

Q = heat flow per unit area

$\Delta\theta$ = temperature rise = $\theta \, (\mu, \bar{p})$
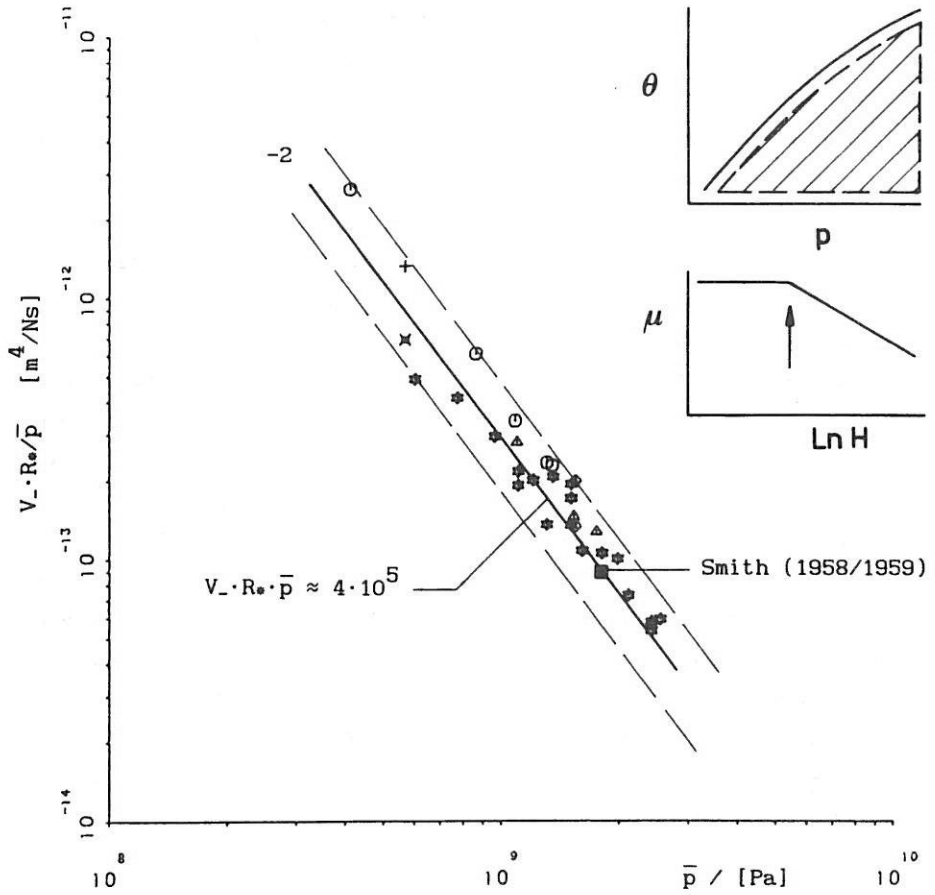
Fig. 5.28: Transitions of the "solid-state" friction curves
represented by $V_- \cdot R_* / \bar{p}$ as a function of $\bar{p}$.

⊙ : 5P4E, △ : Santotrac-50, ⋈ : HVI-160S, ◇ : Gadenia-30,
+ : Vitrea-100, ✿ : HVI-650 and ∎ : Smith (1958/1959).

with $\qquad Q = \bar{\tau}_l \cdot V_- = \mu \cdot \bar{p} \cdot V_- \qquad$ (5.1) becomes:

$$Nu = \frac{\mu \cdot \bar{p} \cdot V_- \cdot R_*}{\lambda \cdot \theta(\mu, \bar{p})} \qquad (5.2)$$

Equation (5.2) shows, together with the $V_- \cdot \bar{p} \cdot R_* \approx 4 \cdot 10^5$ relationship,
that temperature effects cause the decrease in friction. Using $V_- \cdot \bar{p} \cdot R_*$

as the parameter in figures 5.24, 5.25 and 5.26, instead of $\eta_1 \cdot V_+/\bar{p}$, yields curves which almost lie on top of each other.

It should be noted here that the friction curves, shown in figures 5.24 to 5.26 have nothing to do with ML or BL or with the transition ML-BL. The lubrication is entirely governed by conditions as present in EHL contacts.

By this method of measurement, $\bar{\tau}_1/\bar{p}$ values for the different lubricants can be obtained very easily as a function of temperature. In the table of appendix B some results are given.

Many LCC's operate in the solid-state regime of the lubricant. For mineral oils at moderate temperatures, 50 to 70°C, this behaviour manifests itself already at relatively low Hertzian contact pressures, say, 0.8 GPa. For this reason many authors like Czichos (1972, 1974[a,b], 1976, 1977), Begelinger and de Gee (1972, 1974, 1976, 1982), Ku et al. (1978[a,b]), who studied the failure of LCC's, pointed out that the sliding velocity is an important variable. In their measurements at higher sliding velocities, LCC's start to operate in the solid-state regime of figure 3.4. However, heat dissipation in the contact causes a temperature rise and the LCC will operate in the liquid-state regime. In the next section the consequence of such a temperature rise will be outlined.

5.3.1.4 Miscellaneous

In the above tests friction curves were obtained by measuring the friction of an LCC at constant contact pressure and temperature, while the velocity was changed. By this method of measuring experiments were carried out at a certain point in the temperature-pressure graph of figure 3.4. It is interesting to study the frictional behaviour of LCC's by keeping the pressure and the velocity constant and only changing temperature. In this way the temperature rise at the inlet of the contact, due to heat dissipation in the contact, is roughly simulated. By choosing a suitable pressure- and temperature range the transition curve of the "solid- to the liquid like behaviour" of the lubricant is passed. In figure 5.29 and 5.30 the friction curves for Santotrac-50 and 5P4E, measured in this way, are presented.
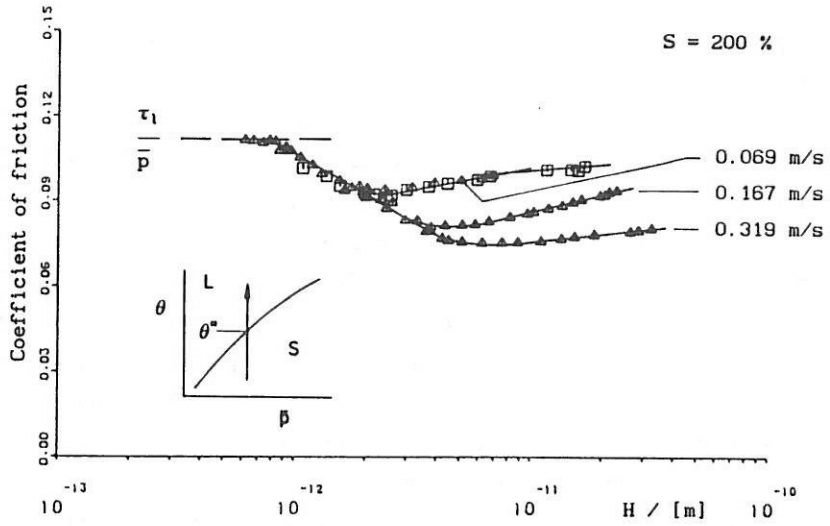
Fig. 5.29: Friction due to solid-liquid behaviour of Santotrac-50.
$\triangle$: $\bar{p}$ = 0.61 GPa, θ = var., R_* = 25 mm and V_+ = 6.9, 16.7 and 31.9 cm/s.
$\square$: $\bar{p}$ = 1.0 GPa, θ = var., R_* = 6.25 mm and V_+ = 19.5 cm/s.
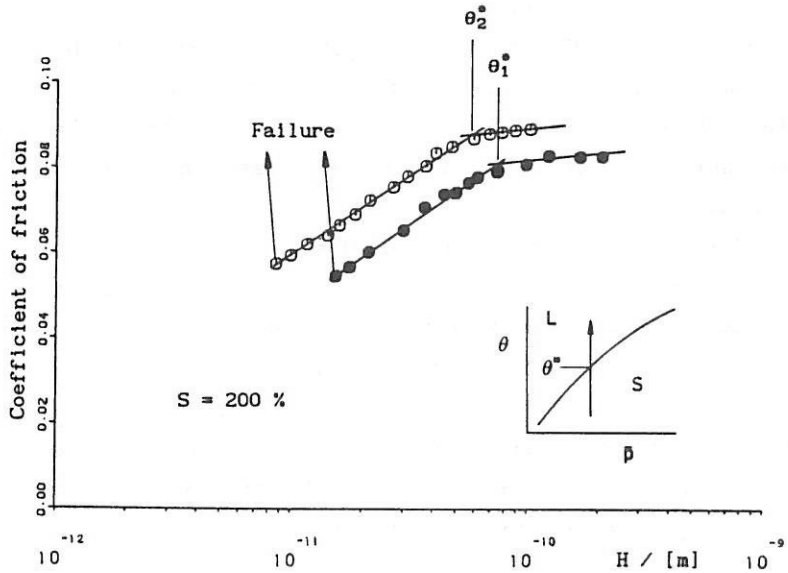
Fig. 5.30: Friction due to solid-liquid behaviour of 5P4E at
S = 200 %. θ_1^* and θ_2^* are plotted in figure 3.4.
o : $\bar{p}$ = 0.31 GPa, θ = var., R_* = 25 mm and V_+ = 0.123 m/s.
$\bullet$: $\bar{p}$ = 0.25 GPa, θ = var., R_* = 25 mm and V_+ = 0.161 m/s.

These figures show a different type of friction curve compared to the ones presented in the previous sections if μ still is depicted as a function of H. The heat generation during an experiment is almost constant - μ varies only little - as was the case during the other experiments. Thus, such frictional behaviour in time (as found with rising the temperature) is to be expected for LCC's which function under a heavy "thermal load". Such a system starts in the solid-state behaviour regime of the lubricant, $\mu = \tau_1/p$. Due to the heat generation, the solid elements rise in temperature and with that the contact inlet temperature. This temperature rise depends on the thermal properties of the contact and on the heat capacity of the total system in which that particular contact is functioning. Once in the liquid-state regime ($\mu < \tau_1/p$), the inlet viscosity further drops with rising temperature and with this the value of H decreases. This decrease in H goes on until a stationary temperature is established. If there is no such temperature, the ML regime is reached (or even passed) and failure can occur.

The experiments with 5P4E show a transition in the coefficient of friction curve which coïncides with the transition solid- to liquid-state behaviour. For 5P4E this temperature agrees very well with the results of Alsaad et al. (1978). (see in figure 3.4 the points marked ●).

The coefficient of friction in the solid-state regime decreases with increasing temperature and velocity, i.e., more heat generation in the contact. Thus, a temperature dependent τ_1 is observed, see also figure 5.24. Also, these experiments show that no ML-friction measurements with 5P4E were possible. For Santotrac-50 this solid- to liquid-state transition is not observed. The dependence of τ_1 on θ and the frictional behaviour of Santotrac-50 as a function of $\bar{p}$ and θ in the liquid-state regime make cause this transition in the friction curve to be not well defined.

5.3.1.5 Summary

Different lubricants have been investigated in LCC's with respect to their influence on the frictional behaviour in the ML-regime and the transitions EHL-ML and ML-BL.

Depending on the behaviour of the lubricant (as governed by the operating variables) and on the method of measuring, all kinds of friction curves can be obtained. The traditional Stribeck-curves are only found under certain circumstances. Friction measurements showed:

- For mineral- and synthetic lubricants the transitions EHL-ML and ML-BL are governed by $H = c \cdot \bar{p}^{-1/2}$ and $\eta_1 V_+ = c$, respectively, if the LCC, made of AISI-52100 with a roughness of $Ra_t \sim 2.5 \cdot 10^{-8}$ m, operates in the lubricant's liquid state regime.

- At BL two friction levels are found if the contact operates in the liquid-state regime of the lubricant: A value for the coefficient of friction of appr. $\mu \sim 0.13$ which is characteristic for BL and a level with a value of $\mu \sim 0.08$ to ~ 0.11 depending on the lubricant. In the latter case friction is governed by the properties of the lubricant for all lubrication modes, i.e., EHL, ML and quasi "BL" (micro-EHL) respectively.

- The position of the transitions is not affected by the existence of micro-EHL. In the case of micro-EHL the surfaces almost do not suffer damage, being an interesting topic if wear is to be avoided at severe operating conditions.

- LCC's operating with a solid-state behaviour of the lubricant showed a transition in the friction curves which is governed by $V_- \cdot \bar{p} \cdot R_* \approx 4 \cdot 10^5$. It appeared that this is caused by temperature effects.

- The use of H or film thickness h as the parameter to indicate the operating condition of an LCC is useless when this LCC is expected ($\bar{p}$ and θ_1) to function in the solid-state behaviour regime of the lubricant.

5.3.2   Roughness

5.3.2.1   Surface characterization

From the definition for ML, i.e. the lubrication mode by which the
applied load is transmitted from one surface to the other both by
interacting asperities and by the pressure generated in the lubricant,
it can be concluded that if there is no surface roughness there would
be no ML-regime. Unfortunately, surfaces without roughness do not
exist in practice; they always possess a certain micro-geometry and
this micro-geometry mainly determines the frictional behaviour of an
LCC.
In the past a lot of attention has been paid to the phenomena,
associated with surface roughness. However, as yet "surface roughness"
has not been defined really adequately, see for instance Greenwood
(1984). The common descriptions which characterize roughness can be
split up into two groups, i.e. the deterministic- or simple
statistical descriptions and by descriptions based on random process
theory. In deterministic or simple statistical descriptions the
surface is assumed to be consisting, for instance, of a number of
summits per unit area all having the same curvature and a Gaussian
summit height distribution, the Greenwood and Williamson (1966) model.
If surface roughness is treated as a two dimensional random noise
problem then the theory of random processes can be applied. The random
noise theory was introduced by Rice (1945), generalized by
Longuet-Higgins (1957), developed by Whitehouse and Philips (1978,
1982) and elaborated by Greenwood (1984). Greenwood (1984) showed that
a small number of parameters is sufficient to describe a rough
surface. These are $r = \sigma_m^2/(\sigma \cdot \sigma_k)$ and $\phi = \arcsin (\frac{1}{2} \cdot h \cdot \sigma_k/\sigma_m)$ with
respectively σ, σ_m and σ_k being the RMS height, slope and curvature of
a profile measurement at a certain sampling interval h. However, the
absolute values of these variables strongly depends on the sampling
interval h as well as on the subtleties of the specific calculation

method which is employed in the computer program. The sampling length should be chosen depending on the application envisaged, as proposed for LCC's by Leaver et al. (1974).

Until yet, neither of these methods satisfactorily characterizes surface roughness in a quantitative way. Good qualitative results are obtained, although some discrepancies still exist.

In practice surface roughness is mostly characterized by a single parameter, such as the RMS- of CLA roughness value. These values only give an indication of the distribution of roughness heights, not of the roughness texture. Surfaces may have the same RMS- or CLA values, but totally differ in asperity shape. The CLA- or RMS values, which relatively do not differ much from each other, are independent of the roughness wavelength. Nevertheless, in this thesis the CLA roughness value in the sliding direction will be used as parameter for characterizing surface roughness. The reason for this is that the determination of other surface properties, as pointed out by Greenwood (1984), is not straightforward.

5.3.2.2   Surface roughness effects on lubrication and the transitions EHL-ML and ML-BL

To study the effect of surface roughness on the transitions EHL-ML and ML-BL a series of experiments have been carried out with AISI-52100 specimens having a CLA surface roughness of ~ 0.01 μm to ~ 1 μm. The surfaces were prepared as described in section 4.3. Measurements were conducted on the two-disc machine in the liquid-state regime of HVI-650 and Sebacate, at mean pressures of 0.70 and 0.82 GPa respectively and at a slip ratio of 50 %. A nearly constant pressure for these experiments was chosen in order to avoid pressure effects in determining the relation between the surface roughness and the transitions EHL-ML and ML-BL. The results of these measurements, i.e. transitions represented by H as a function of the combined CLA surface roughness, Ra_t, are depicted in figure 5.31. The

combined CLA surface roughness, Ra_t, is defined by $Ra_t = (Ra_1^2 + Ra_2^2)^{1/2}$, where Ra_1 and Ra_2 are the CLA surface roughness values of the opposing surfaces respectively. These CLA roughness values are obtained by measuring them with the stylus of the Taylor-Hobson apparatus in the sliding direction with a cut-off length of 0.8 mm.
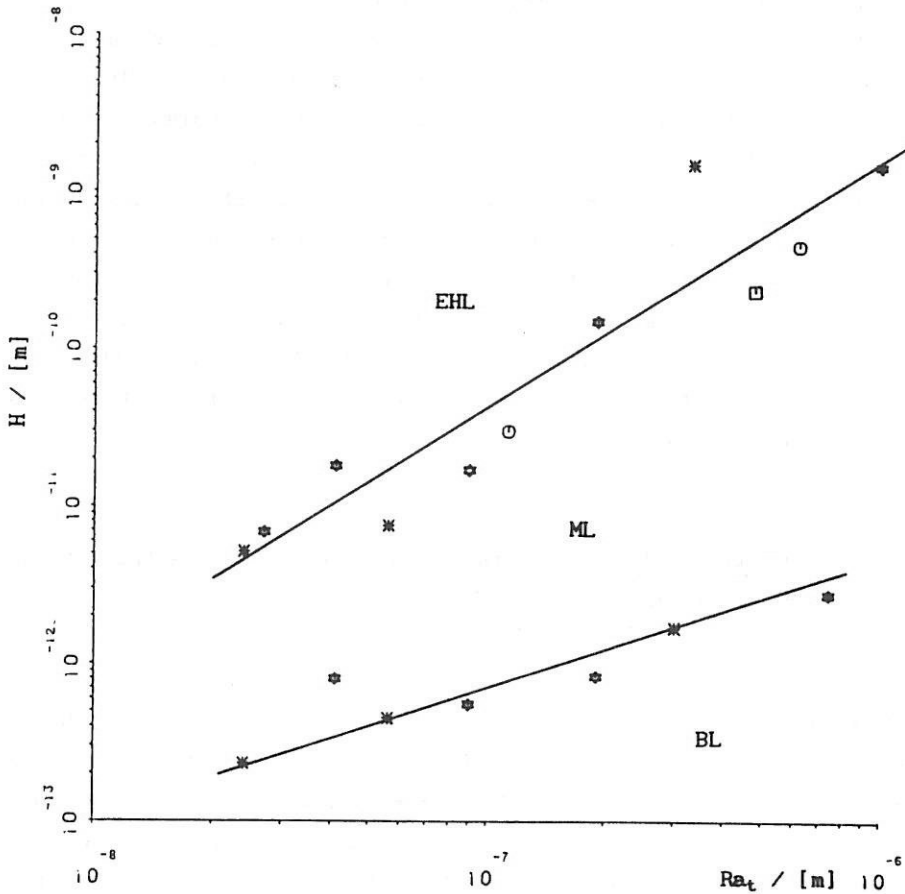
Fig. 5.31: CLA surface roughness and the transitions EHL-ML and ML-BL, (✳) Sebacate, ~ 22°C and (✦) HVI-650, ~ 97°C. The black marked results are obtained at $\bar{p}$ = 0.70 GPa, else $\bar{p}$ = 0.82 GPa.
(□) Poon and Haines (1966/1967), $\bar{p}$ = 0.76 GPa.
(⊙) Smith (1959), $\bar{p}$ = 0.71 GPa.

It is seen from figure 5.31 that the transition EHL-ML depends more strongly on roughness than the transition ML-BL. For the transition EHL-ML the relationship between H and Ra_t can be characterized by H $\therefore$ $Ra_t^{\sim 1.75}$ and for the transition ML-BL, H is almost linearly proportional with Ra_t. These results agree rather well with those of Poon and Haines (1966/1967) and Smith (1959). A remark concerning running-in with regard to these results is necessary. The running-in method as described in section 5.2.5 was not applicable for rough surfaces with Ra > 0.1 μm. These surfaces kept running-in, i.e., a continuous shift of the μ - ln H curve occurs. Therefore, it would not be possible to determine transitions at these large roughness values. Thus, it was decided that for these rough surfaces a running-in period was to be omitted and the friction curves were to be obtained at once, using the quasi-stationary friction method for each data point. For these tests the initial roughness was taken to be the determining factor for the transition EHL-ML. The roughness in the track, measured after the experiment, is related to the transition ML-BL. The consequence of this is that the transitions are determined from μ - ln H curves which have a smaller slope for the friction curve representing the ML-regime. Consequently, somewhat higher values for the transition EHL-ML and somewhat lower values of H for the ML-BL transition are determined. Nevertheless, the dependence of H as a function of Ra_t for the transition EHL-ML is more pronounced than for the transition ML-BL.

In figure 5.32 the transitions EHL-ML and ML-BL as a function of Ra_t are presented for mean pressures which varied between 0.1 and 0.2 GPa. The results for the transition EHL-ML are completed by measurements from μ - V_- friction curves of Gartner (1964). According to these results the transition EHL-ML is characterized by H $\therefore$ $Ra_t^{\sim 1.5}$ and the transition ML-BL is linearly proportional to Ra_t.
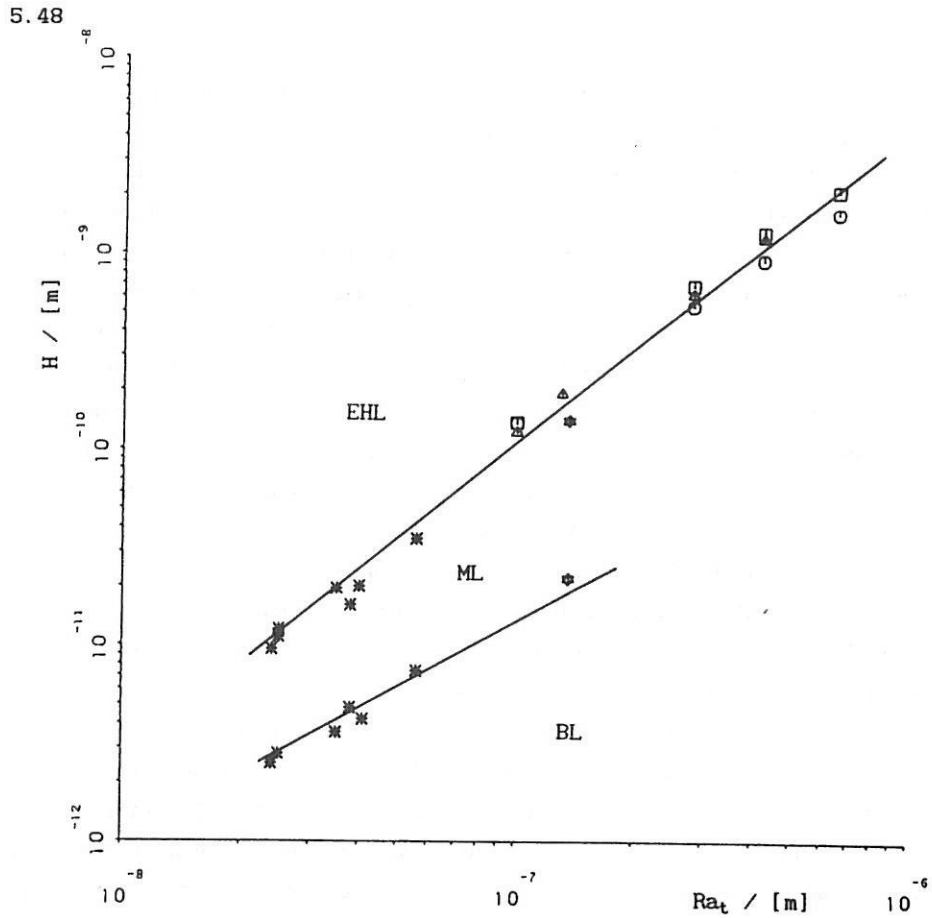
Fig. 5.32: Transition EHL-ML represented by H as a function of
Ra$_t$ at $\bar{p}$ = 0.1 - 0.2 GPa and 200% slip.
  ※ : Sebacate and ✿ : HVI-650.
  △, □ and ☉ : Gartner (1964).

Figures 5.31 and 5.32 show that the dependence of the transition
EHL-ML (represented by H) on the surface roughness (represented by
Ra$_t$) is not fully straightforward and has some discrepancies. This is
due to the small number of data points and to the experimental
technique used for the very rough surfaces. On the other hand the data
are in agreement with data from literature. In general, the
transitions are characterized by $H \approx Ra_t^k$ where $k \sim 1.5$ for the
transition EHL-ML and $k \sim 1$ for the transition ML-BL.

In section 5.3.1.2 micro-EHL has been measured for the different

lubricants. The coefficients of friction, measured in the BL- and quasi "BL"-region, are plotted in figure 5.33 against the combined CLA surface roughness. It can be seen that above a certain value of Ra_t no micro-EHL is observed and that below this value micro-EHL is possible. This figure indicates that Ra_t is one of the controlling variables for the existence of micro-EHL. However, the characterization of the micro-geometry by Ra_t is still leaving much to be desired.
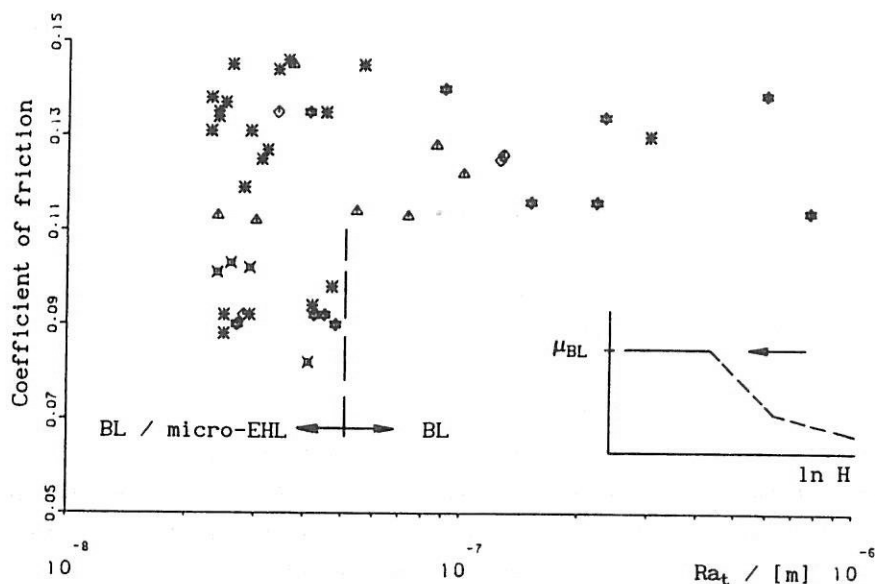
Fig. 5.33: BL and micro-EHL in relation with Ra_t.
　　　　※ : Sebacate, △ : Santotrac-50, ✕ : HVI-160S,
　　　　◇ : Gadenia-30 and ✿ : HVI-650.

In fact, the slopes and/or the curvatures of the roughness peaks are supposed to be of importance in the formation of micro-EHL. However, data on the slopes and/or the curvatures of the micro-contacts involved in the contact processes are not available. In section 5.4 it is shown that the geometry at the inlet of a contact has an enormous influence on the generation of a lubricant film in that contact.
From figure 5.33 it can be seen that surface roughness does not influence the coefficient of friction in the BL-regime.

5.3.2.3   Conclusions

As could be expected, surface roughness has an enormous influence on the transitions EHL-ML and ML-BL respectively. This roughness influence is most pronounced for the EHL-ML transition. These transitions can be characterized analytically by:

$$\frac{H}{Ra_t^k} = 1 \cdot \bar{p}^{\ m}$$

(5.3)

where:

	k	l	m
EHL-ML	1.5	$3.1 \ 10^4$	-0.5
ML-BL	1	$1.25 \ 10^4$	-1

$0.1 \ GPa < \bar{p} < 1.5 \ GPa$
and
$2.5 \cdot 10^{-8} \ m < Ra_t < 100 \cdot 10^{-8} \ m$

Expression (5.3) agrees well with the experimental results for the EHL-ML transition presented in literature and with the often used h/σ_t ratio ($H/Ra_t^{1.5} \therefore \{h/Ra_t\}^{1.5}$). It is seen again that the operational number H and the film thickness h correlate quite well.

An increase in surface roughness, increases the width of the ML-regime according to:

$$\frac{H_{EHL-ML}}{H_{ML-BL}} = 2.5 \cdot \bar{p}^{\ 0.5} \cdot Ra_t^{0.5}$$

(5.4)

This is in agreement with the suggestion that if Ra_t becomes zero the ML-regime vanishes and a direct transition from EHL to BL occurs.

Micro-EHL can not be captured with a single parameter like Ra_t. It also depends on other micro-geometry parameters. Deformation is also supposed to play a role, because all variables which characterize surface roughness, are measured at undeformed surfaces.

5.3.3   Material

The deformation of the surfaces depends on their elasticity moduli. AL 7075-T651, appendix E, has been used as the material to study the effect of the elasticity modulus on the transitions and, moreover, of the influence of deformation on lubrication, in particular micro-EHL. This material was also used by Tevaarwerk (1976) to study the effects of elasticity in EHL. The elasticity modulus of AL-7075-T651 is three times smaller compared to that of AISI-52100. At the same contact pressure and equivalent radius R_*, the elastic compliance of the Aluminum specimen for the elliptical/circular contact situation will be 9 times larger than that of steel specimen.

Unfortunately, this study failed because the wear in the ML-regime was too high. Due to wear, relatively large contact areas are formed, which reduce the mean contact pressure to values of only a few MPa. Wear occurring at the specimen combination of AL 7075-T651 and AISI-52100 was less dramatic. However, no comparable results became available. Friction measurements with AL 7075-T651 yielded μ - ln H curves from which the transitions at low pressures could be obtained. These results are included in figure 6.4. The AL 7075-T651/AL 7075-T651 and AL 7075-T651/AISI-52100 specimen combinations are presented in figure 6.4 by ⊞ and + respectively. The transitions obtained from these measurements relate very well with the extrapolated high pressure results. However, no micro-EHL was observed. It is obvious that AL 7075-T651 is not suitable as a material for concentrated contacts operating in the ML- or BL-regime.

5.4   SOME ADDITIONAL OBSERVATIONS

In this section some measurements are discussed which yielded some remarkable results compared to those of previous tests.

Sebacate

Of the other lubricants used in this research program it is known that they possess a liquid- and a solid behaviour. Micro-EHL was established for several lubricants, section 5.3.1.2. Sebacate can also show a solid like behaviour. However, until yet no transition from liquid- to solid like behaviour has been observed. Pressures generated in micro-contacts of 2 to 3 GPa are not unusual, Johnson et al. (1972). Thus, micro-EHL at Sebacate lubricated systems may also be possible. In figure 5.34 some friction curves of Sebacate LCC's have been presented. Apart from the different shapes of these friction curves, also measured for other lubricants, three instead of two possible levels of the coefficient of friction were observed at those operating conditions where normally BL occurs.

A value of $\mu \sim 13.5 \cdot 10^{-2}$, typical for BL, and a value of $\mu \sim 9.4 \cdot 10^{-2}$ are found. The latter agrees well with the results of Evans (1983) with relation to plastic shear of the lubricant, i.e., $\tau_1 \sim 0.1 \cdot p$ or $\mu = \tau_1/p \sim 0.1$. Thus, the τ_1/p ratio for Sebacate is expected to be this value of $9.4 \cdot 10^{-2}$. Besides these two friction levels, as already discussed in section 5.3.1.2, a third level is a few times measured with $\mu \sim 5.5 \cdot 10^{-2}$. The transitions determined from these friction curves have been plotted in fig. 5.12 and are marked ❀ and ✖ respectively. The transition EHL-ML of these measurements corresponds with the other Sebacate results, the ML-quasi "BL" transition shifts to higher values of H.

This low friction level ($\mu \sim 5.5 \cdot 10^{-2}$) might be caused by some rheological behaviour of Sebacate which is not yet known. Evans (1983) observed for 5P4E an elastic- non linear-plastic behaviour additional to the rheological aspects of lubricants as discussed in section 3.2.3. This behaviour was observed for a certain pressure- and temperature range. A similar behaviour for Sebacate, a synthetic
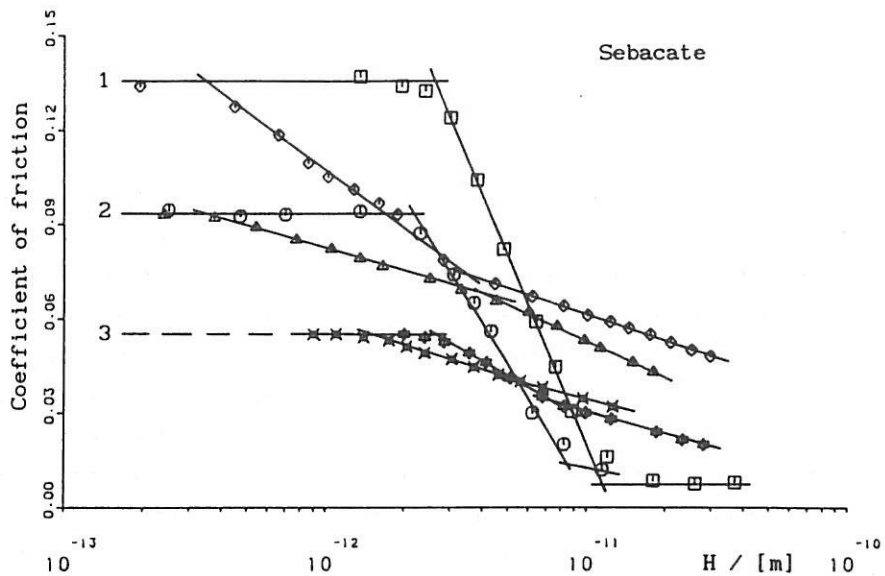
Fig. 5.34: Three friction levels for Sebacate in the "BL"-regime.

    □ : $\bar{p}$ = 0.12 GPa, θ = 67°C and R_* =   98 mm.

    ☺ : $\bar{p}$ = 0.18 GPa, θ = 28°C and R_* =   98 mm.

    ✿ : $\bar{p}$ = 0.29 GPa, θ = 20°C and R_* =   25 mm.

    ⋈ : $\bar{p}$ = 0.58 GPa, θ = 22°C and R_* =   25 mm.

    △ : $\bar{p}$ = 0.89 GPa, θ = 22°C and R_* = 6.25 mm.

    ◊ : $\bar{p}$ = 1.34 GPa, θ = 20°C and R_* =   19 mm.

liquid like 5P4E, may be possible. Figure 2.3 of Bair and Winer shows for Sebacate (diester) near the BL-regime a reduced coefficient of friction which can be more than 3 times the $\tau_1/\bar{p}$ ratio at mean pressures of 0.71 GPa and 0.84 GPa respectively. This indicates that their "τ_1"/$\bar{p}$ ratio must have been of the order of $5 \cdot 10^{-2}$ to obtain values for the coefficient of friction in the BL-regime of the order of $15 \cdot 10^{-2}$. The shift of the ML-BL transition, figure 5.12, is an unsolved phenomena as yet.

The friction curve, marked with Δ in figure 5.34, shows that the tangent, representing the friction in the ML-regime, not always has to increase compared to the tangent which represents friction in EHL.

Inlet

All the experiments discussed before were carried out on LCC's with an inlet region possessing such a configuration that pressure can be generated for the Hertzian contact region, as illustrated in figure 3.1. On the S-tribometer, strip-plate specimen combinations have been tested. These specimen were made from a piston-ring and a liner. The strip, with a large crown radius, had a misalignment with the plate in the sliding direction, as shown in figure 5.35. With this setup an inlet configuration in the sliding direction as in the previous experiments is produced. In the opposite sliding direction no inlet or an insufficient inlet is present. The effect of this contact configuration on friction is given in figure 5.35. It can be seen that, at the same operational variables and element properties, a totally different frictional behaviour exists for a contact with and without a sufficient inlet region. The well known friction curve was obtained for the contact situation with an inlet region. Without- or with an insufficient inlet region the contact stays in the BL-regime.
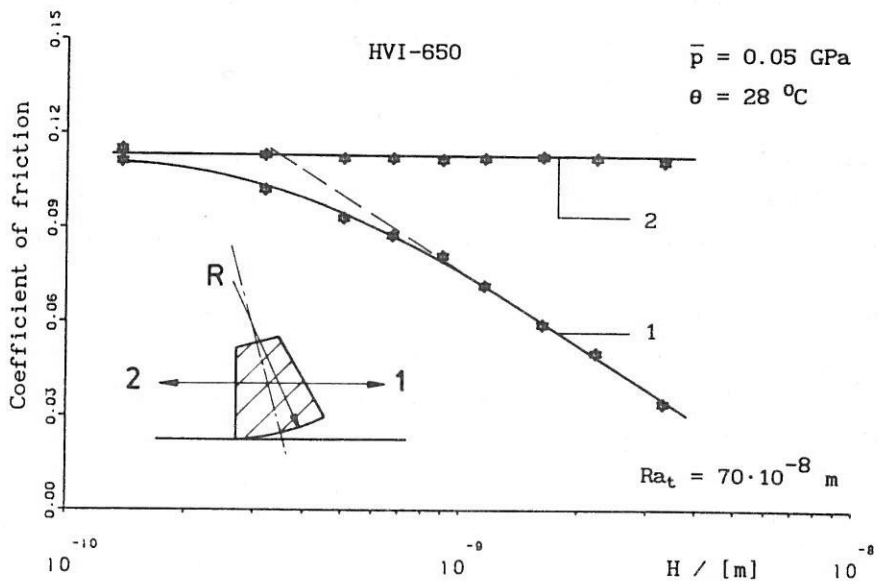
Fig. 5.35: Contact configuration and the effect on friction.

This means that the use of the parameter H or film thickness h is of no use for contact situations where no, or only an insufficient, inlet region is present. The question arises whether a sufficient inlet region is present or not. The answer to this question can not be given for the time being. It is known from the hydrodynamic lubrication theory (see for instance Cameron's (1966) essay on the Michell bearing) that a small angle of, say $2 \cdot 10^{-3}$ rad., is necessary to establish hydrodynamic action. This angle is so small that a small amount of wear, together with some deformation, can easily introduce a sufficient inlet region and subsequently the usual frictional behaviour for LCC's as a function of the lubrication number occurs.

In the contact situation, as presented in figure 5.35, wear takes place. However, the strip made from the piston-ring was covered with a (hard) Chrome layer of 0.5 mm. Therefore, the wear was low and had no influence on the contact configuration during these experiments.

CHAPTER 6:   ANALYSIS AND DISCUSSION

6.1   REVIEW AND ANALYSIS OF THE MAIN CONCLUSIONS

In chapter 5 the results were presented of friction experiments performed at LCC's and represented with the operational- and the lubrication number as derived in chapter 3. This lubrication number contains the operational variables and the relevant element properties under which the LCC is functioning. The relevance of this lubrication number is studied in relation to friction and its value to distinguish the different modes of lubrication of an LCC. From friction experiments, carried out with LCC's, it is clear that a distinction has to be made whether the lubricant in an LCC is expected to behave (according to the inlet temperature θ_1 and applied pressure $\bar{p}$) like a liquid or like a solid. This differentiation is applied to these experiments which results in the following main conclusions.

6.1.1   Liquid-state behaviour of the lubricant

- The area of contact remains largely confined to the Hertzian contact area throughout all lubrication modes, i.e. EHL, ML and BL (the small amount of wear that may occur is probably of a corrosive- or a micro-abrasive nature.

- The sum velocity is the controlling parameter for both the transitions EHL-ML and ML-BL. Contrary to the opinion of many authors, the sliding velocity is not characteristic for these transitions. For the pure rolling situation, ML and BL does not manifests itself in friction.

- The transitions EHL-ML and ML-BL are controlled by the lubricant viscosity in the inlet of the LCC. Friction, caused by shearing the lubricant, depends on the viscosity in the contact.

- The operational number $H = \eta_1 \cdot V_+ / \bar{p}$ appears to be a measure for the separation of the surfaces. The product $\eta_1 \cdot V_+$ can be regarded as a measure for the pressure generation in the inlet of an LCC; see equation (1.1). Owing to this, H is equal to the ratio of possible pressure generation to the applied pressure. It

determines if the pressure generation is large enough to prevent contact between the opposing surfaces at a certain applied contact force (pressure) and element properties, thus preventing the EHL-ML transition from taking place. Below a certain value of $\eta_1 \cdot V_+$ and constant element properties, pressure generation is negligible and the normal load is transmitted entirely by the interacting asperities, the transition ML-BL.

The result that η_1 and V_+ are controlling both the transitions EHL-ML and ML-BL, confirms the necessity of hydrodynamic action in the inlet of the macro-contact throughout the whole ML-regime. If there is insufficient inlet present, no pressure generation takes place and BL prevails.

- If the lubrication number is used, the type of lubricant does not influence the transitions EHL-ML and ML-BL. The level of friction, however, depends on the lubricant and differs with it in each lubrication mode.

- The rheological behaviour of the lubricant in the macro-contact changes if the operating conditions for an LCC are changing. This also occurs when a contact enters more and more into the ML-regime by changing for instance the sum velocity, while keeping the other operating conditions constant. In figure 3.5 the dotted line (1) schematically represents the change in rheological behaviour for a contact that, just before it enters the ML-regime, is of an elastic-non linear viscous nature. The lubricant behaviour in the macro-contact ultimately becomes Newtonian when the BL-regime is reached. The drawn line (2) expresses the rheological change in the micro-contacts. Note that the transition from elastic-non linear viscous to elastic-plastic behaviour decreases proportionally with decreasing V_+. Therefore, if micro-geometry allows lubrication in the micro-contacts, the rheological behaviour in these micro-contacts can become of elastic-plastic nature.

Owing to the rheological behaviour of the lubricant, different types of friction curves (Stribeck like) may be obtained. These friction curves showed that the "minimum friction concept" for determining the transition from full-film lubrication to mixed

lubrication is not applicable.

- As expected, roughness has a significant influence on both the transitions EHL-ML and ML-BL. However, this influence of roughness is more pronounced for the EHL-ML transition, as pointed out in equation (6.2).

  The roughness measurements show that a roughness height parameter, like Ra_t used in this study, characterizes a rough surface rather well with relation to the transitions EHL-ML and ML-BL. The other micro-geometry variables like slope, curvature, wavelength appear to have a minor effect on the transitions. Friction, however, appears to also depend on other geometry variables, which are characteristic for describing the micro-geometry.

- The transitions EHL-ML and ML-BL can, in general, be specified by:

$$H/Ra_t^k = 1 \cdot \bar{p}^m \qquad (6.2)$$

where k is 1.5 and 1, l is $3.1 \cdot 10^4$ and $1.25 \cdot 10^4$ and m is -0.5 and -1.0 for the transition EHL-ML and ML-BL respectively.

These transitions are presented in figure 6.1, where H/Ra_t is depicted as a function of the mean Hertzian contact pressure.

With this figure it is possible to predict in which lubrication mode a particular lubricated concentrated contact operates; this as a function of the relevant element properties (R_*, Ra_t and E_*) and operational variables (V_+, $\theta_1 \to \eta_1$ and $N \to \bar{p}$) under liquid-like behaviour of the lubricant.

- The relation between the minimum film thickness h and $H = \eta_1 \cdot V_+/\bar{p}$ for a circular contact is, using Moes et al. (1972):

$$h_{min} = 0.32 \; \alpha^{0.55} \; E_*^{0.40} \; N^{0.15} \; H^{0.70} \qquad (6.1)$$

For the transitions EHL-ML and ML-BL at a moderate mean pressure of 0.60 GPa it has been found; $H_{EHL-ML} = 6 \cdot 10^{-12}$ m and $H_{ML-BL} = 8 \cdot 10^{-13}$ m respectively, where $\alpha = 1.4 \cdot 10^{-8}$ Pa^{-1}, $E_* = 2.3 \cdot 10^{11}$ Pa, N = 1000 N and $Ra_t = 2.5 \cdot 10^{-8}$ m. Substituted in equation (6.1), this yields for the transition EHL-ML: $h_{min}/Ra_t \approx 0.9$. If
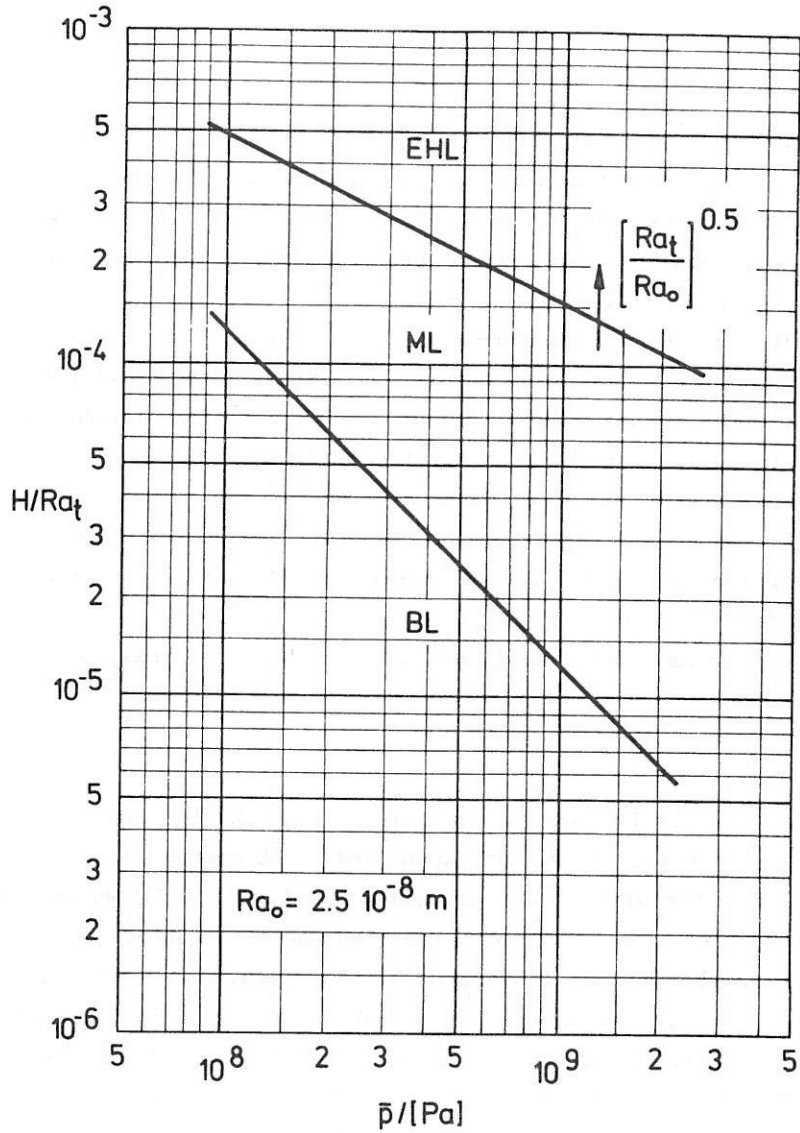
Fig. 6.1: H/Ra_t as a function of $\bar{p}_{Hertz}$.

$$\text{EHL-ML} : H/Ra_t^{1.5} = 3.1\ 10^4\ \bar{p}^{-0.5}$$

$$\text{ML-BL} : H/Ra_t = 1.25\ 10^4\ \bar{p}^{-1}$$

the "smooth EHL" theory is applied to the transition ML-BL, then $h_{min}/Ra_t \approx 0.2$ is obtained. These somewhat low h/Ra_t values are rather in agreement with values of h/Ra_t as presented in literature for similar pressures. However, for a pressure region of 0.1 to 1.5 GPa, h/Ra_t for the EHL-ML transition varies with a factor of, say, 2.5 and for the ML-BL transition h/Ra_t varies

with a factor of, say, 6.

- In a large part of the ML-regime friction increases linearly with decreasing ln H; in general: $\mu_{ML} = C_1 + C_2$ ln H. Therefore, using (5.4), friction in the ML regime can be specified by:
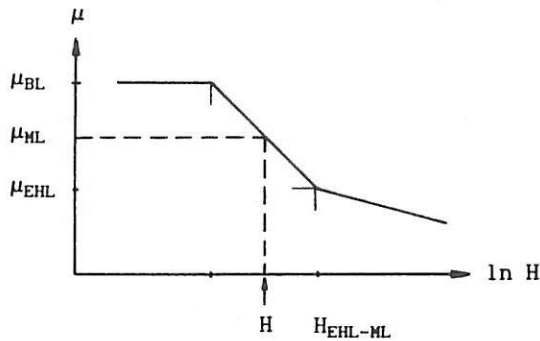
$$\mu_{ML} \approx \mu_{EHL} + \frac{(\mu_{BL} - \mu_{EHL})}{\ln (2.5 \cdot \bar{p}^{0.5} \cdot Ra_t^{0.5})} (\ln H_{EHL-ML} - \ln H) \quad (6.3)$$

Since μ_{EHL} can be obtained from the well known EHL theory a prediction of μ in the ML regime as a function of the operating conditions is possible if μ_{BL} is known.

- The transition ML-BL is pressure independent. The consequence of this is that a contact which operates in the ML-regime at constant $\eta_1 V_*$ and constant element properties does not enter the BL-regime by solely rising the pressure.

The reason for this pressure independence is; At the transition ML-BL, the total applied normal load is carried by the interacting asperities. By rising the normal force (and with that the macro-contact pressure, $\bar{p}_{Hertz}$) the mean contact pressure in the micro-contacts nearly remains the same, Greenwood et al. (1966, 1967 and 1970). For the lubrication of these micro-contacts the pressure of the macro-contact is not relevant. Instead of $\bar{p}_{Hertz}$ the mean pressure in the real contacts is becoming of interest.

According to Greenwood et al. (1966, 1970) the mean pressure in the micro-contacts is equal to $\bar{p}_c \therefore E_* \cdot \sqrt{(\sigma/\beta)}$. With increasing

surface roughness (σ) the real contact pressure increases and therefore to get some of the micro-contacts lubricated (transition ML-BL) $\eta \cdot V_*$ has to increase (Note: not all asperity contacts do have a pressure equal to $\bar{p}_c$). The same happens if the mean radius of the summits decreases. By reducing E_* and keeping the same surface roughness the transition ML-BL has to shift to lower values of $\eta \cdot V_*$. However, the measurements with Al 7075-T651 did not show this effect.

- Low pressure measurements did not often show a friction level in the quasi "BL"-region equal to τ_l/p. Raising the pressure, but remaining in the lubricants liquid-state regime, measurements showed that it is more easy to obtain a value of τ_l/p of about 0.1. At low pressures the contact is operating in the Newtonian regime of fig.3.5. Starting in this regime and decreasing only the sum velocity, the micro-contacts do not easily enter the elastic-plastic regime, in contradistinction to the high pressure situation presented in figure 3.5, the elastic - non linear viscous behaviour situation. Furthermore, the deformation of the roughness is larger at higher contact pressures. The curvatures of the roughness summits decrease (Tripp et al.(1987)) and with that a better condition for lubrication is created for the micro-contacts. Quantitative statements concerning this topic are not available yet. The measurements with Al 7075-T651, which were meant to study the effect of elasticity and with that the effect of deformability of the surfaces, were not successful.

6.1.2   Expected solid-state behaviour of the lubricant

- In this case, the lubrication number H/Ra_t or a film thickness to roughness ratio h/Ra_t appear to be no relevant parameters to express the severity of the operational conditions under which an LCC is operating. The inlet viscosity does not play a role with respect to the frictional behaviour at expected solid-state behaviour of the lubricant in the contact. Also, in case solid-state lubrication changes to ML (as shown in figure 5.25)

no relation with the inlet viscosity has been found. This change occurs for totally different H values at the same element properties.

- Measurements in the solid-state regime of figure 3.4 show a transition in the friction curve. This frictional behaviour is controlled entirely by the rheological behaviour of the lubricant in the contact and has nothing in common with ML. This statement is justified by calculating the friction of an LCC at a certain pressure p and at a constant inlet temperature θ_1.
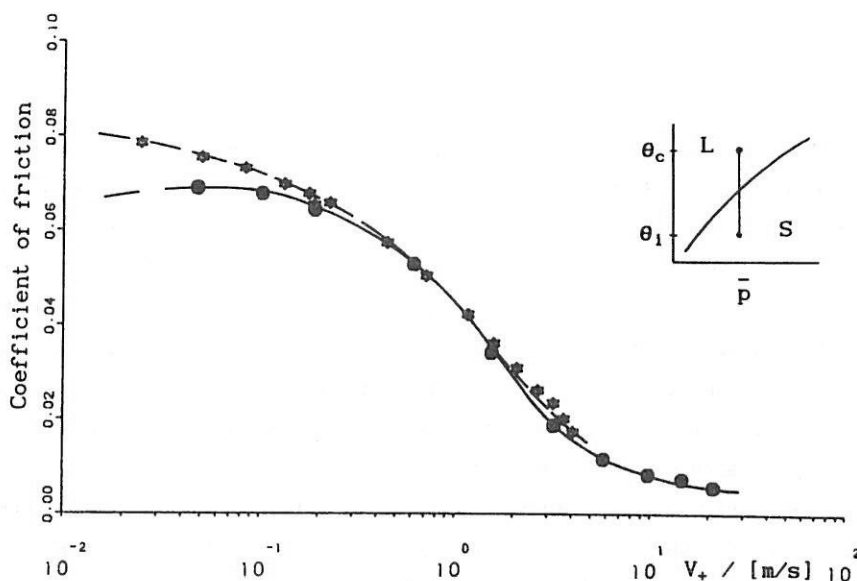
Fig 6.2: Comparison between measured (✽) and calculated friction (●) for HVI-650 at $\bar{p}$ = 0.82 GPa, θ_1 = 27 ^{0}C and S = 100 %.

Figure 6.2 shows that the calculated friction agrees very well with the measured friction in the declining part of the friction curve. In these thermal friction calculations the rheological parameters τ_0, G and η , valid in the liquid-like regime, have been used (τ_1 is not taken into account). These calculations show that, due to temperature rise in the contact, the lubricant behaviour changes from solid- to liquid-state.

This transition in the friction curve, caused by solid-state to

liquid-state behaviour, is roughly specified by $V_- \cdot \bar{p} \cdot R_* \approx 4 \cdot 10^5$. Archard (1958/1959) showed that the temperature rise in a contact is mainly controlled by the Péclet number. For concentrated contacts Péclet can be written as $Pé = V_- \cdot r_H / K$. K is the thermal diffusivity and equal to $\lambda / \rho C_p$, where λ is the thermal conductivity, ρ the density and C_p the specific heat. Using equations (c-12) and (c-14), r_H becomes equal to $3 \cdot \pi \cdot \bar{p} \cdot R_* \cdot E_*^{-1}$ and herewith $Pé = 3 \cdot \pi \cdot V_- \cdot \bar{p} \cdot R_* \cdot E_*^{-1} / K$. The experimentally found relation $V_- \cdot \bar{p} \cdot R_* = $ Const. is in agreement with this.

6.1.3 Summary

The frictional behaviour of an LCC under conditions of solid-state or liquid-state behaviour of the lubricant seems to be equivalent. That is, a decrease in friction is present with increasing lubrication number. However, they essentially differ from each other. In the case of liquid-like behaviour of the lubricant the rise of the coefficient of friction is caused by asperity interaction, BL or micro-EHL. If solid-like behaviour prevails, the decrease in friction at increasing lubrication number is entirely related to lubricant behaviour caused by heat dissipation in the contact.

On the basis of the above findings a flow diagram, depicting the lubrication mode and the frictional behaviour of an LCC, can be drawn up, as presented in figure 6.3. The advantage of this diagram is that, in principle, it can be seen very easily which lubrication mode an LCC is operating in and which frictional behaviour can be expected. On the basis of the parameters involved, it can be decided what measures have to be taken to avoid a particular lubrication mode.

$\bar{p}, \theta_1$

θ_{LS} — + — | $\bar{P}$

L: $\theta_1 > \theta_{LS}$

S: $\theta_1 < \theta_{LS}$

$V_- \cdot R_* \cdot \bar{p} > 4 \cdot 10^5$

No   Yes

$\theta_c < \theta_{LS}$ $\theta_c > \theta_{LS}$

$\mu = \tau_1/p$ $\mu = \mu_{EHL}$

$\mu_{EHL} = \phi(\eta, \ \tau_0, \ G, \ p, \ \theta, \ \dot{\gamma})$

$\mu_{ML} =$ Equation (6.3)

$\mu_{BL} = \begin{cases} \sim \ (9 \pm 2) \cdot 10^{-2} \ \text{micro-EHL} \\ \sim (13 \pm 2) \cdot 10^{-2} \ \text{BL} \end{cases}$
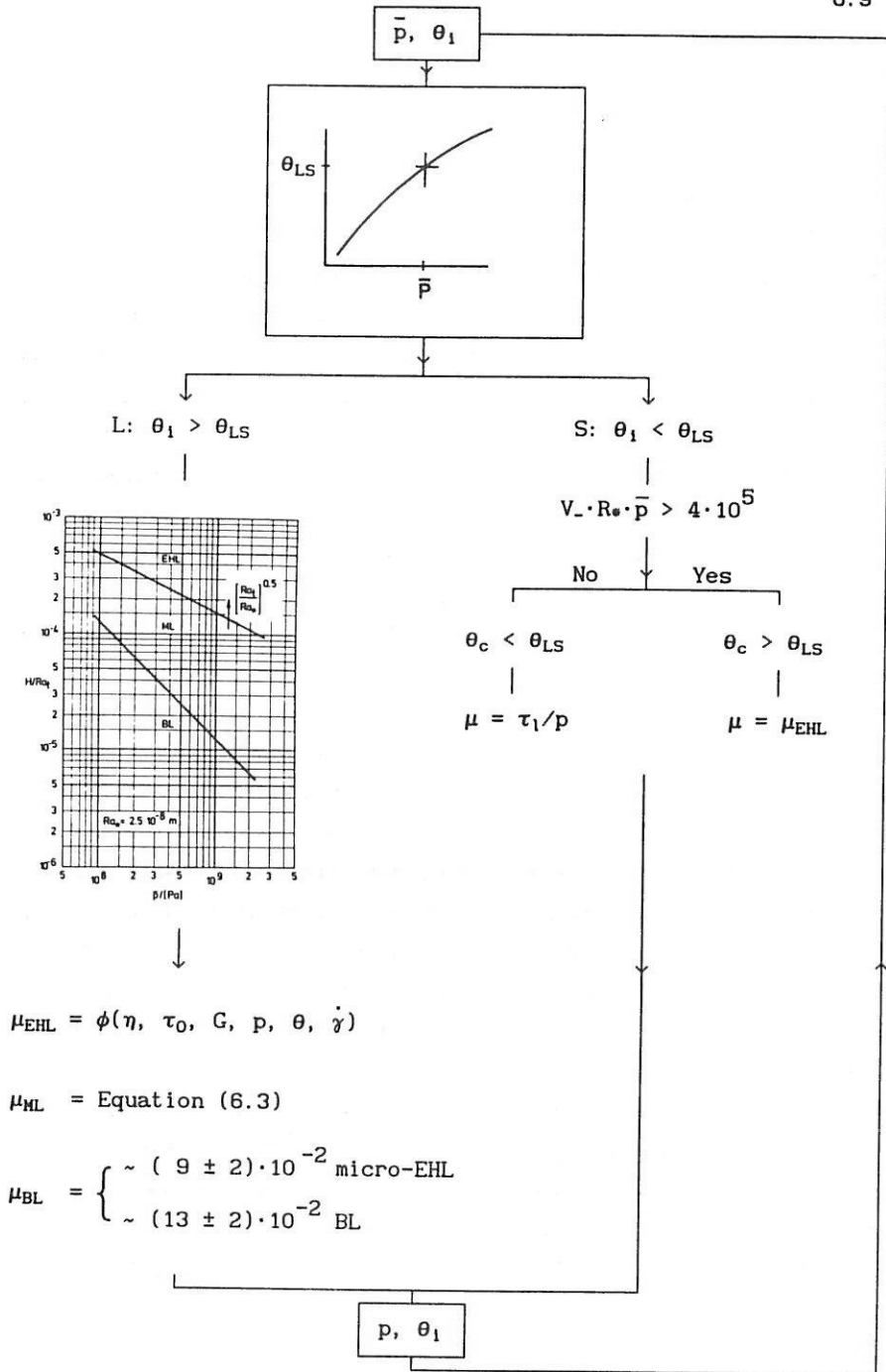
$p, \ \theta_1$

Fig 6.3: Flow diagram to determine frictional
behaviour and lubrication mode of an LCC.

6.2 DISCUSSION

I. Flow diagram.

In the flow-diagram of figure 6.3 two parameters during operation are not yet known.

Firstly, the inlet temperature (θ_1) and with that the inlet viscosity η_1 which strongly depends on θ_1 and decreases with a temperature rise ($\Delta\theta_1$) in the inlet. This temperature rise is caused by heat dissipation in the contact ($\Delta\theta_{11}$) and by shear heating in the inlet itself ($\Delta\theta_{12}$).

Secondly, the micro-geometry parameter Ra_t, determining the transitions EHL-ML and ML-BL, is also of importance for the magnitude of the coefficient of friction present in the situation that $H/Ra_t < 1.25 \cdot 10^4 \cdot \bar{p}^{-1}$.

These variables θ_1 ($\rightarrow \eta_1$) and Ra_t depend on the friction- and wear processes present in the contact.

- Greenwood and Kauzlarich (1973) showed that at high surface velocities the temperature rise $\Delta\theta_{12}$ by shear heating at the inlet can become significant. The average rise is equal to $\eta_1 \cdot V_+^2/(16 \cdot \lambda)$. However, for low surface velocities this effect can be neglected.

  The temperature rise $\Delta\theta_{11}$ in the inlet zone from heat dissipation in the contact is an unsolved problem as yet. It strongly depends upon the heat capacity and on the thermal heat coefficients of the elements and the system in which the contact is operating. For this reason many authors, mentioned in section 5.2.5, find different failure conditions for scuffing to occur.

- No theory is available as yet which predicts roughness values of the surfaces during operation or after a certain operation time (sliding distance). Known is only that, if running-in takes place (without macroscopic wear), Ra_t in sliding direction decreases.

The prediction of the coefficient of friction in the lubrication regime where $H/Ra_t < 1.25\ 10^4 \cdot \bar{p}^{-1}$, is still in its infancy. Only values obtained from experiments are available. Roughly, two levels of coefficient of friction are found in this lubrication area, being resp. 0.13±0.02 and 0.09±0.02, mainly depending on micro-geometry.

II. Extension to low pressures.

In chapter 2 ML is discussed, as it occurs under low pressure conformal (dispersed) contact conditions (HL) and under high pressure contraformal (concentrated) contact conditions (EHL). ML conditions were expected to differ not very much at HL and EHL contact situations.

In figure 6.4 the H/Ra_t - $\bar{p}$ curve is extended to the low pressure regime (HL), supplemented with results of the Al 7075-T651 experiments and results presented in the literature. The low pressure results of section 5.3.3 and those found in literature fit rather well with the extrapolated EHL-ML and ML-BL transitions, which are characterized by equation (6.2). Figure 6.4 shows that for low pressures the transition HL-ML shifts to higher values of H/Ra_t, compared to the extrapolated EHL-ML transition. An intersection would occur if the lines from figures 6.1 or 6.4, representing respectively the transitions EHL-ML and ML-BL for a certain value of Ra_t, would be extrapolated. Using equation (5.4), this intersection occurs at a pressure of appr. 6 MPa if the roughness Ra_t is equal to 2.5 10^{-8} m. This conflicts with the results of figure 2.1, where an ML-region is found to be present at low pressures. The slope of the transition HL-ML in figure 6.4 is tending to -1 in the low pressure region. This means that the transition HL-ML also appears to be nearly pressure independent, a remarkable result. The tendency of pressure independence is also measured at flat sliding contacts. From the results of Gartner (1964) and Hata et al. (1980) the figures 6.5[a,b] have been reproduced. Stribeck's result does not agree with it; see figure 6.5[c] where $n/p_{proj.}$ is depicted as a function of $p_{proj.}$. The first few low pressure datapoints show a decrease of $n/p_{proj.}$ with increasing $p_{proj.}$. At higher values of $p_{proj.}$ the value of $n/p_{proj.}$ increases. The reason for this phenomena might be temperature effects, i.e. a higher transition velocity was necessary due to a decreasing inlet viscosity caused by heat dissipation at high $p_{proj.}$. In figure 6.6 the
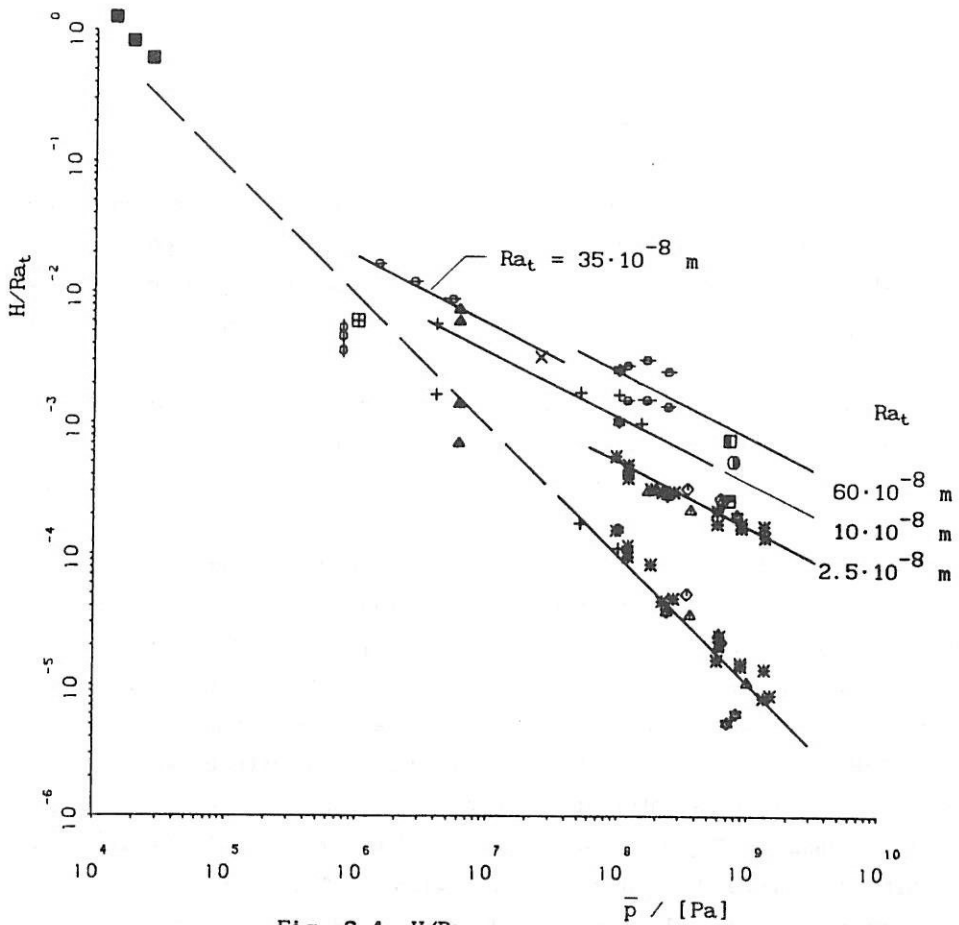
Fig. 6.4: $H/Ra_t - p$.

■ : Hata et al. (1980) Ra=$1.4 \cdot 10^{-8}$ m × : Czichos (1971) Ra=$35 \cdot 10^{-8}$ m

+ : Al 7075-T651   Ra=$8 \cdot 10^{-8}$ m ⊖ : Gartner (1964) Ra=$60 \cdot 10^{-8}$ m

⊖ : Gartner (1964)   Ra=$10 \cdot 10^{-8}$ m ▫ : Smith (1959)   Ra=$60 \cdot 10^{-8}$ m

⊖ : Gartner (1964)   Ra=$35 \cdot 10^{-8}$ m ▲ : Emmens (1988) Ra=$100 \cdot 10^{-8}$ m

◑ : Poon et al.(66/67) Ra=$47 \cdot 10^{-8}$ m ▣ : Smith (1959)   Ra=$11 \cdot 10^{-8}$ m

Φ : Lenning (1960)   Ra = 13, 27, $53 \cdot 10^{-8}$ m

dependence of $H_{(E)HL-ML}$ with relation to $\bar{p}$, represented by $dH/d\bar{p}$, is depicted as a function of $\bar{p}$. It follows that the transition HL-ML becomes more pressure independent with decreasing pressure. Some reservation to this statement has to be made. The information becomes uncertain, due to the limited number of data points and the variability of the roughness values.
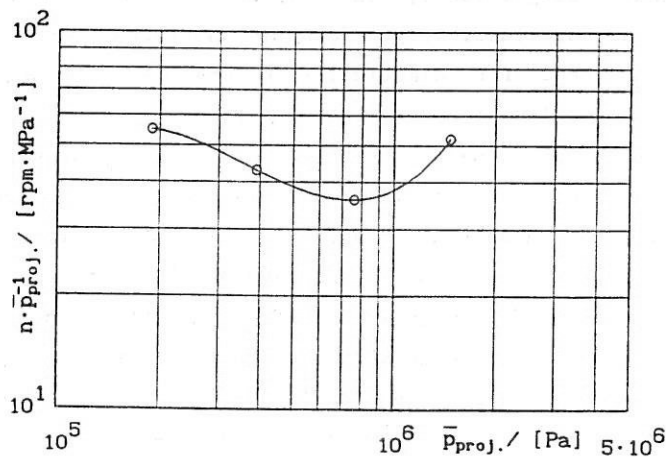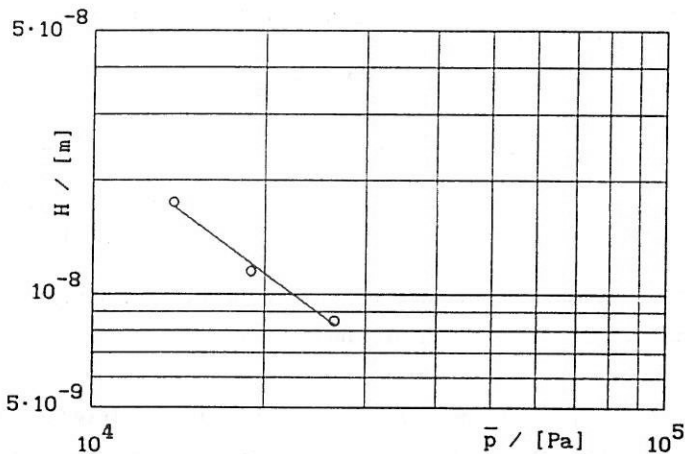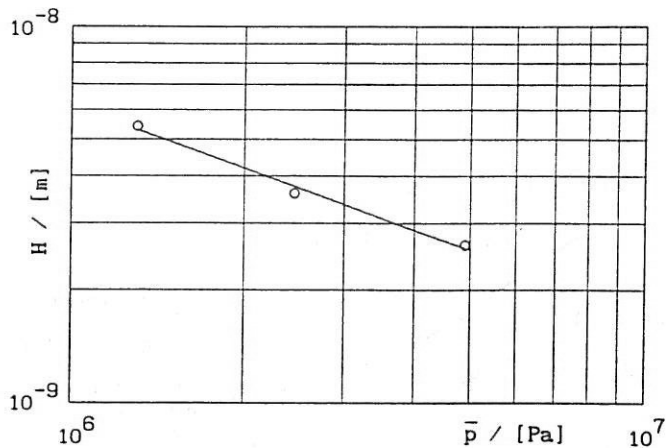
Figure 6.5: The HL-ML transition represented by $H = \eta_1 \cdot V_+ / \overline{p}$ or $n/p_{proj.}$ as a function of pressure.

a) Gartner (1964), b) Hata et al. (1980), c) Stribeck (1902).
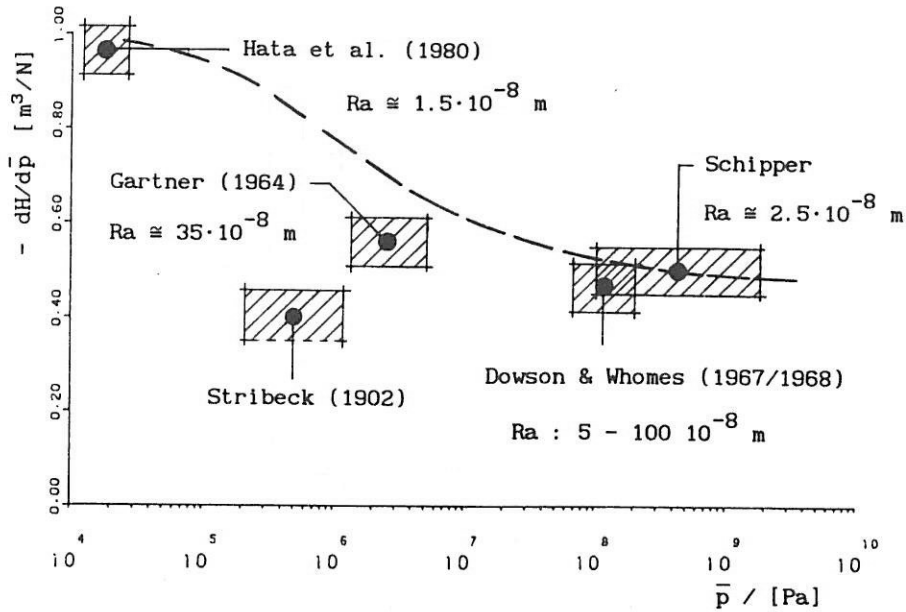
Figure 6.6: The pressure dependence of the (E)HL-ML transition
(dH/dp̄) as a function of the pressure p̄.

Recently, de Gee et al. (1988) presented a transition diagram for
journal bearings, in which the lubrication mode is shown as a function
of normal load and sliding velocity. The diagram has been presented
for rigid as well as for elastically deformable surfaces. From this
diagram it is seen that for elastically deformable surfaces the
transition HL-ML is tending to become independent of pressure.

From the equations to determine the transitions, used in that work, it
can be seen that the ratio of the elastic compliance of the surface
(c) and the surface roughness (Ra), c/Ra, is a relevant parameter. If
c/Ra is small, both the transitions HL-ML and ML-BL are inversely
proportional to p̄, whilst for large values of c/Ra, the transitions
tend to become pressure independent. However, this is conflicting with
the EHL results, where c/Ra is large, while a pressure dependence
still exists. Most of the results, presented in chapter 5, have been
obtained at values of c/Ra of appr. 300.

III. The IRG transition diagram.

In chapter 1 the well known IRG-transition diagram for LCC's is presented. The transitions from region I to region II and from region I to region III are controlled by the product of $p \cdot V_-^x = C$. In this equation the value of x varies from 0.1 to 0.3, depending on the viscosity-temperature characteristic of the lubricant while C depends on viscosity, composition of the lubricant and surface roughness. For these lubricated systems the transition from region II to region III appears to be controlled by a constant contact temperature, θ_c. This transition is influenced by the composition of the materials and by the type of additives in the lubricant. It is interesting to compare the IRG-transition diagram with the transition diagram of figure 6.1. Rewriting equations (6.2) into terms of V_- and $\bar{p}$, using $S = 2 \cdot V_-/V_+$, $H = \eta_1 \cdot V_+/\bar{p}$ and equation (c-14), one obtains :

EHL-ML:

$$V_- = 1.55 \cdot 10^4 \frac{S \cdot Ra_t^{1.5} \cdot \bar{p}^{0.5}}{\eta_1}$$

ML-BL :
(6.4)

$$V_- = 6.25 \cdot 10^3 \frac{S \cdot Ra_t}{\eta_1}$$

These equations yield transition lines as presented in figure 6.7 to distinguish the EHL, ML and BL lubrication regimes. At low pressures the results of the discussion in part II of this section are applicable, i.e., both the transitions HL-ML and ML-BL are pressure independent.
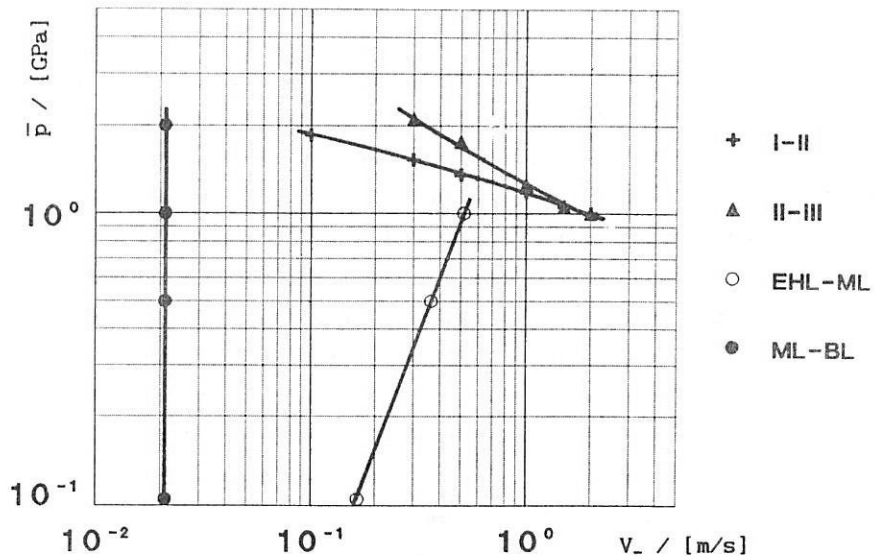
Fig. 6.7: EHL-ML and ML-BL transitions in the IRG-transition diagram.
The IRG-diagram is reproduced from de Gee et al. (1984).

It can be seen from figure 6.7 that region I of the IRG transition
diagram falls apart into three subregions, representing EHL, ML and BL
respectively.

In section 4.5 it is indicated that in experiments performed by
raising the pressure, whilst keeping the other operating conditions
constant, the heat dissipation is enormous. As discussed in section
5.3.1.3. and in this section, part I, the inlet conditions become more
severe (temperature rise in the inlet). For this reason the EHL-ML as
well as the ML-BL transition in figure 6.7 shift to higher values of
V_-, which is going on with increasing inlet temperature. The
transitions in the IRG-diagram depict the situation in which the
contact has already passed the ML-BL transition. They have to be seen
as a total failure of the boundary layers at the micro-contacts due to
heat dissipation or lack of time in re-establishment of the mechanical
removed surface layers. The 5P4E experiments also failed by the latter
mechanism.

CHAPTER 7:   RECOMMENDATIONS

The results presented in this work lead to an improvement in the understanding of friction and transitions in the lubrication of concentrated contacts. Further work in this field to improve the knowledge of LCC's is necessary. Therefore, the next points are of interest in the development of a comprehensive theory for the mixed lubrication region.

1. An interesting topic is to establish micro-EHL at severe operating conditions. The existence of micro-EHL is mainly controlled by micro-geometry. Therefore, more knowledge of the relevant parameters for the micro-geometry is needed especially those parameters which represent the highest interacting roughness summits. One should keep in mind that deformation in the contact may play an important role.

2. Measurements at low pressures have to be carried out to obtain a complete transition diagram for the different lubrication modes to support the statements made in the discussion of chapter 6.

3. Development of a general calculation method of the temperature rise in the inlet ($\Delta\theta_1$) of an LCC caused by heat dissipation in the contact itself.

4. Now that the transitions EHL-ML and ML-BL have been established as a function of the operational variables and of the element properties, it is required to study wear both in the ML- and in the BL-regime.

APPENDICES

APPENDIX A: General nomenclature [*]

a   Minor semi-axis of Hertzian contact.

A   Contact area.

b   Major semi-axis of Hertzian contact.

D   Deborah number, $D = \eta \cdot \bar{V}/(G \cdot a)$.

E   Elasticity modulus.

$E_{\bullet}$ Equivalent elasticity modulus for combined surfaces.

F   Friction force.

F_c Friction force caused by asperity interaction.

F_l Friction force caused by shearing the fluid.

G   Shear modulus.

h   Film thickness.

H   Operational number, $H = \eta_1 \cdot V_+ / \bar{p}$.

k   Wear rate or specific wear coefficient.

N   Normal force.

N_c Normal force carried by asperity interaction.

N_l Normal force carried by hydrodynamic pressure.

p   Pressure.

Q   Heat generation.

r   Radius of Hertzian contact circle.

Ra   CLA surface roughness.

Ra_t Combined CLA surface roughness, $Ra_t = (Ra_1^2 + Ra_2^2)^{1/2}$.

R_{x1} Principal radii at the contact in x-direction, this is the direction of main flow.

R_{x2} Principal radii at the contact in y-direction, perpendicular to the main flow.

[*] note: certain specialized terminology is defined locally.

R_* Equivalent radius of curvature.

s Separation.

S Slipratio, $S = 200 \cdot V_- / V_+$ [%].

V Velocity.

V_+ Sum velocity, $V_+ = V_1 + V_2$.

V_- Sliding velocity, $V_- = |V_1 - V_2|$.

$\bar{V}$ Mean rolling velocity, $\bar{V} = V_+/2$.

x Cartesian coordinate in the direction of motion of the surfaces and mean lubricant flow.

y Cartesian coordinate perpendicular to direction of motion.

z Cartesian coordinate through film thickness.

α Pressure viscosity index in the Barus equation, $\eta = \eta_0 \cdot e^{\alpha \cdot p}$

β Mean radius of the asperity summits.

$\dot{\gamma}$ Shear strain rate, $\dot{\gamma} = \partial V / \partial z$.

$\dot{\gamma}_e$ Shear strain rate due to elastic effects.

$\dot{\gamma}_v$ Shear strain rate due to viscous effects.

η Dynamic viscosity.

η_1 Dynamic viscosity inlet contact.

η_0 Dynamic viscosity at $\theta = \theta_0$ and atmospheric pressure.

θ Temperature.

λ Film thickness to roughness ratio, $\lambda = h/\sigma_t$.

μ Coefficient of (sliding) friction.

ν Poisson's ratio.

σ RMS surface roughness.

σ_t Combined RMS surface roughness, $\sigma_t = (\sigma_1^2 + \sigma_2^2)^{1/2}$.

τ Shear stress.

τ_l Limiting shear stress.

τ_0 Eyring shear stress.

Φ Functional relationship.

Superscripts:

$\char`\^{}$ as in $\hat{V}$: maximum value

$-$ as in $\bar{p}$: averaged property over the contact.

Subscripts:

1,2 as in V_1 : refers to properties of individual surfaces.

bl   as in A_{bl} : refers to boundary lubricated.

ml   as in A_{ml} : refers to micro-EHL.

ma   as in A_{ma} : refers to macro lubricated contact.

l   as in F_l : refers to lubricant.

c   as in F_c : refers to asperity contact.

Abbreviations:

BL   :   Boundary Lubrication.

CLA   :   Center Line Average.

DF   :   Dry Friction.

EHL   :   Elasto Hydrodynamic Lubrication.

HL   :   Hydrodynamic Lubrication.

LCC   :   Lubricated Concentrated Contact.

ML   :   Mixed Lubrication.

RMS   :   Root Mean Square.

APPENDIX B: Lubricant properties.

Oil Properties		1) SEBACATE		2) SANTOTRAC* 50		3) SANTOVAC-5* 5P4E		4) HVI-650*	
		η	α	η	α	η	α	η	α
	20°C	21.2	1.61	–	–	–	–	–	–
	30	14.7	1.53	45.6	3.30	–	4.01	900	3.02
η	40	10.7	1.42	28.4	2.87	266	3.50	450	2.75
(m Pa·s)	50	8.0	1.36	19.4	2.51	140	3.02	240	2.48
	60	6.2	1.29	13.1	2.28	79	2.63	140	2.29
	70	4.9	1.25	9.6	2.06	48	2.30	85	2.10
α	80	4.0	1.22	7.3	1.91	31	1.98	55	1.95
$(m^2/N) \cdot 10^8$	90	3.3	1.18	5.7	1.77	21	1.71	37	1.84
	100	2.8	1.16	4.6	1.65	15	1.49	27	1.75
	110	–	–	3.8	1.58	10	1.30	20	1.68
	120	–	–	3.1	1.50	8	1.12	15	1.64
Z		0.55		–		–		0.59	
s_0		1.04		1.21		1.45		1.28	
ρ	40°C	911		889		1184		888	
kg/m³	100	875		855		1140		853	
Literature* $\tau_1/\bar{p}$		–		40°C $11.3 \cdot 10^{-2}$		40–100°C $6.8 \cdot 10^{-2}$		40°C $9.0 \cdot 10^{-2}$	
$\tau_1/\bar{p}$	40°C 80	$9.4 \cdot 10^{-2}$ ($\approx$25°C)		– $10.8 \cdot 10^{-2}$ (63°C)		$8.7 \cdot 10^{-2}$ –		$9.2 \cdot 10^{-2}$ $8.6 \cdot 10^{-2}$	
Symbol		※		△		☽		✿	

* Evans, (1983).

Oil Properties		5) TURBO** T68 η	6) VITREA** 100 η	7) HVI-*** 160S η	8) GADENIA** 30 η
η (m Pa·s)	20°C	183.3	297.1	–	–
	40	58.4	87.4	90.1	91.8
	50	35.8	52.8	–	55.3
	100	7.1	9.6	9.7	10.0
Z		0.62	–	0.63	–
s_0		1.26	1.25	1.24	1.25
ρ kg/m³	15°C	876	890	878	897
$\tau_1/\bar{p}$	40°C	–	–	$8.7 \ 10^{-2}$	$9.0 \ 10^{-2}$
	80	–	–	–	$8.0 \ 10^{-2}$
Symbol		+	×	⋈	◇

** SHELL, "smeermiddelen voor industrie en scheepvaart".

*** SHELL, report TNGR 0042.74

1) A synthetic hydrocarbon, di-(2 ethyl hexyl), for low temperature applications.

2) A synthetic cycloaliphatic hydrocarbon plus additives especically developed for its high traction properties. Additives: Antiwear (zinc dialkyl dithiophosphate), oxidation inhibitor, antifoam, V.I. improver (Polymethacrylate).

3) A mixed isomeric five-ring polyphenyl ether, developed for use in high temperature applications and high vacuum technology.

4) A high viscosity (HVI) mineral oil predominantly paraffinic.

5) A mineral oil developed for "gasturbine" installations under high temperature conditions. Additives: Oxidation inhibitor, antifoam and metal deactivator.

6) A clean mineral oil, predominantly paraffinic, developed for not heavily loaded contacts.

7) A mineral oil predominantly paraffinic.

8) A mineral oil with additives such as antiwear, oxidation inhibitor, antifoam, etc. This oil is developed for medium speed diesel engines and highly loaded contacts.
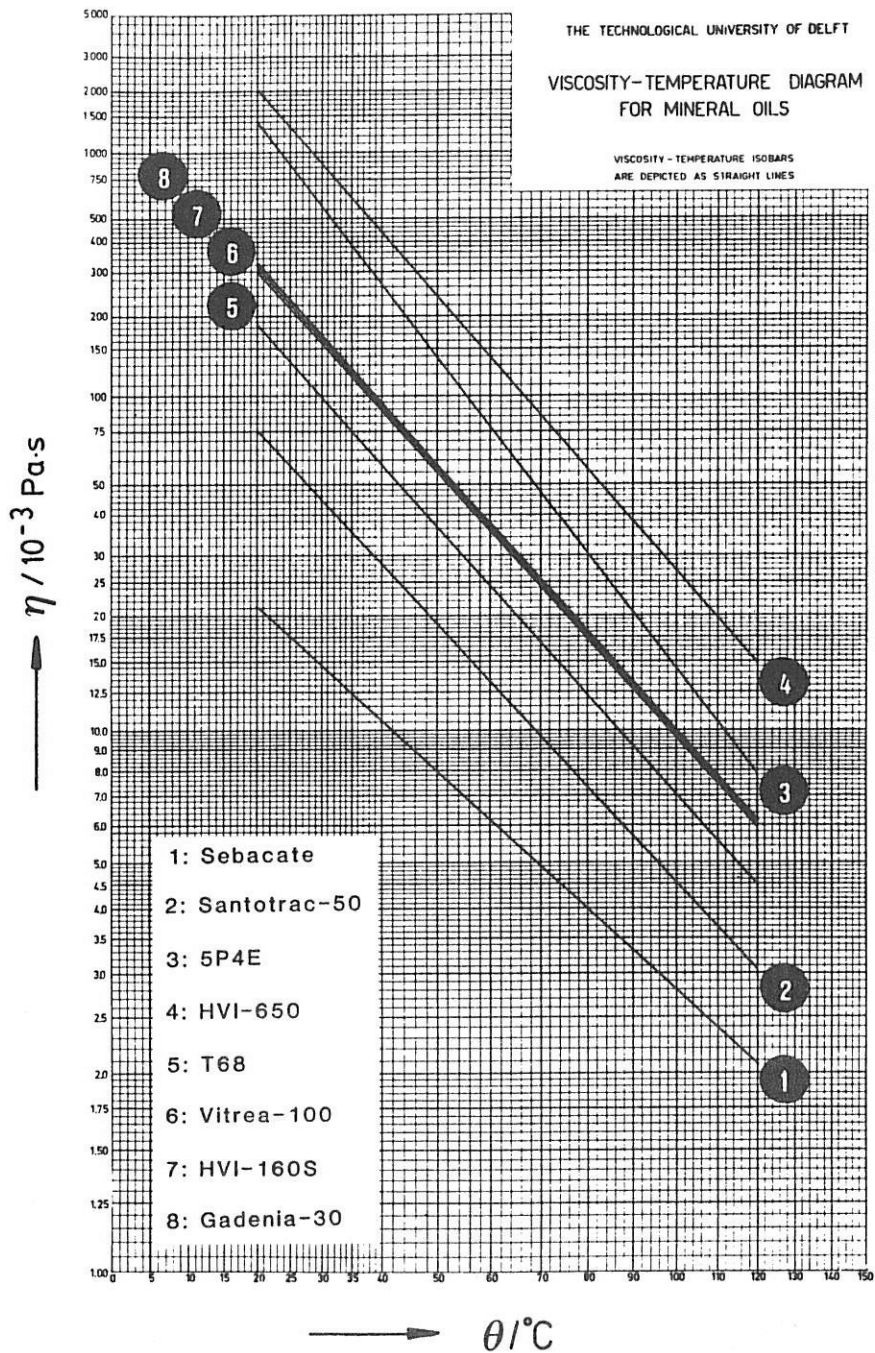
Fig. B1: Viscosity-temperature diagram.

APPENDIX C: Summary of the Hertzian contact formulas.

In tribology many contact situations are present in which curved bodies, such as cylinders and spheres are in contraformal contact, schematically represented in figure C1.
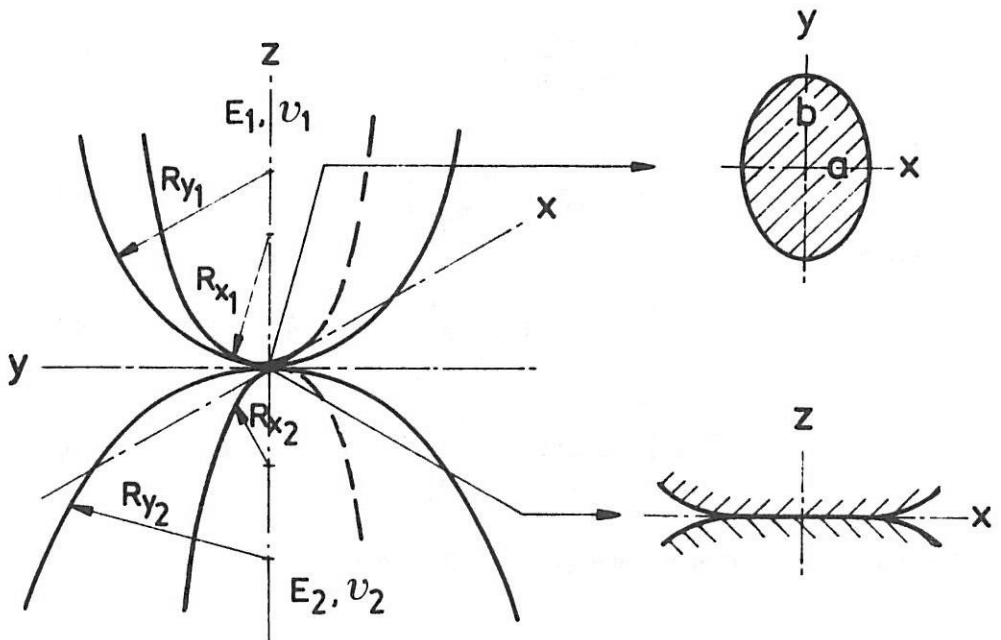
Fig. C1: Contraformal contact.

Hertz (1881) gave for elasto-statical contraformal contacts without friction at the interface the solution for contact area, contact pressure and elastic compression as a function of normal force, geometry and elastic moduli. The Hertzian equations contain elliptical integrals, whose values must be found from tables. Reusner (1977) and Greenwood (1985) gave approximate expressions for the Hertzian solutions. The equations for elliptical contact areas are according to Hertz:

contact area:

$$a = \alpha \left[\frac{3 \cdot N \cdot R_{\bullet}}{E_{\bullet}} \right]^{1/3} \qquad (c-1)$$

$$b = \beta \left[\frac{3 \cdot N \cdot R_{\bullet}}{E_{\bullet}} \right]^{1/3} \qquad (c-2)$$

elastic approach:

$$c = \gamma \left[\frac{9 \cdot N^2}{8 \cdot E_{\bullet}^2 \cdot R_{\bullet}} \right]^{1/3} \qquad (c-3)$$

pressure:

$$\overline{p} = \frac{2}{3} \hat{p} = \frac{1}{\pi \alpha \beta} \left[\frac{N \cdot E_{\bullet}^2}{9 \cdot R_{\bullet}^2} \right]^{1/3} \qquad (c-4)$$

in which

$$\frac{1}{R_{\bullet}} = \frac{1}{R_x} + \frac{1}{R_y} = \frac{1}{R_{x1}} + \frac{1}{R_{x2}} + \frac{1}{R_{y1}} + \frac{1}{R_{y2}} \qquad (c-5)$$

$$\frac{2}{E_{\bullet}} = \left(\frac{1 - \nu_1^2}{E_1} + \frac{1 - \nu_2^2}{E_2} \right) \qquad (c-6)$$

The values of α, β and γ are given by Reusner:

$$\lambda = \frac{R_y}{R_x} \qquad (c-7)$$

$$k = \{ \lambda \cdot \ln(4 \cdot \lambda^{1/2}) \}^{1/2} - 0.13 \cdot \ln(4 \cdot \lambda) \qquad (c-8)$$

$$\beta = \{ \frac{2}{\pi} \cdot (k^2 - 1 + 0.7375 \cdot \ln(4.8979 \cdot k) +$$
$$0.4296 \cdot \frac{1}{k^2} \cdot \ln(2.532 \cdot k) \}^{1/3} \qquad (c-9)$$

$$\alpha = \beta/k \qquad (c-10)$$

$$\gamma = \frac{2}{\pi\beta} \ln(4\cdot k) + 0.1671\cdot \frac{1}{k^2}\cdot \ln(3.0176\cdot k) \qquad (c-11)$$

For circular contacts α, β and γ are equal 1, a = b = r.

$$r = \left[\frac{3\cdot N\cdot R_*}{E_*} \right]^{1/3} \qquad (c-12)$$

$$c = \left[\frac{9\cdot N^2}{8\cdot E_*^2\cdot R_*} \right]^{1/3} \qquad (c-13)$$

$$\bar{p} = \frac{1}{3\pi} \left[\frac{3\cdot N\cdot E_*^2}{R_*^2} \right]^{1/3} \qquad (c-14)$$

The equations for line-contacts, according to Hertz are:

$$a = \left[\frac{8\cdot w\cdot R_*}{\pi\cdot E_*} \right]^{1/2} \qquad (c-15)$$

$$\bar{p} = \frac{\pi}{4}\cdot \hat{p} = \frac{\pi}{4}\cdot \left[\frac{w\cdot E_*}{2\cdot \pi\cdot R_*} \right]^{1/2} \qquad (c-16)$$

For more detailed information concerning contact mechanics, the reader is referred to Johnson (1985).

APPENDIX D: Film thickness equations.

During the last decades a large number of film thickness formulas are given in literature, see table D1. A Distinction is made between the minimum- and central film thickness, see fig. 3.1. Most of these equations are composed of 4 dimensionless groups. The general representation of these equations is by numbers of Dowson and Higginson (1966) and Hamrock and Dowson (1977):

$$H_{min.} = c_1 \cdot G^{C2} \cdot U^{C3} \cdot W^{C4} \cdot f(k) \qquad (d-1)$$

In which:

$$H_{min.} = \frac{h_{min.}}{R_x} \qquad \text{: film thickness parameter}$$

$$G = \alpha \cdot E_* \qquad \text{: material parameter}$$

$$U = \frac{\eta_1 \cdot \overline{V}}{E_* \cdot R_x} \qquad \text{: velocity parameter}$$

circular: $\qquad\qquad\qquad\qquad\qquad\qquad$ (d-2)

$$W = \frac{N}{E_* \cdot R_x^2}$$

line:

$$W = \frac{w}{E_* \cdot R_x}$$

$\left.\right\}$: load parameter

$f(k)$ = expression, depending on the contact ellipticity ratio $k = b/a$; for line- and circular contacts it is equal 1.

Table D1:

	c_1	c_2	c_3	c_4	$f(k)$
Line contacts:					
Dowson & Higginson (1966)	1.60	0.60	0.70	-0.13	1
Hamrock & Jacobsen (1984)	3.07	0.57	0.71	-0.11	1
Circular contacts:					
Archard & Cowking (1965/1966)[*]	1.40	0.74	0.74	-0.074	1
Cheng (1970)	1.55	0.725	0.725	-0.058	1
Westlake & Cameron (1972)[**]	4.80	0.70	0.827	-0.143	1
Elliptical contacts:					
Hamrock & Dowson (1977)	3.63	0.49	0.68	-0.073	$1-e^{-0.68 \cdot k}$
Chittenden et al. (1985[a,b])	3.68	0.49	0.68	-0.073	$1-e^{-0.67 \cdot k}$

[*] : $H_{centr.}$ instead of H_{min}

[**] : Jackson (1976)

Line: $H_{min}/H_{centr.} \approx 0.75$ Circular: $H_{min}/H_{centr.} \approx 0.6$

Moes et al. (1965,1985), Johnson (1970), showed that it is possible to describe the EHL regime with 3 dimensionless groups. Moes defined:

a.   line contacts:

$$H_{min.} = \frac{h_{min.}}{R_x} \left(\frac{E_* \cdot R_x}{\eta_1 \cdot V_+} \right)^{1/2} \quad ; \quad H_{Moes} = H_{Dowson} \, (2 \cdot U)^{-1/2}$$

$$M = \frac{w}{E_* \cdot R_x} \left(\frac{E_* \cdot R_x}{\eta_1 \cdot V_+} \right)^{1/2} \quad ; \quad M = W \cdot (2 \cdot U)^{-1/2} \qquad (d-4)$$

$$L = \alpha \cdot E_* \left(\frac{E_* \cdot R_x}{\eta_1 \cdot V_+} \right)^{-1/4} \quad ; \quad L = G \cdot (2 \cdot U)^{1/4}$$

For line contacts Moes derived an equation which is valid for the whole EHL-regime, see Lubrecht et.al. (1986). The given line contact equations in table D1 are restricted to only a part of the EHL- regime.

The formula reads:

$$H_{min.} = [\{(0.99 \cdot M^{-1/8} \cdot L^{3/4})^r + (2.05 \cdot M^{-1/5})^r \}^{s/r} +$$

$$(2.45 \cdot M^{-1})^s]^{1/s}$$

$$(d-5)$$

$$\text{where:} \quad s = 4 - e^{-L/2} - e^{-2/M}$$

$$r = e^{\{1 - 4/(L+5)\}}$$

b.   circular-, elliptical contacts:

$$H_{min.} = \frac{h_{min.}}{R_x} \left[\frac{E_\bullet \cdot R_x}{\eta_1 \cdot V_+} \right]^{1/2} \cdot \Gamma_e^{-1}$$

$$M_\bullet = \frac{N}{E_\bullet \cdot R_x{}^2} \left[\frac{E_\bullet \cdot R_x}{\eta_1 \cdot V_+} \right]^{3/4} \cdot \lambda^{1/2} \qquad (d-6)$$

$$L = \alpha \cdot E_\bullet \left[\frac{E_\bullet \cdot R_x}{\eta_1 \cdot V_+} \right]^{-1/4}$$

with: $\lambda = R_x / R_y$

$$\Gamma_e = 1 - e^{-0.82 \cdot \lambda^{-0.75}}$$

For circular- and elliptical contacts there is at this moment no film thickness equation available which is valid for the whole EHL-regime. An approximation given by Moes et al. (1985) is:

$$H_{min.} = 1.7 \cdot M_\bullet^{-1/12} \cdot L^{11/20} \qquad (d-7)$$

The validity of the given equations (table D1) is depending on the EHL-conditions ($M_\bullet$ and L). Each equation is obtained from calculations carried out in a particular region of the whole EHL-regime.

Lubrecht (1987) calculated the minimum film thickness for circular contacts. The results are presented in figure D1. It is seen that the minimum film thickness drops to very low values at high values of $M_\bullet$. This phenomenon is not included in the formulas given in table D1 and equation (d-7). The transition from EHL to ML occurs at $M_\bullet$ values of $\approx$ 200 to $\approx$ 4000 and L values varying between $\approx$ 1 to $\approx$ 10, the shaded

area in figure D1. The central film thickness does not show such behaviour as found for the minimum film thickness for M_* values of appr. 100 to 200. It seems that $h_{centr.}$ can be used in the region where $M_* > 200$. However, no solution could be obtained for such high M_* values to be sure of that. However, for the contact between the two mating surfaces h_{min} is important and for the calculation of the coefficient of friction $h_{centr.}$ is of interest.

Another aspect with relation to the presented film thickness formulas is the existence of solidification of the lubricant. The lubricant model used in these calculations is based upon Barus which allows an infinite viscosity. Bair and Winer (1979) indicated that viscosity has a limited value. To study the effect of solidification of the lubricant with relation to the validity of the given filmthickness formulas the next analysis is made for line- and circular contacts. Rewriting the equations (c-14), (c-16), (d-4) and (d-6) yields:

$$\text{Line contact} \qquad M = 2 \cdot \pi \cdot (\alpha \cdot \hat{p}/L)^2 \quad = 32/\pi \cdot (\alpha \cdot \bar{p}/L)^2$$

$$\text{Circular contact} \qquad M = 2/3 \cdot \pi^3 \cdot (\alpha \cdot \hat{p}/L)^3 = 9/4 \cdot \pi^3 \cdot (\alpha \cdot \bar{p}/L)^3$$

(d-8)

From figure 3.4 one obtains for the liquid to solid transition :

5P4E	$\alpha p = 10.0 \pm 0.5$	$\theta : 30 - 100\ ^oC$
HVI-650	$\alpha p = 18.5 \pm 1$	$\theta : 30 - 60\ ^oC$
SANTOTRAC-50	$\alpha p = 21.7 \pm 0.2$	$\theta : 30 - 60\ ^oC$

It appears that for the transition from liquid- to solid-like behaviour of a particular lubricant the product of $\alpha \cdot p$ is almost constant. This results in equation (d-8) yielding lines as presented in figure D2.

The question arises if the calculated EHL film thicknesses obtained near the L - S transition are valid for real EHL contact situations. It seems that a better lubricant model is necessary. Conry et al. (1987) showed the influence of non-Newtonian behaviour on film thickness. For lubricants like Sebacate the model can still be applied.
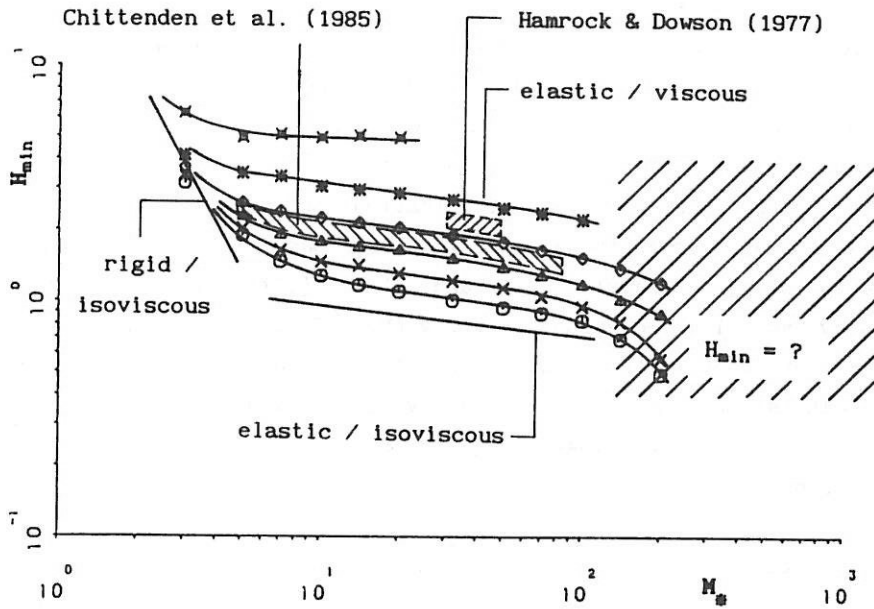
Fig. D1: Film thickness as a function of M_* and L for circular contacts, reproduced from Lubrecht (1987). For ⊙, x, ▲, ◇, ✳ and ⋉ L is 0, 1, 2.5, 5, 10 and 25 respectively. The shaded area represents common L and M_* values near the EHL-ML transition.
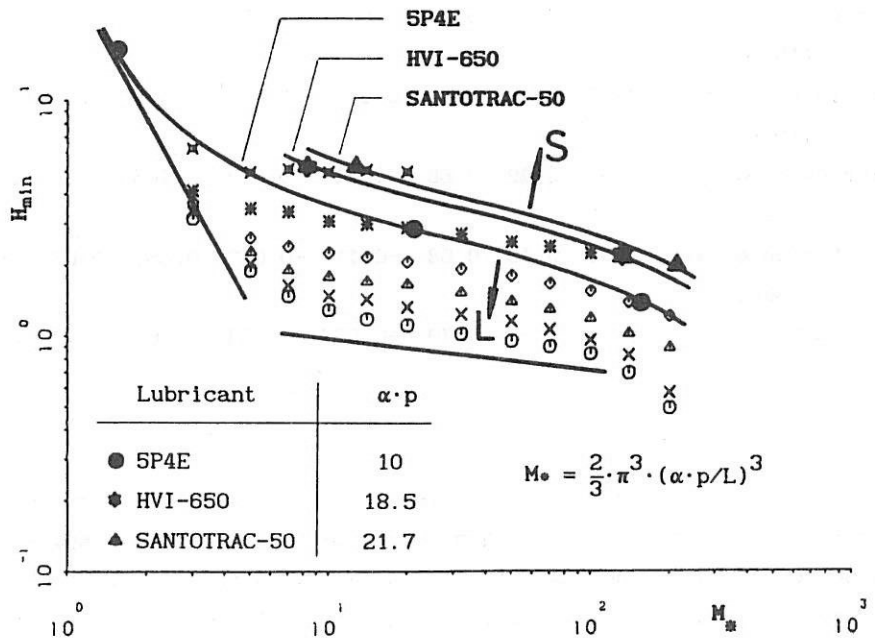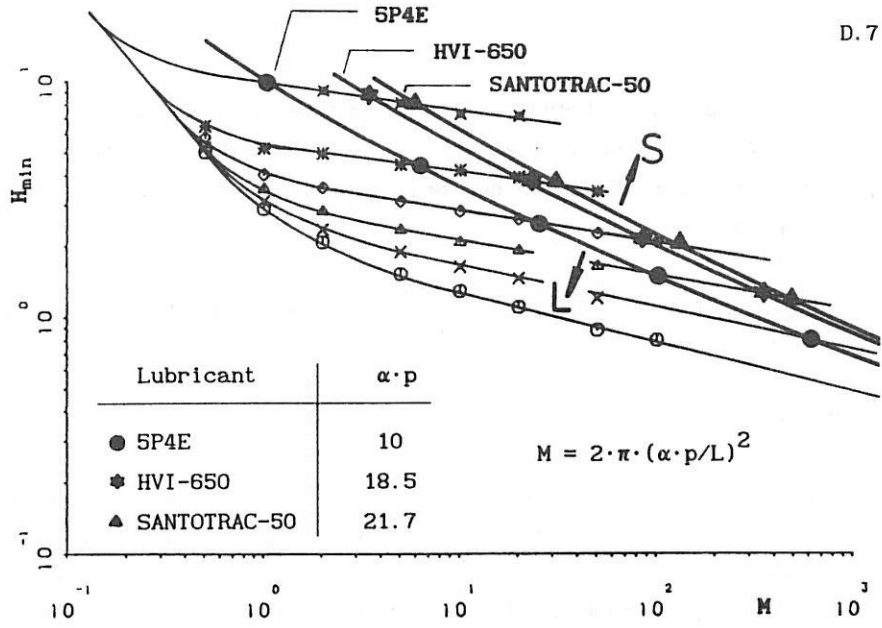
Fig. D2: L-S transition for 5P4E, HVI-650 and Santotrac-50 in the film thickness figures of Moes (1985) for line- and circular contacts. For ⊙, ×, △, ◇, ✳ and ✖ L is 0, 1, 2.5, 5, 10 and 25 respectively.

a. Line contact, b. Circular contact.

In table D2 the influence of the variables, E_*, R_x etc., on the different film thickness equations (of table D1) for the circular- and elliptical contact situation has been investigated. Equation (d-1) is rewritten in:

$$h_{min.} = c_1 \cdot \alpha^{c_2} \cdot \eta_1^{c_3} \cdot E_*^{c_4} \cdot N^{c_5} \cdot R_x^{c_6} \cdot V_+^{c_7} \cdot f(k) \qquad (d-9)$$

Table D2:

	c_1	c_2	c_3	c_4	c_5	c_6	c_7	$f(k)$
Archard & Cowking (1965/1966)	0.84	0.74	0.74	0.074	-0.074	0.408	0.74	1
Cheng (1970)	0.94	0.73	0.73	0.058	-0.058	0.391	0.73	1
Westlake & Cameron (1972)	2.71	0.70	0.83	0.016	-0.143	0.459	0.83	1
Hamrock & Dowson (1977)	2.27	0.49	0.68	-0.117	-0.073	0.466	0.68	$1-e^{-0.68k}$
Chittenden et.al. (1985)	2.30	0.49	0.68	-0.117	-0.073	0.466	0.68	$1-e^{-0.82k}$
Moes & Bosma (1985)	1.70	0.55	0.70	-0.067	-0.083	0.467	0.70	$\lambda^{-1/24} \cdot \Gamma_e$ (d-6)

Now some discrepancies become clear; for instance, the constant c_4 for the elasticity modulus is sometimes positive, which is impossible. These equations are not used in this work. It is seen also that the exponents can differ by almost a factor 2 from one equation to another. The differences between Hamrock & Dowson, Chittenden et al. and Moes are small. However, caution is needed with the use of them, because their validity is limited. For lack of correct film thickness formulas in this thesis the equations of Moes, Chittenden and those of Hamrock & Dowson are used for calculating friction in EHL contacts.

APPENDIX E: AISI-52100 and AL 7075-T651

Material Properties	AISI-52100[*]	AL 7075-T651[**]
E $\quad$ N/m^2 ν ρ $\quad$ kg/m^3 λ $\quad$ W/m^{0}C C_p $\quad$ J/kg^{0}C H $\quad$ N/m^2	$213 \cdot 10^9$ 0.29 7875 46 490 $755 \cdot 10^7$	$74 \cdot 10^9$ 0.30 2800 120 960 $165 \cdot 10^7$
percent of alloy elements	C $\quad$ 1.1 Mn $\quad$ 0.4 Si $\quad$ 0.3 Ni $\quad$ 0.1 Cr $\quad$ 1.5 Mo $\quad$ 0.005 V $\quad$ 0.01	Fe $\quad$ 0.5 Mn $\quad$ 0.3 Si $\quad$ 0.4 Cu $\quad$ 1.2-2.0 Cr $\quad$ 0.18-0.35 Mg $\quad$ 2.1-2.9 Zn $\quad$ 5.1-6.1 Ti $\quad$ 0.2
Heat Treatment	According to SKF specifications	T651 - Solution heat $\quad$ treated 3 hr at 466^{0}C - Quenched in cold $\quad$ water - Stretched, aged 4 $\quad$ days at 20^{0}C then $\quad$ 24 hr at 121^{0}C.

[*] : SKF

[**] : Schipper (1977), ASTM B210-76.

APPENDIX F: Electric contact resistance measurement.

A way to establish if there is any contact between the two surfaces is to measure the contact resistance across them. In figure F1 the electric circuit is given which is used at these ML experiments.
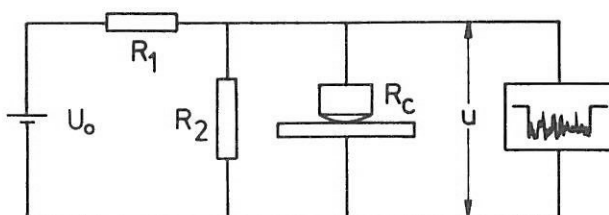
$$R_1 = 56 \ k\Omega, \ R_2 = 1 \ k\Omega, \ U_o = 1 \, V.$$

Fig. F1: Electric circuit.

The measured voltage u is defined by:

$$u = \frac{U_0}{1 + \dfrac{R_1}{R_2} + \dfrac{R_1}{R_c}} \qquad \text{(f-1)}$$

If the specimens are separated by a lubricant film then a potential difference of $U_0/(1 + R_1/R_2)$ is measured, but when there is good electrical contact between the two opposing surfaces, $R_c < 0.1 \ \Omega$ no potential difference is recorded. In figure F2 an observed signal, measured in the ML-regime on the S-tribometer, is shown.

Fig. F2: Contact "resistance" measurement.

Unfortunately, this method only gives an indication that there is electric conductivity present. No quantitative values concerning contact area can be obtained from it. Also this method does not always predict if there is contact between the surfaces or not. The load can be transmitted entirely by interacting asperities and still no electrical conductivity is observed, see section 5.3.1.1.

APPENDIX G: References.

Akhmatov, A.S., 1966, "Molucular physics of boundary lubrication", Israel program for scientific translations, Daniel Davey & Co., New York.

Alsaad, M., Bair, S., Sanborn, D.M., and Winer, W.O., 1978, "Glass transitions in lubricants: its relation to elastohydrodynamic lubrication (EHL)", ASME JOLT, Vol. 100, pp 404-417.

Altrogge, W., 1950, "Zur gesetzmässigkeit der Mischreibung", Ph.D. Thesis, University of Munich, Germany, in German.

Amontons, G., 1699, "De la resistance cause'e dans les machines", Mem. Acad. R. Sci., Vol. 3, pp 206-275.

Archard, J.F., 1958/1959, "The temperature of rubbing surfaces", Wear, Vol. 2, pp 438-455.

Archard, J.F. and Cowking, E.W., 1965/1966, "Elastohydrodynamic lubrication of point contacts", Elastohydrodynamic Lubrication, Inst. Mech. Engrs., Vol. 180, Part 3b, pp 47-56.

Amuzu, J.A.K., Briscoe, B.J., and Tabor, D., 1977, "Friction and shear strengths of polymers", ASLE Trans., Vol. 20 (40), p 354.

Bair, S. and Winer, W.O., 1979, "Shear strength measurements of lubricants at high pressure", ASME JOLT, Vol. 101, pp 251-257.

Bair, S. and Winer, W.O., 1982, "Regimes of traction in concentrated contact lubrication", ASME JOLT, Vol. 104, pp 382-391.

Barlow, A.J., Erginsav, A. and Lamb, J. 1967, "Viscoelastic relaxation of super cooled liquids", Proc. Roy. Soc. of London, Vol. A 298, p 481.

Beeck, O., Givens, J.W. and Smith, A.E., 1940, "On the mechanism of boundary lubrication; I The action of long chain polar compounds", Proc. Roy Soc. of London, Vol. A 177, pp 90-118.

Begelinger, A. and de Gee, A.W.J., 1972, "Boundary lubrication of sliding concentrated steel contacts", Wear, Vol. 22, pp 337-357.

Begelinger, A. and de Gee, A.W.J., 1974, "Thin film lubrication of sliding point contacts of AISI-52100 steel", Wear, Vol. 28, pp 103-114.

Begelinger, A. and de Gee, A.W.J., 1976, "On the mechanism of lubricant film failure in sliding concentrated steel contacts", ASME JOLT, Vol. 98, pp 575-579.

Begelinger, A. and de Gee, A.W.J., 1982, "Failure of thin film lubrication - a detailed study of the lubricant film breakdown mechanism", Wear, Vol. 77, pp 57-63.

Bell, J.C. and Dyson, A., 1972a, "The effect of some operating factors on the scuffing of hardened steel discs", Inst. Mech. Engrs., Second symposium on Elastohydrodynamic Lubrication, Leeds, England, C 11/72, p 68.

Bell, J.C. and Dyson, A., 1972b, "Mixed friction in a Elastohydrodynamic system", Inst. Mech. Engrs., Second symposium on Elastohydrodynamic Lubrication, Leeds, England, C 12/72, pp 68-76.

Bell, J.C., Dyson, A., and Hardley, J.W., 1975, "The effects of rolling and sliding speeds on the scuffing lubricated steel discs", ASLE Trans. Vol. no. 1, pp 62-63.

Bell, J.C., Kannel, J.W. and Allen, C.M., 1964, "The rheological behaviour of the lubricant in the contact zone of a rolling contact system", ASME Trans., J. Basic Engng., Vol. 86, p 423.

Berthe, D. and Godet, M., 1973, "A more general form of Reynolds equation - application to rough surfaces", Wear, Vol. 27, pp 345-357.

Biel, C., 1920, "Die Reibung in Gleitlagern bei Zusatz von Voltöll zu Mineralöl und bei Veränderung der Umlaufzahl und der Temperatur", VDI, Vol. 64, pp 449-452 and pp 483-485.

Blok, H., 1937, "Theoretical study of temperature rise at surfaces of actual contact under oiliness lubrication conditions", Proc. General Discussion on Lubrication and Lubricants, Vol. 2, p 222.

Blok, H., 1963, "Hydrodynamic effects on friction in rolling with slippage", Proceedings of a symposium held at the General Motors research company, Warren, Michigan, October 1960.

Bowden, F.P. and Tabor, D., 1950, "The friction and Lubrication of solids", Pt.I, Oxford University Press.

Bowden, F.P. and Tabor, D., 1964, "The friction and lubrication of solids", Pt.II, Oxford University Press.

Briscoe, B.J., Scruton, B. and Willis, F.R., 1973, "The shear strength of thin lubricant films", Proc. Roy. Soc. London, Vol. A 333, pp 99-114.

Buckingham, E., 1914, "On physically similar systems; illustrations of the use of dimensional equations", Phys. Rev., Vol. 4, pp 347-376.

Buckingham, E., 1915, "Model experiments and the forms of empirical equations", T 37, pp 263-296.

Burwell, J.T., 1957, "Survey of possible wear mechanisms", Wear, Vol. 1, p 119.

Bush, A.W., Skinner, P.H. and Gibson, R.D., 1984 "The effect of surface roughness in elastohydrodynamic lubrication", Wear, Vol. 96, pp 177-202.

Cameron, A., 1966, "Principles of lubrication", Longmans.

Campbell, W.E., 1969, "Boundary Lubrication, an appraisal of world literature", Ed. by F.F. Ling et.al., ASME, New York, pp 87-117.

Carper, H.J. and Ku, P.M., 1975, "Thermal and scuffing behaviour of disks in sliding-rolling contact", ASLE Trans., Vol. 18, no. 1, pp 39-47.

Carper, H.J., KU, P.M. and Anderson, E.L., 1973, "Effect of some material and operating variables on scuffing", Mechanism and Machine Theory, Vol. 8, pp 209-225.

Cheng, H.S., 1965, "A refined solution to the thermal-elasto hydrodynamic lubrication of rolling and sliding cylinders", ASLE Trans., Vol. 8, p 397.

Cheng, H.S., 1970, "A numerical solution of the elastohydrodynamic film thickness in an elliptical contact", ASME JOLT, Vol. 92, pp 155-162.

Chittenden, R.J., Dowson, D., Dunn, J.F. and Taylor, C.M., 1985a, "A theoretical analysis of the isothermal elastohydrodynamic lubrication of concentrated contacts. I. Direction of lubricant entrainment with the major axis of the Hertzian contact ellipse", Proc. Roy. Soc. of London, Vol. A 397, p 245.

Chittenden, R.J., Dowson, D., Dunn, J.F. and Taylor, C.M., 1985b, "A theoretical analysis of the isothermal elastohydrodynamic lubrication of concentrated contacts. II General case, with lubricant entrainment along either principal axis of the Hertzian contact ellipse or at some intermediate angle", Proc. Roy. Soc. of London, A 397, p 271.

Chow, L.S.H. and Cheng, H.S., 1976, "The effect of surface roughness on the average film thickness between lubricated rollers", ASME JOLT, Vol. 98, pp 117-124.

Christensen, H., 1971, "Some aspects of the functional influence of surface roughness in lubrication", Wear, Vol. 17, pp 149-162.

Christensen, H. and Tonder, K., 1973, "The hydrodynamic lubrication of rough journal bearings", ASME JOLT, Vol. 95, pp 166-172.

Conry, T.F., Wang, S. and Cusano C., 1987, "A Reynolds-Eyring equation for elastohydrodynamic lubrication in line contacts", ASME JOT, Vol. 109, p 648.

Crook, A.W., 1963, "The lubrication of rollers. IV. measurement of friction and effective viscosity", Phil. Trans. Roy. Soc. (London), Vol. A 255, p 281.

Czichos, H., 1971, "Untersuchungen über die Verteilung Metallischer und nichtmetallischer Kontaktanteile bei Mischreibung", Wear, Vol. 17, pp 209-217.

Czichos, H., 1974a, "Failure modes of sliding lubricated concentrated contacts", Wear, Vol. 28, pp 95-101.

Czichos, H., 1974b, "Failure criteria in thin film lubrication, the concept of a failure surface", Tribology, Vol. 7, pp 14-20.

Czichos, H., 1974c, "The principles of system analysis and their application to tribology", ASLE Trans., Vol. 17, p 306.

Czichos, H., 1976, "Failure criteria in thin film lubrication: investigation of the different stages of film failure", Wear, Vol. 36, pp 13-17.

Czichos, H., 1977, "Influence of asperity contact conditions on the failure of sliding elastohydrodynamic contacts", Wear, Vol. 41, pp 1-14

Czichos, H., 1978, " Tribology, a systems approach to the science and technology of friction, lubrication and wear", Elsevier, Amsterdam.

Czichos, H. and Kirschke, K., 1972, "Investigations into film failure (transition point) of lubricated concentrated contacts", Wear, Vol. 22, pp 321-336.

Davies, C.B., 1957, "A review of boundary lubrication with particular reference to the conference papers", Proc. Conf. on Lubrication and Wear, Instn. Mech. Engrs., p 319.

Dowson, D. and Higginson, G.R., 1959, "A numerical solution to the elastohydrodynamic problem", J. Mech. Engrg. Sci., Vol. 1, no. 1, p 6.

Dowson, D. and Higginson, G.R., 1966, "Elasto-Hydrodynamic Lubrication", Pergamon Press, Oxford.

Dowson, D. and Withaker, A.V., 1965, "Elastohydrodynamic problem of rolling and sliding contacts lubricated by a Newtonian fluid", Proc. Instn. Mech. Engrs., Vol. 180, Pt 3B, p 57.

Dowson, D. and Whomes, T.L., 1967/1968, "Effect of surface quality upon the traction characteristics of lubricated cylindrical

contacts", Proc. Instn. Mech. Engrs. Vol. 182, Pt1, no. 14, pp 292-299.

Elrod, H.G., 1973, "Thin-film lubrication theory for Newtonian fluids with surfaces possessing striated roughness or grooving", ASME JOLT, Vol. 95, pp 484-489.

Elrod, H.G., 1977, "A review of theories for the fluid dynamic effects of roughness on laminar lubrication films", Proceedings of 4th Leeds-Lyon Symposium on Tribology, pp 11-26.

Elrod, H.G., 1979, "A general theory for laminar lubrication with Reynolds roughness", ASME JOLT, Vol. 101, pp 8-14.

Emmens, W.C., 1988, "The influence of surface roughness on friction", ASM International 15th Biennial Congress, paper no. 8814-002, pp 63-70.

Ertel, A.M., 1939, "Hydrodynamic Lubrication based on new principles", Akad. Nauk SSSR, Prikadnaya Mathematica i Mekhanika, Vol. 3, no. 2, pp 41-52.

Evans, C.R., 1983, "Measurement and mapping of the rheological properties of elastohydrodynamic lubricants", Ph. D. Thesis, University of Cambridge.

Evans, C.R. and Johnson, K.L., 1986a, "The rheological properties of elastohydrodynamic lubricants", Proc. Instn. Mech. Engrs., Vol. 200, C5, p 303.

Evans, C.R. and Johnson, K.L., 1986b, "Regimes of traction elasto-hydrodynamic lubrication", Proc. Instn. Mech. Engrs., Vol. 200, C5, p 313.

Evans, C.R. and Johnson, K.L., 1987, "The influence of surface roughness on elastohydrodynamic traction", Proc. Instn. Mech. Engrs., Vol. 201, C2, pp 145-150.

Fein, R.S., 1969, "Chemistry in concentrated conjunction lubrication", NASA Symposium on Interdisciplinary approach to the lubrication of concentrated contacts", NASA SP-237, pp 489-527.

Fein, R.S. and Kreutz, K.L., 1968, "Discussion on boundary lubrication", Interdiciplinary approach to friction and wear, Ed. P.M. Ku, NASA Sp-181, pp 358-376.

Forrester, P.G., 1946, "Kinetic friction in or near the boundary region; II The influence of sliding velocity and other variables on kinetic friction in or near the boundary region", Proc. Roy. Soc. of London, Vol. A 187, pp 439-463.

Fowles, P.E., 1969, "The application of elasto hydrodynamic lubrication theory to individual asperity-asperity collisions", ASME JOLT, Vol. 91, pp 464-476.

Fowles, P.E., 1971a, "Extension of the elastohydrodynamic theory of individual asperity-asperity collisions to the second half of the collision", ASME JOLT, Vol. 93, pp 213-215.

Fowles, P.E., 1971b, "A thermal elastohydrodynamic theory for individual asperity-asperity collisions", ASME JOLT, Vol. 93, pp 383-397.

Fowles, P.E., 1975, "The statistical application of a thermal EHL theory for individual asperity-asperity collisions on the sliding contact of rough surfaces", ASME JOLT, Vol. 97, pp 311-320.

Furey, M.J., 1963, "Surface roughness effects on metallic contact and friction", ASLE Transactions, Vol. 6, pp 49-59.

Furey, M.J. and Appeldoorn, J.K., 1962, "The effect of lubricant viscosity on metallic contact and friction in a sliding system", ASLE Transactions, Vol. 5, pp 149-159.

Gartner, F., 1964, "Die Mischreibung bei Linienberührung", Ph.D. Thesis, University of Munich, Germany (in German).

Gee, A.W.J. de, 1976, "Selection of materials for lubricated journal bearings", Wear, Vol. 36, pp 33-61.

Gee, A.W.J. de, 1988, "Tribotechniek deel E: Toestandsdiagrammen", Report I9A, University of Twente, Enschede, The Netherlands.

Gee, A.W.J. de, Begelinger, A. and Salomon, G., 1984, "Failure mechanisms in sliding lubricated concentrated contacts", 11th Leeds-Lyon Symposium on mixed lubrication and lubricated wear, Butterworths, London.

Godfrey, D., 1968, "Boundary lubrication", Ed. P.M. Ku, NASA Sp-181, "Interdisciplinary approach to Friction and Wear", pp 335-384.

Godfrey, D., 1978, "Review of usefulness of new surface analysis instruments in understanding boundary lubrication", Proc. Int. Conf. Fund. of Tribology, MIT Cambridge Mass.

Goglia, P.R., Conry, T.F. and Cusano, C., 1984a, "The effects of irregularities on the elasto hydrodynamic lubrication of sliding line contacts, Part I single irregularities", ASME JOLT, Vol. 106, pp 104-112.

Goglia, P.R., Cusano, C. and Conry, T.F., 1984b, "The effects of irregularities on the elasto hydrodynamic lubrication of sliding line contacts, Part II wavy surfaces", ASME JOLT, Vol. 106, pp 113-119.

Greenwood, J.A., 1984, "A unified theory of surface roughness", Proc. Roy. Soc. of London, Vol. A 393, pp 133-157.

Greenwood, J.A., 1985, "Formulas for moderately elliptical Hertzian contacts", ASME JOT, Vol. 107, pp 501-504.

Greenwood, J.A. and Kauzlarich, J.J., 1973, "Inlet shear heating in elastohydrodynamic lubrication", ASME JOLT, Vol. 95, pp 417-426.

Greenwood, J.A. and Tripp, J.H., 1967, "The elastic contact of rough spheres", ASME J. of Appl. Mech., Vol. 89, pp 153-159.

Greenwood, J.A. and Tripp, J.H., 1970, "The contact of two nominally flat rough surfaces", Proc. Inst. Mech. Engrs., Vol. 185, pp 625-633.

Greenwood, J.A. and Williamson, J.B.P., 1966, "Contact of nominally flat surfaces", Proc. Roy. Soc. of London, Vol. A 295, pp 300-319.

Grubin, A.N. 1949, "Fundamentals of the hydrodynamic theory of lubrication of heavily loaded cylindrical surfaces", Central Scientific Research Institute for Technology and Mechanical Engineering, book no. 30, Moscow, D.S.I.R. translation, pp 115-166.

Hamrock, B.J. and Dowson, D., 1977, "Isothermal EHL of point contacts, Part III: fully flooded results", ASME JOLT, Vol. 99, pp 264-276.

Hamrock, B.J. and Jacobson, B.O., 1984, "Elasto-hydrodynamic lubrication of line contacts", ASLE Trans., Vol. 27, pp 275-287.

Hardy, W.B., 1936, "Collected Works", Cambridge University Press.

Hardy, W.B. and Bircumshaw, I., 1925, "Boundary Lubrication. Plane surfaces and the limitations of Amoutons Law", Proc. Roy. Soc. of London, Vol. A 108, pp 1-27.

Hata, H., Nakahara, T. and Aoki, H., 1980, "Measurement of friction in lightly load hydrodynamic sliders with striated roughness", Annual meeting of the ASME on surface roughness effects in hydrodynamic and mixed lubrication, Ed. Rohde S.M. and Cheng H.S. Chicago, Illinois, USA, pp 75-92.

Herrebrugh, K., 1968, "Solving the incompressible and isothermal problem in EHL through an integral equation", ASME JOLT, Vol. 90, pp 262-270.

Hersey, M.D., 1915, "On the laws of lubrication of journal bearings", ASME Transactions, Vol. 37, pp 167-202.

Hertz, H., 1881, "Ueber die Berührung fester elastischer Körper", J. Reine Angew. Math. Vol. 92, pp 156-171.

Hirst, W. and Moore, A.J., 1974, "Non-Newtonian behaviour in EHL", Proc. Roy. Soc. of London, Vol. A 337, pp 101-121.

Hirst, W. and Moore, A.J., 1975, "The elastohydrodynamic behaviour of polyphenyl ether", Proc. Roy. Soc. of London, Vol. A 344, pp 403-426.

Hirst, W. and Moore, A.J., 1978, "Elastohydrodynamic lubrication at high pressures", Proc. Roy. Soc. of London, Vol. A 360, pp 403-425.

Hirst, W. and Moore, A.J., 1979, "EHL at high pressures II. Non Newtonian behaviour", Proc. Roy. Soc. of London, Vol. A 365, pp 537-565.

Hirst, W. and Moore, A.J., 1980, "The effect of temperature on traction in elastohydrodynamic lubrication", Phil. Trans. Roy. Soc. A., Vol. 298, pp 183-208.

Holmberg, K., 1984, "Friction in low speed lubricated rolling and sliding contacts", Ph. D. Thesis, Technical research centre of Finland.

Jackson, A., 1976, "Film thickness in EHL point contacts: revision of Westlake and Cameron's equations", ASLE Trans., Vol. 19, p48.

Johnson, K.L., 1970, "Regimes of elastohydrodynamic lubrication", J. Mech. Eng. Sci, Vol. 12, pp 9-16.

Johnson, K.L., 1985, "Contact mechanics", Cambridge University press, Cambridge.

Johnson, K.L. and Cameron, R., 1967, "Shear behaviour of elasto hydrodynamic oil films at high rolling contact pressures", Proc. Instn. Mech. Engrs., Vol. 182, Pt-I, no. 14, p 307.

Johnson, K.L. and Greenwood, J.A., 1980, "Thermal analysis of an Eyring fluid in elastohydrodynamic traction", Wear, Vol. 61, pp 353-374.

Johnson, K.L., Greenwood, J.A. and Poon, S.Y., 1972, "A simple theory of asperity contact in elastohydrodynamic lubrication", Wear, Vol. 19, pp 91-108.

Johnson, K.L. and Roberts, A.D., 1974, "Observations of viscoelastic behaviour of an elastohydrodynamic lubricant film", Proc. Roy. Soc. of London, Vol. A 337, pp 217-242.

Johnson, K.L. and Tevaarwerk, J.L., 1977, "Shear behaviour of EHD oil films", Proc. Roy. Soc. of London, Vol. A 356, p 215.

Ku, P.M., Staph, H.E. and Carper, H.J., 1978a, "Frictional and thermal behaviors of sliding-rolling concentrated contacts", ASME JOLT, Vol. 100, pp 121-128.

Ku, P.M., Staph, H.E. and Carper, H.J., 1978b, "On the critical contact temperature of lubricated sliding-rolling discs", ASLE Trans., Vol. 21, no. 2, pp 161-180.

Lammers, R.W., 1986, "Experimentele bepaling van de overgang volle-film smering naar gemengde smering op een twee-schijven machine", Msc. Thesis, University of Twente, Enschede, The Netherlands (in Dutch).

Leaver, R.H., Sayles, R.S. and Thomas, T.R., 1974, "Mixed lubrication and surfaces topography of rolling contacts", Proc. Instn. Mech. Engrs., Vol. 188, no 44/74, pp 461-470.

Lenning, R.L., 1960, "The transition from boundary to mixed friction", Lubrication Engineering, Vol. 16, no. 12, pp 575-482.

Longuet-Higgins, M.S., 1957, "The statistical analysis of a random moving surface", Phil. Trans. Roy. Soc. of London, Vol. A 249, pp 321-387.

Lubrecht, A.A., 1987, "The numerical solution of the elastohydrodynamically lubricated line- and point contact problem using multigrid techniques", Ph.D. Thesis, University of Twente, Enschede, The Netherlands.

Lubrecht, A.A., Breukink, G.A.C., Moes, H., Napel, W.E. ten and Bosma, R., 1986, "Solving Reynolds equation for EHL line contacts by application of a multi-grid method", Proc. of the 11th Leeds-Lyon symposium on Tribology.

Matveevsky, R.M., 1965, "The critical temperature of oil with point and line contact machines", ASME Trans., Journal of Basic Engineering, Vol. 17, pp 754-760.

McKee, S.A., 1927, "The effect of running in an journal bearing performance", ASME Trans., Vol. 49, p 1335.

Michell, A.G.M., 1950, "Lubrication - its principles in practice", Blackie and Son, London and Glasgow, pp 281-291.

Moes, H., 1965, "Discussion of paper R1", Instn. Mech. Engrs., Vol. 180, Part 3B, p 244.

Moes, H. and Bosma, R., 1972, "Film thickness and traction in EHL at point contact", Instn. Mech. Engrs., EHL Symposium, London, England, c 38/72, pp 149-152.

Moes, H. and Bosma, R., 1985, "Survey diagrams for filmthickness in elastohydrodynamic lubrication", Internal memo, University of Twente, Enschede, The Netherlands.

Niemann, G. and Gartner, F., 1966, "Die Mischreibung bei Linienberührung", VDI, Vol. 108, no. 6, pp 201-209.

Oh, K.P., 1984, "The numerical solution of dynamically loaded elastohydrodynamic contact as a non linear complementarity problem", ASME JOT, Vol. 106, pp 88-95.

Oh, K.P., 1985, "The formulation of the mixed lubrication problem as a generalized nonlinear complementarity problem", ASME JOT, Vol. 107, p 201.

Patir, N. and Cheng, H.S., 1978, "An average flow model for determining effects of three dimensional roughness on partial hydrodynamic lubrication", ASME JOLT, Vol. 100, pp 12-17.

Patir, N. and Cheng, H.S., 1979, "Application on the average flow model to lubrication between rough sliding surfaces", ASME JOLT, Vol. 101, pp 220-230.

Petrusevich, A.I., 1951, "Fundamental conclusions from the contact hydrodynamic theory of lubrication", Iz. Akad. Nauk. S.S.S.R. (OTN), Vol. 2, p 209.

Phan-Thien, N., 1981a, "On the effect of parallel and transverse stationary random surface roughness in hydrodynamic lubrication", Proc. Roy. Soc. of London, Vol. A 374, pp 569-591.

Phan-Thien, N., 1981b, "On the effects of the Reynolds and Stokes surface roughnesses in a two-dimensional slider bearing", Proc. Roy. Soc. of London, Vol. A 377, pp 349-362.

Poon, S.Y., and Haines, D.J., 1966/1967, "Frictional behaviour of lubricated rolling-contact elements", Proc. Instn. Mech. Engrs., Vol. 181, Pt 1, no. 16, p 363.

Reusner, H., 1977, "Druckflächen belastung und Oberflächen verschiebung im Walzcontact", Ph. D. thesis, University of Karlsruhe, Germany (in German).

Reynolds, O., 1886, "On the theory of lubrication and its application to Mr. Tower's experiments, including an experimental determination of the viscosity of olive oil", Trans. Roy. Soc. of London, Vol. 177 (part 1), pp 157-235.

Rice, S.O., 1945, "Mathematical analysis of random noise", Bell System Tech. J., Vol. 24, pp 46-156.

Roelands, C.J.R., 1966, "Correlation aspects of the viscosity-temperature-pressure relationship of lubrication oils", Ph.D. thesis, University of Delft, The Netherlands.

Rowe, C.N., 1973, "Interdisciplinary approach to liquid lubricant technology", Ed. P.M. Ku, NASA Sp-318, p 527.

Rowe, G.W., 1966, "Boundary lubrication", Principles of lubrication, A. Cameron, John Wiley & Sons, Chap. 20.

Safa, M.M.A., 1982, "Elastohydrodynamic studies using thin film transducers", Ph. D. thesis, University of London, England.

Sakurai, T., 1981, "Role of chemistry in the lubrication of concentrated contacts", ASME JOLT, Vol. 103, p 473.

Schipper, D.J., 1977, Report nr. WB/TM 27/77, University of Twente, Enschede, The Netherlands (in Dutch).

Smith, F.W., 1958/1959, "Lubricant behaviour in concentrated contact systems - the castor oil - steel system", Wear, Vol. 2, pp 250-263.

Smith, F.W., 1959, " Lubricant behaviour in concentrated contact - some rheological problems", ASLE Trans., Vol. 3, pp 18-25.

Spiegel, K., 1973, "Ueber den Einfluss elastischer Deformationen auf die Tragfähigkeit von Radialgleitlagern", Schmiertech. Tribol., Vol. 20, pp 3-9.

Stribeck, R., 1902, "Die wesentlichen Eigenschaften der Gleit- und Rollenlager", VDI-Zeitschrift, Vol. 46, pp 1341-1348, pp 1432-1438 and pp 1463-1470.

Sun, D.C. and Chen, K.K., 1977, "First effects of Stokes roughness on hydrodynamic lubrication technology", ASME series F, Vol. 99, pp 2-9.

Tabor, D., 1951, "The hardness of metals", Oxford University Press.

Tabor, D., 1982a, "Status and direction of tribology as a science in the 80's - understanding and prediction", Proc. of an international conference on tribology for the 80's, ed. Loomis, W.R., NASA-Cleveland, Ohio, pp 1-16.

Tabor, D., 1982b, "Future directions of research in adhesion and friction - status of understanding", Proc. of an international conference on tribology for the 80's, ed. Loomis, W.R., NASA-Cleveland, Ohio, pp 116-137.

Tallian, T.E., McCool, J.J. and Sibley, L.B., 1965, "Partial elastohy-drodynamic lubrication in rolling contact", Proc. Instn. Mech. Engrs. Vol. 180, no. Pt 3B, p 169.

Tamai, Y. and Rightmire, B.G., 1965, "Mechanism of boundary lubrication and the edge effect", Trans. ASME, J. of Basic Engrg., Vol. 68, p 735.

Teale, J.L. and Lebeck, A.O., 1980, "An evaluation of the average flow model for surface roughness effects in lubrication", ASME JOLT, Vol. 102, pp 360-367.

Tevaarwerk, J.L., 1976, "The shear of elastohydrodynamic oil films", Ph.D Thesis, University of Cambridge, Cambridge.

Tonder, K., 1977a, "Lubrication of surface having area-distributed isotropic roughness", ASME JOLT, Vol. 99, pp 323-330.

Tonder, K., 1977b, "Mathematical verification of the applicability of modified Reynolds equations to striated rough surfaces", Wear, Vol. 44, pp 329-343.

Tonder, K., 1980a, "Numerical investigation of lubrication of doubly periodic unit roughness", Wear, Vol. 64, pp 1-14.

Tonder, K., 1980b, "Simulation of the lubrication of isotropically rough surfaces", ASLE-Trans., Vol. 23, pp 326-333.

Tonder, K. and Christensen, H., 1972, "Lubrication of cylindrical rollers with surface corrugations", Wear, Vol. 20, pp 309-314.

Tripp, J.H., 1983, "Surface roughness effects in hydrodynamic lubrication: The flow factor method", ASME JOLT, Vol. 105, pp 458-465.

Tripp, J.H., Houpert, L.G., Ioannides, E. and Lubrecht, A.A., 1987, "Dry and lubricated contact of rough surfaces", Private communication.

Tzeng, S.T. and Saibel, E., 1967, "Surface roughness effect on slider bearing lubrication", ASLE Trans., Vol. 10, pp 334-338.

Venner, C.H., 1988, University of Twente, Enschede, The Netherlands, private communication 1988.

Vogelpohl, G., 1954, "Die Stribeck-kurve als Kennzeichen des allgemeinen Reibungsverhaltens geschmierter Gleitflächen", VDI, Vol. 96, no. 9, pp 261-268.

Vogelpohl, G., 1958, "Betriebssichere Gleitlager", Springer-Verlag, Berlin.

Westlake, F.J. and Cameron, A., 1972, "Interferometric study of point contact lubrication", Inst. Mech. Engrs., EHL Symposium, Leeds, England, C 39/72.

Whitehouse, D.J. and Phillips, M.J., 1978, "Discrete properties of random surfaces", Phil. Trans. R. Soc. London, Vol. A290, pp 267-298.

Whitehouse, D.J. and Philips, M.J., 1982, "Two-dimensional discrete properties of random surfaces", Phil. Trans. R. Soc. London, Vol. A 305, pp 441-468.

Acknowledgements

- Geboren te Kampen op 30 mei 1955.

- Lagere Technische School te Kampen, 1967-1970.

- Middelbare Technische School te Zwolle, afdeling der Werktuigbouw-kunde, 1970-1972.

- Hogere Technische School te Zwolle, afdeling der Werktuigbouwkunde, 1972-1977, met als afstudeeropdracht:

   "De scheurgroei in Aluminium AL 7075-T651".

- Universiteit Twente, 1977-1983.
  In deze periode de studie onderbroken i.v.m. militaire dienstplicht. De studie aan de U.T., afdeling der Werktuigbouwkunde afgesloten bij de leerstoel Tribologie met de opdracht getiteld:

   "Computer simulatie van dynamisch belaste lagersystemen".

- Van sept. 1983 tot sept. 1987 in dienst van de Stichting voor de Technische Wetenschappen (S.T.W.). In deze periode is dit werk tot stand gekomen.

- Sedert sept. 1987 tijdelijk verbonden aan de Universiteit Twente als universitair docent.